STABILIZATION OF EXPANSIVE SOILS USING SILICA FUME AND LIME

A THESIS SUBMITTED TO
THE GRADUATE SCHOOL OF NATURAL AND APPLIED SCIENCES
OF
MIDDLE EAST TECHNICAL UNIVERSITY

BY

HAYRİ GÜZEL

IN PARTIAL FULFILLMENT OF THE REQUIREMENTS
FOR
THE DEGREE OF MASTER OF SCIENCE
IN
CIVIL ENGINEERING

SEPTEMBER 2023

Approval of the thesis:

STABILIZATION OF EXPANSIVE SOILS USING SILICA FUME AND LIME

submitted by **HAYRİ GÜZEL** in partial fulfillment of the requirements for the degree of **Master of Science** i**n Civil Engineering, Middle East Technical University** by,

Prof. Dr. Halil Kalıpçılar
Dean, Graduate School of **Natural and Applied Sciences** _____

Prof. Dr. Erdem Canbay
Head of the Department, **Civil Engineering** _____

Prof. Dr. Erdal Çokça
Supervisor, **Civil Engineering, METU** _____

Examining Committee Members:

Prof. Dr. Kemal Önder Çetin
Civil Engineering, METU _____

Prof. Dr. Erdal Çokça
Civil Engineering, METU _____

Assoc. Prof. Dr. Nejan Huvaj Sarıhan
Civil Engineering, METU _____

Prof. Dr. Nihat Sinan Işık
Civil Engineering, Gazi Uni. _____

Assoc. Prof. Dr. Abdullah Sandıkkaya
Civil Engineering, Hacettepe Uni. _____

Date: 04.09.2023

I hereby declare that all information in this document has been obtained and presented in accordance with academic rules and ethical conduct. I also declare that, as required by these rules and conduct, I have fully cited and referenced all material and results that are not original to this work.

Name Last name : Hayri Güzel

Signature :

ABSTRACT

STABILIZATION OF EXPANSIVE SOILS USING
SILICA FUME AND LIME

Güzel, Hayri
Master of Science, Civil Engineering
Supervisor : Prof. Dr. Erdal Çokça

September 2023, 164 pages

The issue of expansive soils is a global concern that presents numerous complexities for professionals in the field of civil engineering. When exposed to water, these types of soils exhibit swelling and undergo shrinkage upon drying. The prevailing and cost-effective approach to stabilize these soils involves the utilization of admixtures that effectively mitigate volumetric alterations. This study aims to investigate the impact of incorporating silica fume and lime on mitigating the swelling potential and improving the unconfined compression characteristics. The preparation of the expansive soil has been done in the laboratory by mixing kaolinite and bentonite. The expansive soil has been modified with silica fume at different weight percentages. The determination of grain size distribution, consistency limits, compaction characteristics, swelling percentage, and unconfined compressive strength, deformation modulus of the mixtures have been conducted. The specimens have been undergoing a curing process ranging from 7 and 28 days. The experimental study revealed the impact of silica fume and lime on the swelling potential and unconfined compression characteristics of artificially prepared expansive soil specimens under laboratory conditions. The research findings show that the inclusion of silica fume and lime in the samples resulted in a threefold increase in unconfined compression strength compared to samples without additives.

Additionally, the swelling potential dropped to one-fifteenth of no additive sample swelling potential, and the deformation modulus increased by a factor of five.

Keywords: Expansive Soil, Soil Stabilization, Swelling Potential, Silica Fume, Lime,

ÖZ

ŞİŞEN ZEMİNLERİN SİLİS DUMANI VE KİREÇ KULLANILARAK STABİLİZASYONU

Güzel, Hayri
Yüksek Lisans, İnşaat Mühendisliği
Tez Yöneticisi: Prof. Dr. Erdal Çokça

Eylül 2023, 164 sayfa

Şişen zeminler konusu, inşaat mühendisliği alanındaki profesyoneller için çok sayıda karmaşıklık sunan küresel bir sorundur. Bu tür zeminler suya maruz kaldıklarında şişme gösterir ve kuruduktan sonra büzülmeye uğrarlar. Bu zeminleri stabilize etmek için geçerli ve uygun maliyetli yaklaşım, hacimsel değişiklikleri etkili bir şekilde azaltan katkıların kullanılmasını içerir. Bu çalışma, silis dumanı ve kireç ilavesinin şişme potansiyelini azaltma ve serbest basınç özelliklerini iyileştirme üzerindeki etkisini araştırmayı amaçlamaktadır. Genişleyen zeminin hazırlanması, kaolinit ve bentonit karıştırılarak laboratuvarda yapılmıştır. Genişleyen zemin farklı ağırlık yüzdelerinde silis dumanı ile modifiye edilmiştir. Karışımların tane boyutu dağılımı, kıvam limitleri, sıkıştırma özellikleri, şişme yüzdesi ve serbest basınç dayanımı, deformasyon modülü belirlenmiştir. Numuneler 7 ve 28 gün arasında değişen bir kür sürecinden geçirilmiştir. Deneysel çalışma, silis dumanı ve kirecin laboratuvar koşullarında yapay olarak hazırlanan şişen zemin numunelerinin şişme potansiyeli ve serbest basınç özellikleri üzerindeki etkisini ortaya koymuştur. Araştırma bulguları, silis dumanı ve kirecin numunelere dahil edilmesinin, katkı maddesi içermeyen numunelere kıyasla serbest basınç dayanımında üç kat artışa neden olduğunu göstermektedir. Ayrıca, şişme potansiyeli katkısız numunenin şişme potansiyelinin on beşte birine düşmüş ve deformasyon modülü beş kat artmıştır.

Anahtar Kelimeler: Şişen Zemin, Zemin Stabilizasyonu, Şişme Potansiyeli, Silis Dumanı, Kireç,

To My Family

ACKNOWLEDGMENTS

I want to express my most profound appreciation to my supervisor, Prof. Dr. Erdal Çokça, for his priceless guidance, never-ending understanding, remarkable patience, and support throughout every stage of this research study.

I would like to express my gratitude to the instructors at Middle East Technical University (METU) for their valuable contributions to enhancing my understanding of engineering principles during my engineering education.

Furthermore, I would like to especially thank Associate Professor Dr. Kartal Toker for his invaluable feedback and encouragement, which significantly influenced the methodology employed in my experiments and the interpretation of my findings.

I want to thank Mr. Kamber Bilgen, the METU Soil Mechanics Laboratory technician, for his invaluable assistance in implementing laboratory procedures and developing experimental methodologies.

I express my sincere thanks to my father Ahmet Güzel, to my mother Selma Güzel, and my sister Ezgi Güzel Uysal for their endless support throughout my life.

Friends, lab mates, and colleagues: Tuğçe, Sefa, Berkan, Moutasem, Anıl, Arda, Eray, Mehmet, Melih, and Elife are all appreciated for the enjoyable experiences shared while collaborating and engaging in social activities.

TABLE OF CONTENTS

ABSTRACT v

ÖZ vii

ACKNOWLEDGMENTS x

TABLE OF CONTENTS xi

LIST OF TABLES xv

LIST OF FIGURES xvi

LIST OF ABBREVIATIONS xxi

LIST OF SYMBOLS xxiii

CHAPTERS

1 INTRODUCTION 1

1.1 Objective of the Study 5

1.2 Scope of the Study 5

2 LITERATURE REVIEW 7

2.1 Expansive Soil 7

2.1.1 Clay Mineralogy 7

2.1.1.1 Kaolinite Group 10

2.1.1.2 Mica-Like Group 12

2.1.1.2.1 Illite 12

2.1.1.3 Smectite Group 13

2.1.1.3.1 Montmorillonite 13

2.2 Adsorbed Cations and Cation Hydration 17

2.3 Clay Micelle 18

2.4 Diffuse Double Layer 20
2.5 Cation Exchange Capacity 21
2.6 Clay Structure 21
2.7 Swelling Mechanism 22
2.7.1 Crystalline and Osmotic Expansion Approach 23
2.7.2 Interparticle or Intercrystalline 23
2.8 Factors Effecting Swelling 26
2.9 Stabilization of Expansive Soils 30
2.9.1 Chemical Additives 34
2.9.1.1 Lime Stabilization 35
2.9.1.1.1 Lime Stabilization Mechanisms 36
2.9.1.1.1.1 Cation Exchange 37
2.9.1.1.1.2 Flocculation and Agglomeration 38
2.9.1.1.1.3 Pozzolanic Reactions 40
2.9.1.1.1.4 Carbonation 41
2.9.1.2 Silica Fume Stabilization 42
2.9.1.2.1 Silica Fume Production 42
2.9.1.2.2 Properties of Silica Fume 43
2.9.1.2.3 Stabilization Mechanism of Silica Fume 45
2.9.1.2.4 Previous Studies Conducted by Silica Fume 47
3 EXPERIMENTAL STUDY 55
3.1 Purpose 55
3.2 Materials 55
3.3 Preparation of the Samples 58

3.4 Sample Properties 61
3.5 Test Procedures 75
3.5.1 Free Swell Test 75
3.5.1.1 Preparing the Specimen 75
3.5.1.2 Test Procedure 75
3.5.1.3 Results 78
3.5.2 Unconfined Compression Test 83
3.5.2.1 Preparing The Specimen 83
3.5.2.2 Test Procedure 85
3.5.2.3 Results 86
4 DISCUSSION OF RESULTS 95
4.1 Effect of Stabilizers on Specific Gravity, Gs 95
4.2 Effect of Stabilizers on Grain Size Distribution 95
4.3 Effect of Stabilizers on Maximum Dry Density, $\rho_{dry,max}$ and Optimum Moisture Content, w_{opt} 96
4.4 Effect of Stabilizers on Consistency Limits 99
4.5 Effect of Stabilizers on Activity, A_c 100
4.6 Effect of Stabilizers on Swell Percentage 102
4.7 Effect of Cure on Swell Percentage 105
4.8 Effect of Stabilizers on Unconfined Compressive Strength 107
4.9 Effect of Cure on Unconfined Compressive Strength 109
4.10 Effect of Stabilizers on Deformation Modulus, E_{50} 112
4.11 Effect of Cure on Deformation Modulus, E_{50} 114
5 CONCLUSIONS 117

REFERENCES

APPENDICES 137

A. Swell Percent vs Square-Root of Time Graphs of Treated Samples 137

B. Axial Compressive Stress vs Axial Strain of Treated Samples 148

C. Swell Rate vs Percent Additive 159

D. Net Swell Percentage and Stabilization Percentages 161

LIST OF TABLES

TABLES

Table 2.1 Some important properties of key clay minerals (Nelson & Miller, 1992) 16
Table 2.2 Factors affecting the soil's ability to shrink and swell (Nelson & Miller, 1992) 27
Table 2.3 Stress State Factors affecting the shrink-swell behavior (Nelson & Miller, 1992) 28
Table 2.4 Factors in the surrounding environment that might affect swelling or shrinkage (Nelson & Miller, 1992) 29
Table 2.5 Soil Stabilization approaches applied to expansive soils (Nelson & Miller, 1992) 32
Table 3.1 Chemical Compositions of Kaolinite, Bentonite, Lime, and Silica Fume 57
Table 3.2 Percent Additive in Each Sample 59
Table 3.3 Saturation Values at Maximum Dry Density State 63
Table 3.4 Sample Properties 64
Table 4.1 Strain Values at Peak and Failure Unconfined Compressive Strength Values 110
Table 5.1 Optimum Additive Combinations for Each Aspect 119

LIST OF FIGURES

FIGURES

Figure 1.1 Global distribution of reported expansive soil sites (Nelson et al., 2015)2
Figure 2.1 Basic Structural Units in the Silicon Sheet (Murthy, 2002) 9
Figure 2.2 Basic Structural Units in the Octahedral Sheet (Murthy, 2002) 9
Figure 2.3 Synthesis pattern for the clay minerals (Mitchell & Soga, 2005).....10
Figure 2.4 Diagrammatic sketch of the kaolinite structure (Mitchell & Soga, 2005) 11
Figure 2.5 Structure of kaolinite layer (Murthy, 2002).....11
Figure 2.6 Diagrammatic sketch of the structure of illite (Murray, 2006).....12
Figure 2.7 Structure of Illite Layer (Murthy, 2002) 13
Figure 2.8 Diagrammatic sketch of the montmorillonite structure (Mitchell & Soga, 2005).....14
Figure 2.9 Structure of montmorillonite Layer (Murthy, 2002).....14
Figure 2.10 Scanning electron micrographs of clay minerals (Nelson et al., 2015)15
Figure 2.11 Role of cation hydration on soil expansion: (a) low hydration; (b) partial hydration; (c) full hydration. (Nelson et al., 2015) 17
Figure 2.12 A clay micelle showing the concentration of cations near the surface of a clay particle. (Nelson et al., 2015).....18
Figure 2.13 Sediment structures: (a) “flocculated” or “random” orientation; (b) “dispersed” or “oriented” (Nelson et al., 2015).....22
Figure 2.14 Mechanism of swelling proposed by (Popescu, 1986) 25
Figure 2.15 Cation exchange (Prusinski & Bhattacharja, 1999).....38
Figure 2.16 Flocculation and agglomeration (Prusinski & Bhattacharja, 1999).....39
Figure 2.17 Pozzolanic reaction (Prusinski & Bhattacharja, 1999) 41
Figure 2.18 The schematic of the silicon melting process results in silica fume (Tangstad, 2013).....42
Figure 2.19 X-ray diffraction (XRD) pattern of a commercial silica fume (Wang et al., 2020).....44

Figure 2.20 Scanning Electron Microscopy (SEM) image of a commercial silica fume (Wang et al., 2020) 44
Figure 2.21 Transmission Electron Microscope (TEM) image of a commercial silica fume (Wang et al., 2020) 45
Figure 3.1 Kaolinite 55
Figure 3.2 Bentonite 56
Figure 3.3 Hydrated Lime 56
Figure 3.4 Silica Fume 57
Figure 3.5 Sample Preparation Procedure 60
Figure 3.6 Compaction Curves of 3% Lime-Added Set 65
Figure 3.7 Compaction Curves of 5% Lime-Added Set 66
Figure 3.8 Grain Size Distribution Curves of 3% Lime-Added Set 67
Figure 3.9 Grain Size Distribution Curves of 5% Lime-Added Set 68
Figure 3.10 Plasticity Chart (USCS) 69
Figure 3.11 Effect of Addition of Lime and Silica Fume on Specific Gravity 70
Figure 3.12 Effect of Addition of Lime and Silica Fume on Liquid Limit (LL) 71
Figure 3.13 Effect of Addition of Lime and Silica Fume on Plastic Limit (PL) 72
Figure 3.14 Effect of Addition of Lime and Silica Fume on Plasticity Index (PI) 73
Figure 3.15 Classification Chart for Swelling Potential (After Seed et al., (1962)) 74
Figure 3.16 A View of the Specimen Compacted into the Cutting Ring 75
Figure 3.17 Bishop Apparatus 77
Figure 3.18 Percent Swell vs Square-Root of Time relationship for No-Additive Sample 79
Figure 3.19 Effect of Addition of Lime and Silica Fume on Swelling Percent without Curing 80
Figure 3.20 Effect of Addition of Lime and Silica Fume on Swelling Percent with 7 Days of Curing 81
Figure 3.21 Effect of Addition of Lime and Silica Fume on Swelling Percent with 28 Days of Curing 82

Figure 3.22 Equipments for Specimen Compaction for Unconfined Compressive Strength Test 84
Figure 3.23 A View of Static Compaction Done by Hydraulic Jack 84
Figure 3.24 Uniaxial Compression Test Device 86
Figure 3.25 Axial Compressive Stress vs Axial Strain Relationships for No-Additive Sample 88
Figure 3.26 Effect of Addition of Lime and Silica Fume on Unconfined Compressive Strength without Curing 89
Figure 3.27 Effect of Addition of Lime and Silica Fume on Unconfined Compressive Strength with 7 Days of Curing 90
Figure 3.28 Effect of Addition of Lime and Silica Fume on Unconfined Compressive Strength with 28 Days of Curing 91
Figure 3.29 Effect of Addition of Lime and Silica Fume on Deformation Modulus, E_{50} without Curing 92
Figure 3.30 Effect of Addition of Lime and Silica Fume on Deformation Modulus, E_{50} with 7 Days of Curing 93
Figure 3.31 Effect of Addition of Lime and Silica Fume on Deformation Modulus, E50 with 28 Days of Curing 94
Figure 4.1 Effect of Addition of Lime and Silica Fume on Maximum Dry Density 97
Figure 4.2 Effect of Addition of Lime and Silica Fume on Optimum Water Content 98
Figure 4.3 Effect of Addition of Lime and Silica Fume on Activity 101
Figure 4.4 Effect of Addition of Lime and Silica Fume on Stabilization Percentage of Swelling Percent without Curing 104
Figure 4.5 Effect of Addition of Lime and Silica Fume on Stabilization Percentage of Swelling Percent with 7 and 28 Days of Curing 106
Figure 4.6 Effect of Addition of Lime and Silica Fume on Stabilization Percentage of Unconfined Compressive Strength without Curing 108

Figure 4.7 Effect of Addition of Lime and Silica Fume on Stabilization Percentage of Unconfined Compressive Strength with 7 and 28 Days of Curing 111
Figure 4.8 Effect of Addition of Lime and Silica Fume on Stabilization Percentage of Deformation Modulus, E_{50} without Curing 113
Figure 4.9 Effect of Addition of Lime and Silica Fume on Stabilization Percentage of Deformation Modulus, E50 with 7 and 28 Days of Curing..... 115
Figure A.1 Percent Swell vs Square-Root of Time Relationships for 3% L Samples with 0-7-28 Days of Curing 138
Figure A.2 Percent Swell vs Square-Root of Time Relationships for 3% L + 5% SF Samples with 0-7-28 Days of Curing..... 139
Figure A.3 Percent Swell vs Square-Root of Time Relationships for 3% L + 10% SF Samples with 0-7-28 Days of Curing 140
Figure A.4 Percent Swell vs Square-Root of Time Relationships for 3% L + 15% SF Samples with 0-7-28 Days of Curing 141
Figure A.5 Percent Swell vs Square-Root of Time Relationships for 3% L + 20% SF Samples with 0-7-28 Days of Curing 142
Figure A.6 Percent Swell vs Square-Root of Time Relationships for 5% L Samples with 0-7-28 Days of Curing 143
Figure A.7 Percent Swell vs Square-Root of Time Relationships for 5% L + 5% SF Samples with 0-7-28 Days of Curing..... 144
Figure A.8 Percent Swell vs Square-Root of Time Relationships for 5% L + 10% SF Samples with 0-7-28 Days of Curing 145
Figure A.9 Percent Swell vs Square-Root of Time Relationships for 5% L + 15% SF Samples with 0-7-28 Days of Curing 146
Figure A.10 Percent Swell vs Square-Root of Time Relationships for 5% L + 20% SF Samples with 0-7-28 Days of Curing 147
Figure B.1 Axial Compressive Stress vs Axial Strain Relationships for 3% L Samples with 0-7-28 Days of Curing..... 149
Figure B.2 Axial Compressive Stress vs Axial Strain Relationships for 3% L + 5% SF Samples with 0-7-28 Days of Curing 150

Figure B.3 Axial Compressive Stress vs Axial Strain Relationships for 3% L + 10% SF Samples with 0-7-28 Days of Curing 151
Figure B.4 Axial Compressive Stress vs Axial Strain Relationships for 3% L + 15% SF Samples with 0-7-28 Days of Curing 152
Figure B.5 Axial Compressive Stress vs Axial Strain Relationships for 3% L + 20% SF Samples with 0-7-28 Days of Curing 153
Figure B.6 Axial Compressive Stress vs Axial Strain Relationships for 5% L Samples with 0-7-28 Days of Curing 154
Figure B.7 Axial Compressive Stress vs Axial Strain Relationships for 5% L + 5% SF Samples with 0-7-28 Days of Curing 155
Figure B.8 Axial Compressive Stress vs Axial Strain Relationships for 5% L + 10% SF Samples with 0-7-28 Days of Curing 156
Figure B.9 Axial Compressive Stress vs Axial Strain Relationships for 5% L + 15% SF Samples with 0-7-28 Days of Curing 157
Figure B.10 Axial Compressive Stress vs Axial Strain Relationships for 5% L + 20% SF Samples with 0-7-28 Days of Curing 158
Figure C.1 Swell Rate vs Percent Additive Graph of All Samples with 0-7-28 Days of Curing 160
Figure D.1 Net Swell Percentages vs. Percent Additive of Treated 162
Figure D.2 Stabilization Percent in Net Swell Vs Percent Additive Graph of All Treated Samples 163

LIST OF ABBREVIATIONS

ABBREVIATIONS

ACI	: American Concrete Institute
B	: Width of Foundation
CAH	: Calcium Alumina Hydrate
CBA	: Composite Binary Admixture
CBR	: California Bearing Ratio
CEC	: Cation Exchange Capacity
CH	: High Plasticity Clay
CL	: Low Plasticity Clay
CSF	: Combination of Cement and Silica Fume
CSH	: Calcium Silica Hydrate
DDL	: Diffuse Double Layer
FSI	: Free Swell Index
FT-IR	: Fourier Transform Infrared
L	: Lime
LSF	: Lime-Silica Fume
LL	: Liquid Limit
MDD	: Maximum Dry Density
OMC	: Optimum Moisture Content
OWC	: Optimum Water Content

PI : Plasticity Index

PL : Plastic Limit

SEM : Scanning Electron Microscopy

SF : Silica Fume

TEM : Transmission Electron Microscope

UCS : Unconfined Compressive Strength

WS : Wheat Straw

XRD : X-Ray Diffraction

LIST OF SYMBOLS

SYMBOLS

Å	: Angstrom
A_c	: Activity of Clay
c	: Cohesion
C_c	: Compression Index
C_r	: Recompression Index
f	: Flexural Strength
Gs	: Specific Gravity
H_i	: Initial Height of the Sample
H_f	: Final Height of the Sample
m	: Mass of the Sample
ρ	: Density of the Sample
$\rho_{dry,max}$	: Maximum Dry Density Values
V_1	: First Read Volume
V_2	: Last Read Volume
w_{opt}	: Optimum Water Content

CHAPTER 1

INTRODUCTION

The issue of expansive soils is a global concern that presents numerous problems for professionals in the field of civil engineering. They pose a risk of natural disaster and may result in considerable damage to structures if not adequately addressed. This type of soil swells when exposed to water and shrinks when it dries out (Al-Rawas et al., 2002). Moisture infiltration can occur due to various factors, such as excessive rainfall leading to flooding, water leakage from pipes or sewer lines, or a decrease in surface evapotranspiration caused by the presence of buildings or pavement (Çokça, 2001).

There have been reports of expansive soils in a variety of areas of the world, most commonly in the arid or semi-arid regions of the tropical and moderate climate zones like Africa, Australia, China, the Middle East (such as Israel, Egypt), India, South America, the United States, and some regions in Canada (Mishra et al., 2008; Murthy, 2002; Nelson & Miller, 1992). Moreover, it should be noted that expansive soils are present in certain areas of Turkey, specifically within the Central Anatolia, West Anatolia, Southeast Anatolia, and East Anatolia regions (Çokça, 2001). Ankara, the capital of Turkey, is placed in the Central Anatolia region. A certain amount of urban settlement has been built on soil deposits with expansive characteristics (Erguler & Ulusay, 2003).

The issue of swelling soil was initially noticed and documented by the U.S. Bureau of Reclamation in 1938. This phenomenon occurred during the construction of a foundation for a steel siphon at the Owyhee Project in Oregon, as (Chen, 1988) reported. The occurrence of expansive soil consisting areas and the issues related to soil heaving have been documented across six continents and in over 40 countries globally (Nelson et al., 2015). The worldwide spread of reported expansive soil

locations is shown in Figure 1.1. The statements mentioned above do not imply the absence of expansive soils in other regions, as they are prevalent in nearly all geographical areas. Nevertheless, it should be noted that in regions with high humidity, water tables tend to be located close to the surface, and the variations in moisture content that lead to changes in soil volume are typically insignificant, except during long-lasting periods of drought (Arnold, 1984; Charlie et al., 1984; Mishra et al., 2008; Shuai & Fredlund, 1998).

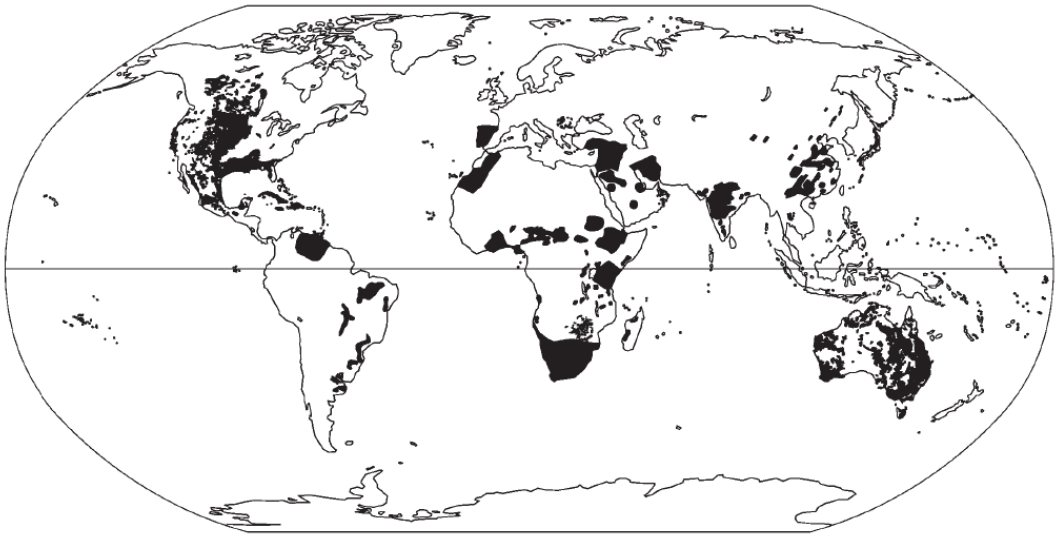

Figure 1.1 Global distribution of reported expansive soil sites (Nelson et al., 2015)

In regions characterized by aridity and semi-aridity, there is significant variation in water content and rainfall quantities across various seasons. Consequently, structures such as small buildings and highways built on expansive soils experience periodic cycles of swelling and shrinkage (Basma et al., 1996). Cracks and fractures occur as a result of the volumetric expansion of expansive clays in various infrastructure elements such as roads, pavements, foundations of structures, sprinkler systems, slab-on-grade members, channel and reservoir linings, sewage lines, and water lines (Çokça, 2001). While the adverse effects relating to this soil do not result in the loss of human life, they do give rise to significant financial implications as a consequence of the soil damage. This soil is referred to as a "hidden disaster" because of this (Snethen, 1986).

The yearly expense attributed to the swelling and shrinking of expansive soils is estimated to be several million euros (Chindris et al., 2017). According to Nelson & Miller (1992) ,the recorded annual losses in the United States resulting from expansive soils reached $798.1 million in 1970, with a projected increase to $997.1 million by the year 2000. The aforementioned values are related exclusively to losses paid for in residential buildings. A factor of 2 to 3 increases the predicted values due to the expense of destroying additional structures, including commercial/industrial buildings and transportation facilities (Nelson & Miller, 1992). The projected yearly expense of damage to facilities and infrastructures resulting from the presence of these sorts of soil is approximately £150 million in the United Kingdom, $1000 million in the United States, $1000 million in China, and several billions of dollars globally (Qi & Vanapalli, 2015; Shi et al., 2002).

There exist various soil stabilization techniques that can be used to stabilize expansive clay soils. The methods utilized involve the application of chemical additives, rewetting, soil replacement, compaction control, moisture control, surcharge loading, and thermal methods (Chen, 1988; Nelson & Miller, 1992). Soil modification through the process of stabilization using various substances has been a subject of consideration for numerous centuries (Baghdadi et al., 1995).

Lime, a calcium-based stabilizer, is commonly utilized in civil engineering projects, such as pavements and foundations, to enhance the convertible shrink-swell characteristics of expansive clays (Puppala, 2016). Nevertheless, lime production raises notable concerns due to its elevated consumption of energy (4000 MJ/tonne) and the subsequent release of greater quantities of carbon dioxide emissions (800 Kg/tonne to get L) into the atmosphere (Oti et al., 2009). In addition, it should be noted that lime exhibits restricted efficacy when exposed to sulfate, leading to significant heaving issues caused by the nucleation and development of ettringite (Aldaood et al., 2014; Ebailila et al., 2022). This phenomenon arises from the reaction process between sulfate, calcium, and alumina in the appearance of water, resulting in the formation of ettringite (Nidzam & Kinuthia, 2010). Within this

particular context, combining industrial byproducts alongside lime and silica fume has been promoted.

Silica fume is a fine solid particle generated during the production of silicon metal, as stated by Kumar Verma et al., (2020). The material that possesses a low unit weight, low compactibility, and high pozzolanic activity is extensively utilized to enhance problematic soils (Goodarzi et al., 2015). The global yearly silica fume production is approximately 1 million tons. Of the overall quantity, 130,000 tons are manufactured within the United States, while Norway contributes 120,000 tons to the total production. Thirteen factories in North America manufacture silicon, silica fume, and ferrosilicon (Türköz et al., 2021).

Additionally, the Eti Elektrometalurji A. facilities in Antalya constitute the source for silica fume production in Turkey. The total annual production quantities of ferrosilicon and silicoferrochrome flue dusts range between 1,000 and 2,000 tons. The silica fume derived from this facility has been utilized as an additive for cement and concrete in numerous academic studies, particularly within universities, starting from the end of the 1980s (Yeginobalı, 2011). Therefore, suitable disposal of SF, regarded as industrial waste, represents a significant concern for environmental specialists due to the potential for harmful effects on health if it is directly released into the environment (Zhang et al., 2016). Therefore, incorporating waste materials, such as SF, in various civil engineering applications presents a notable benefit from an environmental perspective (Türköz et al., 2021).

Numerous investigations have been undertaken to evaluate the efficacy of SF as a soil stabilizer, both in isolation and in combination with other additives. The findings consistently demonstrate the beneficial influence of SF on geotechnical properties (Goodarzi et al., 2016; Kalantari et al., 2011; Kalkan, 2011, 2013; Kalkan & Akbulut, 2004; Phanikumar et al., 2020; Qing et al., 2020). Pozzolans, including natural pozzolana (known as pozzolanic ash), silica fume (derived from silicon smelting), fly ash, rice husk ash, volatile ash, and other similar substances, constitute a diverse group of materials characterized by their siliceous or siliceous and aluminous

composition. Nevertheless, when considered independently, their cementitious properties are minimal or nonexistent (Chung D., 2017). Furthermore, it has been observed that the combination of silica fume and lime demonstrates greater effectiveness compared to their individual use. The addition of lime significantly enhances the effectiveness of stabilization. Several studies (Abd El-Aziz et al., 2004; Alrubaye et al., 2017; Fattah et al., 2015b) have reported that the combined use of additives has led to enhancements in the swell and dispersive characteristics of problematic soils. Additionally, these studies have found significant improvements in shear strength parameters and workability.

1.1 Objective of the Study

The objective of this study was to evaluate the efficacy of adding silica fume, in conjunction with lime, for enhancing the geotechnical characteristics of expansive clay soils. The assessment was conducted by applying direct measurements through the utilization of macrostructure tests. Additionally, the main goal of this study was a combination of two objectives: to mitigate or eliminate the restrictions associated with lime treatment and to generate reliable experimental proof regarding the utilization of silica fume as a means of minimizing economic and environmental costs.

1.2 Scope of the Study

The research began by preparing the expansive soil in the laboratory by mixing kaolinite and bentonite. Then, the artificial expansive soil sample was mixed with 3% to 5% and varying proportions of silica fume (0%, 5%, 10%, 15%, 20%). The sieve analysis, specific gravity, consistency limit, and compaction tests are done to identify and classify soil samples. Free swell and unconfined compression tests were then performed to evaluate swelling and strength properties. Free swell and

unconfined compression tests were conducted for different curing periods (such as no-cure, 7 to 28 days of curing).

CHAPTER 2

LITERATURE REVIEW

2.1 Expansive Soil

Although the swelling issue is connected to clay water absorption, it is not guaranteed that all clays will expand with water (Foster & Survey, 1955). Chemical treatment approaches provided in the literature for stabilizer selection rely on consistency limits characteristics, soil type, and the dimensions of the particles (Hausmann, 1990). However, using an identical chemical additive and quantity to stabilize soils with similar plasticity qualities does not guarantee that their engineering behavior would be alike. The differences in treated soil behavior can be attributed to the natural mineralogical composition of the soils along with the chemical interactions between chemical additions and clay particulates. Accordingly, considering clay mineralogy, as well as other soil parameters such as grain size classification and consistency limits, throughout the treatment design process is essential (Chittoori, 2009).

To truly comprehend the engineering behavior of fine-grained soils, clay mineralogy needs to be investigated first (Yongshan et al., 2002).

2.1.1 Clay Mineralogy

Clay may be characterized by the dimensions and kinds of minerals it contains. In engineering classifications, *clay* is defined as soil components smaller than a specific size, commonly 0.002 mm (2 um). Clay, as a mineral terminology, refers to certain clay minerals that are individuated (Mitchell & Soga, 2005):

1. Having small particle sizes,

2. Having a net negative electrical charge,
3. Having plasticity when mixed with water,
4. Having resistance to high weathering.

The majority of clay mineral particles have a 'plate-like' shape, which provides them with a high specific surface (which refers to a high ratio of surface area to total mass). As a consequence of these factors, the structure of clay mineral particles is considerably affected by surface forces. There is also the possibility of 'needle-shaped' particles being present; however, these are rather uncommon (Knappett & Craig, 2012).

Clay minerals consist of an octahedral sheet and a tetrahedral sheet as their fundamental atomic skeletons. The silica tetrahedral layer is the second structural unit and consists of four oxygen atoms or potentially hydroxyls grouped in a tetrahedral shape around a silicon atom. The silica tetrahedral sheet (Fig. 2.2) is made up of an endless number of tetrahedrons mounted in a hexagonal network along two horizontal axes. The octahedral sheet (Figure 2.3) is composed of tightly arranged oxygens and hydroxyls in which aluminum, iron, and magnesium atoms are placed octahedrally (Murray, 2006).

Both components are negatively charged due to valency mismatches. Therefore, the building blocks are never found alone but always in the context of larger sheet formations. A silica sheet is formed when tetrahedral units share oxygen ions. A gibbsite sheet is formed when octahedral units share hydroxyl ions. In contrast to the gibbsite sheet, which is electrically neutral, the silica sheet preserves a net negative charge. Isomorphous substitution, in which elements other than silicon and aluminum are substituted at a molecular level, can lead to an increased charge misbalance (Knappett & Craig, 2012).

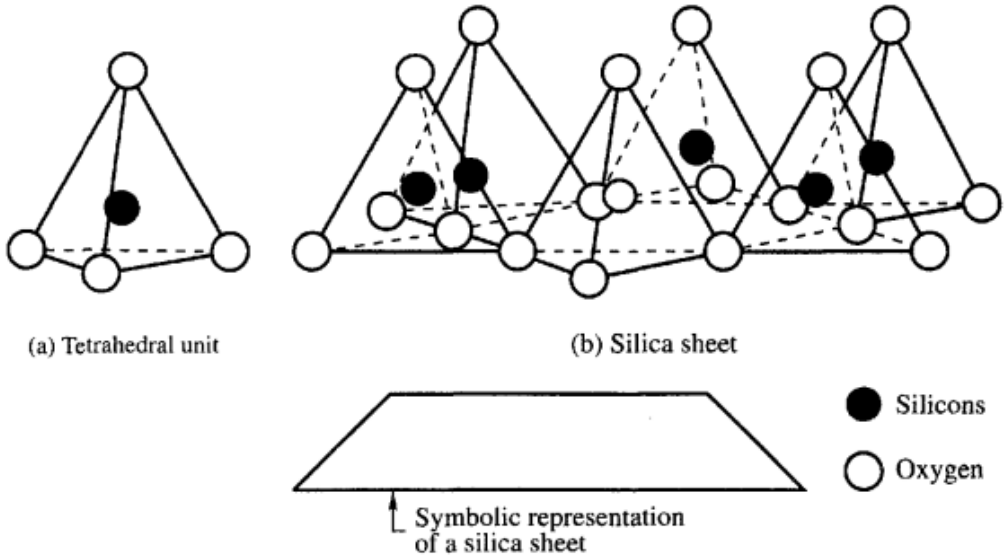

Figure 2.1 Basic Structural Units in the Silicon Sheet (Murthy, 2002)

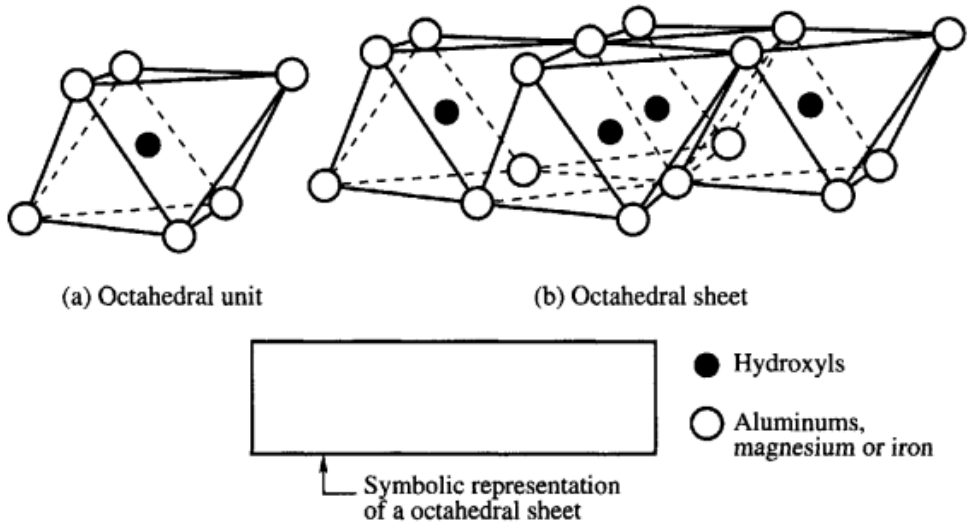

Figure 2.2 Basic Structural Units in the Octahedral Sheet (Murthy, 2002)

In Fig. 2.3, it can be seen how the various clay mineral types are built up from the assembly of atoms into tetrahedral and octahedral units, the subsequent production of sheets, and the stacking of these sheets to form layers (Mitchell & Soga, 2005).

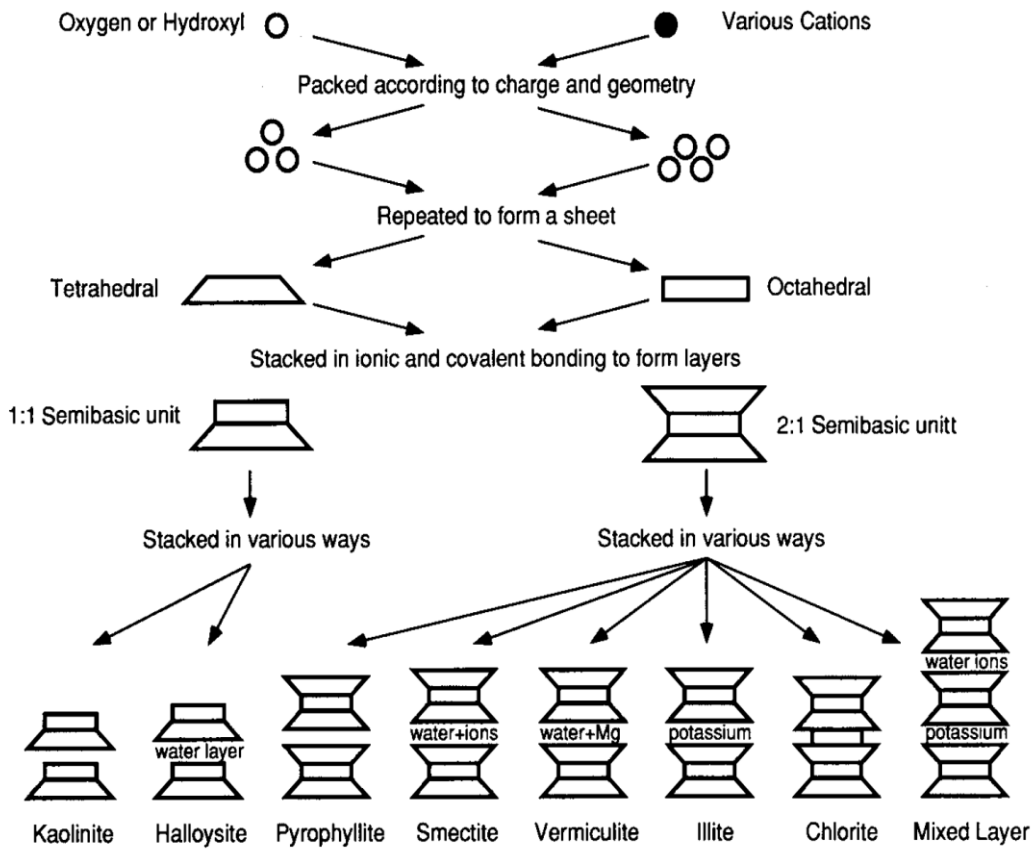

Figure 2.3 Synthesis pattern for the clay minerals (Mitchell & Soga, 2005)

For engineering purposes, three essential structural categories of clay minerals are described as follows (Nelson & Miller, 1992):

- The Kaolinite group is usually not expansive.
- The Mica-like group comprises illites and vermiculites, which can be expansive but do not typically cause major challenges.
- The Smectite group contains montmorillonites, one of the most expansive and problematic clay minerals.

2.1.1.1 Kaolinite Group

The clay mineral kaolinite is formed by a 1:1 semi-basic unit ratio (Barton & Karathanasis, 2002). A single tetrahedral sheet and a single alumina octahedral sheet

are joined in units so that the edges of the silica tetrahedrons and one of the layers of the octahedral sheet create an interconnected layer (Figure 2.4). All silica tetrahedrons point toward the center of the unit composed of silica and octahedral sheets. The silica gibbsite sheets are attached by strong ionic bonds, and the layers are stacked and hydrogen-bonded to create kaolinite (Figure 2.5). Kaolinite crystals have several sheet stackings that are hard to separate due to hydrogen bonding (Murray, 2006). According to Mitchell & Soga, (2005), the bonding is strong enough that there is no swelling of the interlayers when water is in existence.

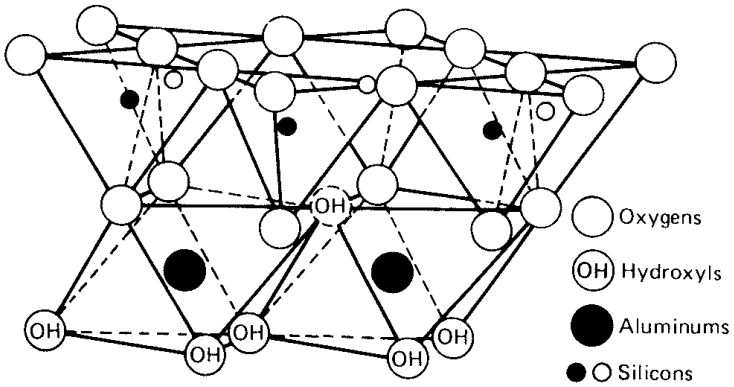

Figure 2.4 Diagrammatic sketch of the kaolinite structure (Mitchell & Soga, 2005)

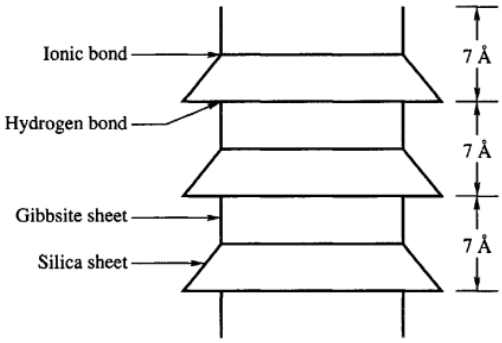

Figure 2.5 Structure of kaolinite layer (Murthy, 2002)

2.1.1.2 Mica-Like Group

2.1.1.2.1 Illite

Illite is a kind of clay mineral mica that was given its name by Grim, (1942). Illite can be thought of as a simplified potassium smectite (Figure 2.6), as its structure is a 2:1 layer with potassium as the interlayer cation. According to Murthy, (2002), the bonds formed with the nonexchangeable K^+ ions are weaker than the hydrogen bonds but stronger than the water bond formed in smectites (Figure 2.7). In contrast to smectites, illite does not swell much when in contact with water. Also, compared to kaolinite, illite displays a medium swell potential and greater activity (Oweis & Khera, 1998).

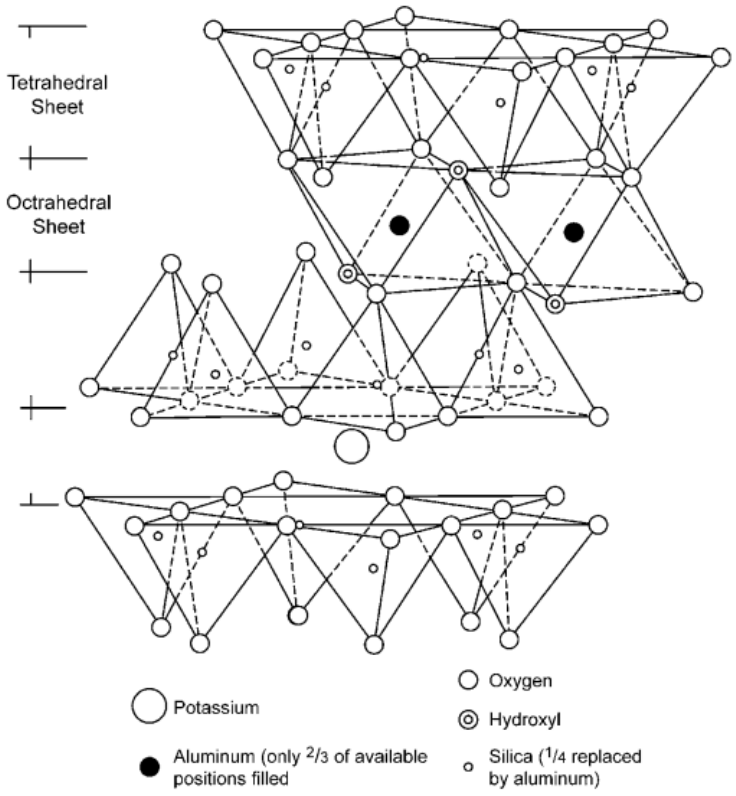

Figure 2.6 Diagrammatic sketch of the structure of illite (Murray, 2006)

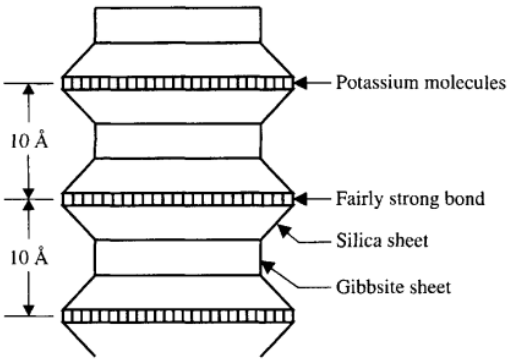

Figure 2.7 Structure of Illite Layer (Murthy, 2002)

2.1.1.3 Smectite Group

According to Murray, (2006), the main components of smectite are the montmorillonites of sodium, calcium, magnesium, iron, lithium, and aluminum, and calcium montmorillonite is the kind of smectite mineral that is most commonly found. Compared to calcium montmorillonite, sodium montmorillonite has a higher water absorption capacity and lower hydraulic conductivity (Grim, 1942).

2.1.1.3.1 Montmorillonite

Layers similar to those found in micas are also observed in montmorillonite minerals (Yong & Warkentin, 1975). Gibbsite sheets have magnesium and iron partially substituting for aluminum, whereas silica sheets have aluminum partially replacing silicon (Figure 2.8). An extremely weak bond is the consequence of water molecules and exchangeable cations other than potassium filling the gap between the combined sheets (Figure 2.9). Additional water can be adsorbed between the combined sheets of montmorillonite, resulting in significant enlargement of the mineral and any sediment containing it (Knappett & Craig, 2012).

High activity and a high liquid limit are both characteristics of montmorillonite clays (Yong & Warkentin, 1975). High swelling and shrinkage properties might be

expected from soils rich in montmorillonite minerals. Bentonite is a kind of clay that is classified as montmorillonite (Murthy, 2002).

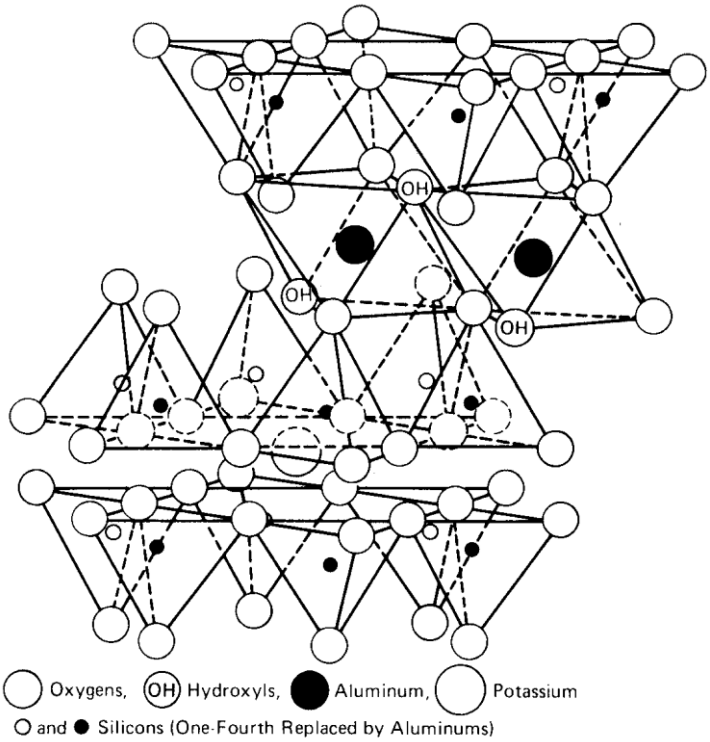

Figure 2.8 Diagrammatic sketch of the montmorillonite structure (Mitchell & Soga, 2005)

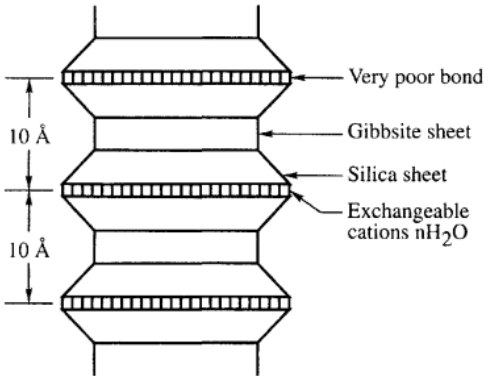

Figure 2.9 Structure of montmorillonite Layer (Murthy, 2002)

Figure 2.10 displays the scanning electron micrographs of these various sorts of minerals.

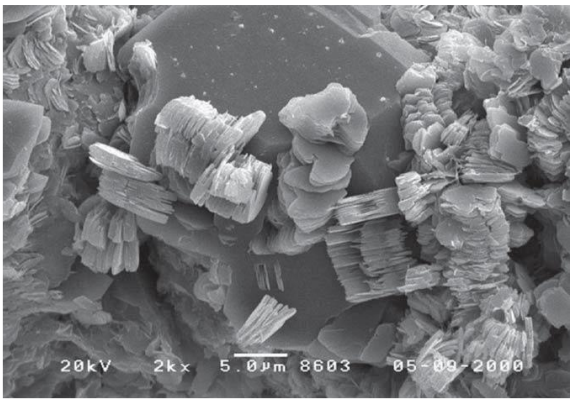

a) Kaolinite

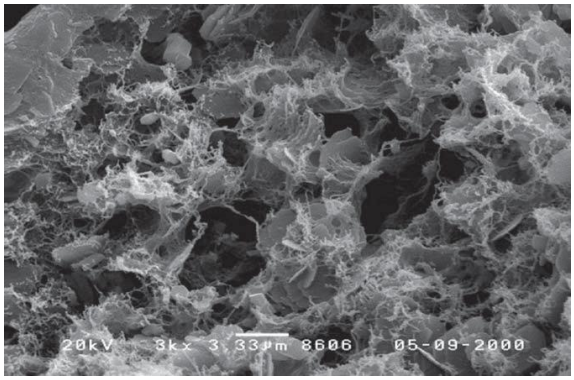

b) Illite

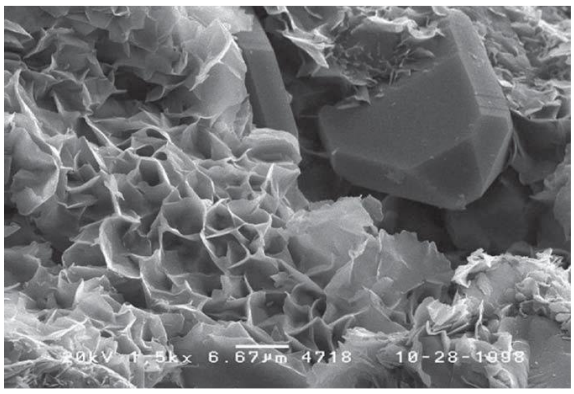

c) Montmorillonite

Figure 2.10 Scanning electron micrographs of clay minerals (Nelson et al., 2015)

In Table 2.1, a summary of the key clay minerals' particle characteristics, as well as their properties, can be found.

Table 2.1 Some important properties of key clay minerals (Nelson & Miller, 1992)

Mineral Group	Basal Spacing (Å)	Interlater Bonding	Specific Surface (m^2/g)	Atterberg Limits			Activity (PI / %Clay)
				LL (%)	PL (%)	SI (%)	
Kaolinites	14.4	Strong hydrogen bonds	10-20	30-100	25-40	25-29	0.33-0.46
Illites	10	Strong potassium bonds	65-100	60-120	35-60	15-17	0.9
Montmorillonites	9.6	Very weak van der Waals bonds	700-840	100-900	50-100	8.5-15	1.5-7.2

2.2 Adsorbed Cations and Cation Hydration

Clay particles have positively charged cations (such as sodium, calcium, magnesium, and potassium) in their surroundings, which helps to neutralize the negative charges that are present on their surfaces. In relation to this, massive quantities of water can accumulate between clay minerals due to the hydration of cations and the absorptive forces generated by the clay crystals themselves (Nelson et al., 2015; Nelson & Miller, 1992). The clay soil's behavior will depend on the types of cations present. Cation hydration's effect on soil expansion is illustrated in Figure 2.11.

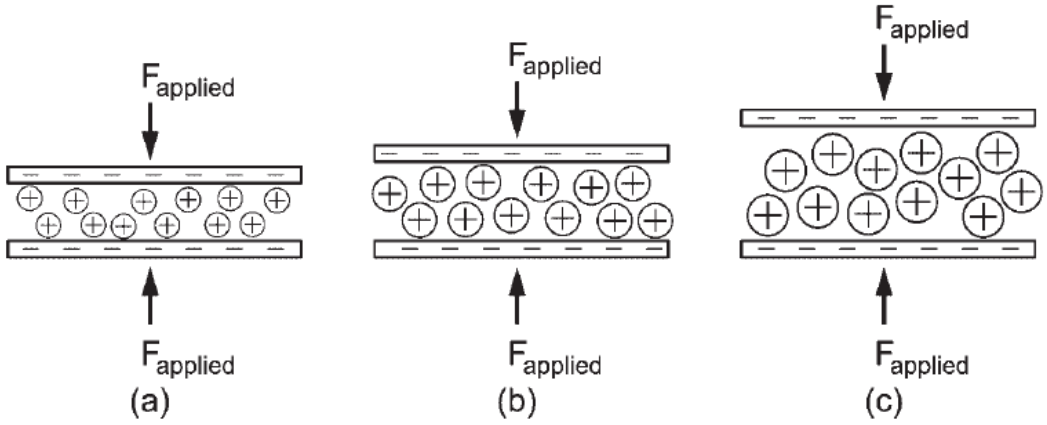

Figure 2.11 Role of cation hydration on soil expansion: (a) low hydration; (b) partial hydration; (c) full hydration. (Nelson et al., 2015)

A soil's cations can be found in a variety of various phases depending on the condition of the soil. In air-dried soils, massive electrostatic forces keep the cations nearby the clay mineral surfaces. When water is present, cation hydration energy increase to a point where they are substantial enough to counteract the forces of interparticle attraction. Therefore, water-adsorbed cations hydrate and expand, forcing dry and closely stuffed particles apart. When a considerable quantity of water is available, the adhesion of cations to clay surfaces is weakened. The attraction caused by electrostatic forces is mitigated by the ions' proneness to migrate towards the less concentrated surrounding solution, thereby moving far from the surfaces of the particles.

2.3 Clay Micelle

In order to examine the characteristics of clay, it is essential to take into account three fundamental constituents, namely the clay mineral component, the cations present, and the accompanying water. To comprehensively examine these three components as an integrated body, it is beneficial to introduce the notion of a clay micelle (Nelson et al., 2015). Figure 2.12 illustrates the representation of a clay micelle. The micelle is formed by the combination of clay particles, cations, the water of hydration, and osmotic water, which is tightly bound to the inner mineral core (Lambe, 1958).

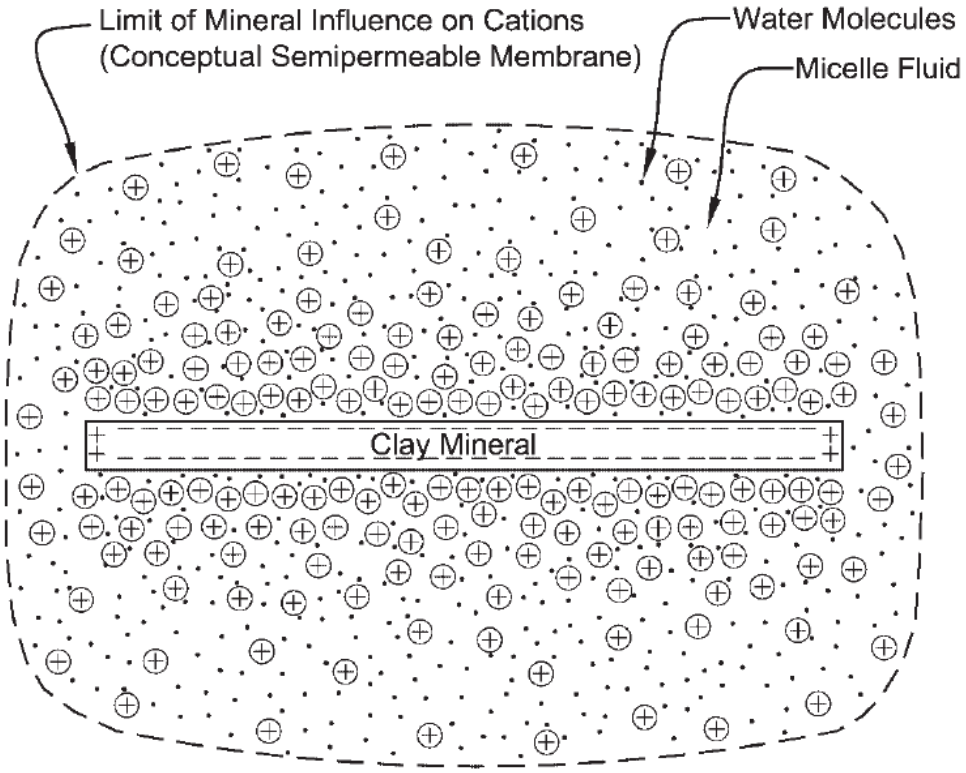

Figure 2.12 A clay micelle showing the concentration of cations near the surface of a clay particle. (Nelson et al., 2015)

The nature of the micelles of different minerals influences soil behavior and its expansive characteristics (Nelson et al., 2015).

In the absence of adsorbed cations, the electrical charges on the surfaces of the clay particles result in the emergence of repulsive forces among the particles at the individual level. The cations present in the micelle form strong adsorption bonds with the surface of the clay mineral, effectively counterbalancing the electrical surface forces. The magnitude of surface forces is highest in close range to the surface of the clay particle and reduces as the distance from the particle increases. The cations that exist in the solution nearest to the clay mineral will experience more substantial restrictions on their ability to migrate away due to the surface forces acting upon them. The observed outcome is the presence of a cation concentration gradient, which exhibits its highest values in nearby to the surface and gradually diminishes as the distance from the surfaces increases, as depicted in Figure 2.12.

At distances significantly far from the clay mineral's surface, the influence of surface forces becomes insignificant, resulting in the cation concentration being equivalent to that found in the unbound water within the soil. In Figure 2.12, such distance is represented by the outside dashed line which is called a conceptual semipermeable membrane in the figure. The dashed line depicted in Figure 2.12 does not indicate an exact and definitive measurement of length but rather indicates a lowering effect from the mineral's surface. Based on the proposed model, the micelle can be characterized as a separate body containing a single clay mineral encircled by a water-based solution. The term "micelle fluid" refers to the water-based solution which is presented in the micelle (Nelson et al., 2015).

The dimensions of the water-based surroundings with the presence of cations within the micelle, commonly referred to as the micelle fluid. On the other hand, it can also be named as diffuse double layer in the proposed theories of Gouy (1910) and Chapman (1913) (Mitchell & Soga, 2005). The thickness of it is predominantly determined by the characteristics of the absorbed cations and the electrical charges present on the clay mineral. The thickness of the micelle fluid in two distinct minerals, which share the same adsorbed cations, is primarily determined by the several exterior structural units. Conversely, the general dimension of the particles has minimal impact on the micelle fluid thickness (Nelson et al., 2015).

Lambe, (1958) reports 200Å micelle fluid thickness for montmorillonite and 400Å for kaolinite. Since kaolinite particles are around 100 times thicker than montmorillonite particles, the ratio of micelle fluid to mineral thickness is about 50 times larger in montmorillonite.

2.4 Diffuse Double Layer

The surface of the clay particle carries a negative charge, while the surrounding solution contains a concentration of positive ions. This combination gives rise to a phenomenon known as a diffuse double layer (DDL), as Bohn et al., (1985) described. The combination of the charged surface and the spreading charge in the neighboring phase is commonly referred to as the diffuse double layer (Nelson & Miller, 1992). The phenomenon in which water molecules with electrical charges are drawn towards the clay particle is called the diffused double layer of water (Murthy, 2002). In addition, a diffuse double layer could be named as diffuse double layer between charged clay surface and the limit on mineral influence on cations explained in the clay micelle section.

The occurrence of concurrent DDLs (Diffuse Double Layers) among clay particles results in the emergence of interparticle repulsive forces, commonly referred to as microscale "swelling pressures." The relationship between the diffuse double layer (DDL) and the swelling potential increases with an increase in the thickness of the DDL. The determination of the thickness of the DDL is influenced by various factors, such as the concentration and valence of the cations present in the water of the soil (Nelson & Miller, 1992). Typically, a higher thickness of the diffusion double layer (DDL) and increased swelling are correlated with reduced cation concentrations and/or the existence of cations exhibiting lower valence (Mitchell, 1976). Therefore, in the case of identical soil structure, a greater degree of swelling would be observed in a sample containing exchangeable sodium (Na^{+}) cations compared to a sample containing calcium (Ca^{2+}) or magnesium (Mg^{2+}) cations.

A decrease in cation concentration, as mentioned by Mitchell & Soga (2005), has been linked to an increase in the thickness of the diffuse double layer and swell potential. The presence of concentrated cations in close proximity to the surface of clay particles gives rise to the repulsive force observed in double-layered systems. Temperature is an additional factor that impacts the thickness of the DDL. A rise in temperature results in an augmentation of the thickness of the diffusion double layer.

2.5 Cation Exchange Capacity

In order to maintain electrical balance, positively charged cations are drawn towards and retained within the interlayers, as well as on the mineral surfaces and edges of the clay particles. A significant proportion of these cations exhibit exchangeability as they have the potential to be substituted by cations of different kinds. There exists variation in the strength of attraction among different types, and it is possible to sort cations into a series based on their respective interactions for attraction, outlined as $Al^{3+} > Ca^{2+} > Mg^{2+} > NH_4^+ > K^+ > Na^+ > Li^+$ by Das (2016).

This series demonstrates that Al^{3+} ions have the ability to substitute Ca^{2+} ions, while Ca^{2+} ions have the capacity to substitute Na^+ ions. The procedure mentioned above is commonly referred to as cation exchange. The term used to describe the amount of exchangeable cations is known as the cation exchange capacity (CEC), which is typically measured in milliequivalents $(meq)^3$ per 100 g of dry clay (Mitchell & Soga, 2005).

2.6 Clay Structure

Nearby clay mineral particles experience both repulsive and attractive forces. The phenomenon of repulsion arises due to the presence of comparable charges within the double layers, with the magnitude of the repulsive force being based on the specific properties of these layers. An augmentation in the valency or quantity of cations will lead to a reduction in the repulsive force. Conversely, a decrease in the

valency or concentration of cations will end in A rise in the repulsive force. The interaction between particles is primarily governed by relatively short-range van der Waals forces, which diminish significantly as the spacing between particles increases. The structural morphology of clay minerals during accumulation is influenced by the net inter-particle forces. This situation allows us to classify clay particle formations as either dispersed (produced by a repulsive net particle force) or flocculated (created by an attracting net particle force). The structures depicted in Figures 2.13 (a) and (b) exemplify the interplay among individual clay mineral particles (Knappett & Craig, 2012).

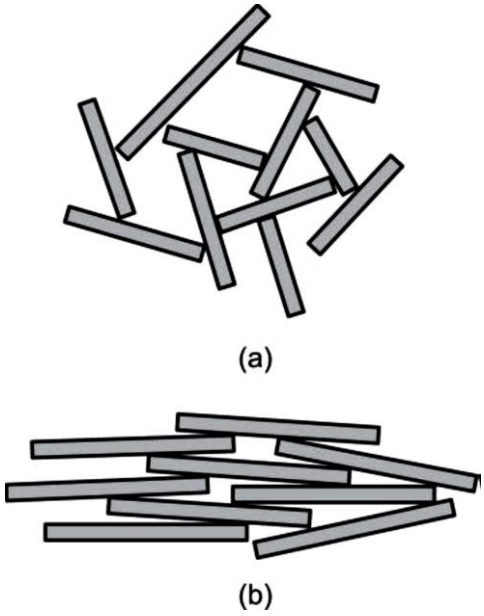

Figure 2.13 Sediment structures: (a) “flocculated” or “random” orientation; (b) “dispersed” or “oriented” (Nelson et al., 2015)

2.7 Swelling Mechanism

There are two different approaches in the literature for explaining the swelling mechanism.

2.7.1 Crystalline and Osmotic Expansion Approach

The model of expansion potential presented in Figure 2.11 is related to the hydration of the adsorbed cations and the osmotic attraction of water into the micelle. This concept helps to explain the nature of swelling in expansive soil (Nelson et al., 2015). Because the energy of hydration is high, the first water that is introduced into a dry soil goes into hydrating the cations. Subsequently, added water goes into satisfying the osmotic forces. Thus, in simple terms, the initial phase of swelling is "crystalline" and due to hydration of the cations as previously described (Slade et al., 1991). After that phase, the concentration of cations between the soil particles causes water to be drawn into the interparticle spacing due to osmotic forces. This second phase of swelling is termed osmotic.

It is unlikely that the two phases of swelling are clearly distinct, and there likely exists a transition zone between the crystalline and osmotic phases.

The process of desiccation in wet soil can result in the reduction of a significant portion of the osmotic water as well as certain amounts of the crystalline water. As a result of this phenomenon, the micelles will undergo a reduction in dimensions, leading to much closer proximity of the constituent particles. Therefore, it is possible for expansive soils to experience a reduction in volume as the water amount drops. Due to this explanation, those particular types of soils are commonly denoted as shrink-swell soils. In natural circumstances, it is highly probable that the shrinkage stage in soil mainly includes the initial extraction of osmotic water. Desiccation of the soil by heat, such as sun-baking or drying in the laboratory, begins to remove more of the water of hydration (Nelson et al., 2015).

2.7.2 Interparticle or Intercrystalline

According to Popescu (1986), the swelling phenomenon has two primary mechanisms:

Interparticle or intercrystalline swelling is a phenomenon that can be observed in various types of clays. In a situation of near dryness, the particles of clay are closely bound together due to capillary tensions. Upon the addition of water to the clay, the intermolecular forces within the clay matrix undergo relief, resulting in the spreading of particles away from neighboring particles (Figure 2.14). The short perpendicular lines depicted in Figure 2.14 symbolize the firm molecular bonds existing between the layers.

The phenomenon of intracrystalline swelling is primarily observed in minerals belonging to the montmorillonite group. The constituent single crystals of montmorillonite are held together by relatively weak interlayer bonds, primarily facilitated by water molecules in conjunction with exchangeable cations. During the process of wetting, water permeates not only the interstices between the individual crystals but also the interlayers within the crystals themselves (Figure 2.14) (Popescu, 1986).

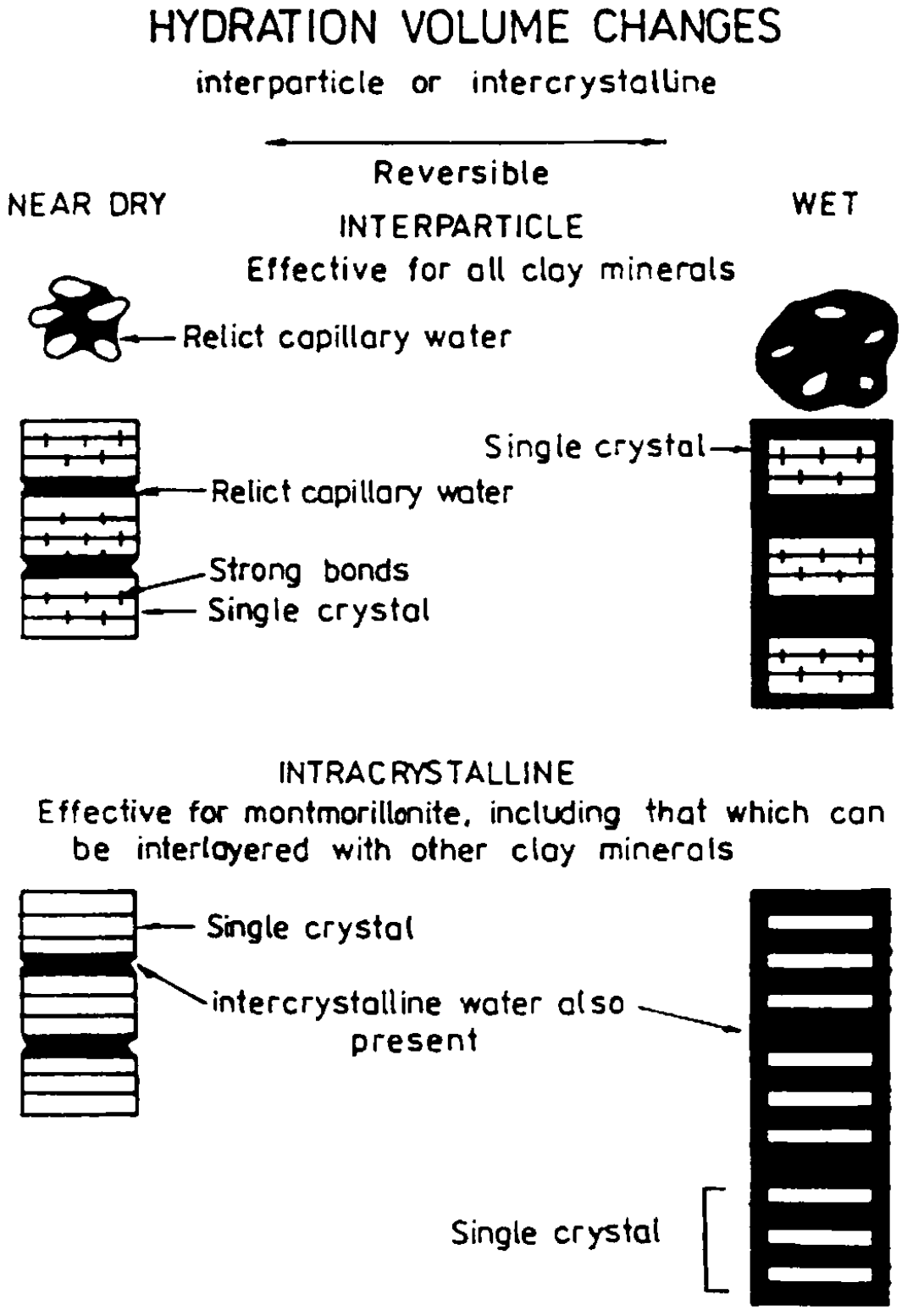

Figure 2.14 Mechanism of swelling proposed by (Popescu, 1986)

2.8 Factors Effecting Swelling

Numerous factors that have an influence on the mechanism of swelling are also complexly associated with, or subject to, the physical properties of soil, such as plasticity or density. The shrink-swell potential of soil is influenced by various factors, which can be categorized into three separate categories (Nelson & Miller, 1992):

- There are soil characteristics that affect the fundamental nature of the internal force field. These characteristics play a crucial role in determining the soil's tendency for shrinkage and swelling.
- Environmental factors step in, influencing the changes that may happen within the internal force system. These external conditions can significantly impact the soil's shrink-swell behavior.
- The state of stress experienced by the soil also contributes to its shrink-swell potential.

By considering these three distinct categories of factors, a comprehensive understanding of soil behavior can be obtained. Tables 2.2, 2.3, and 2.4 provide a comprehensive overview of the various soil and environmental factors that have an influence on the phenomenon of swell and shrink behavior.

Table 2.2 Factors affecting the soil's ability to shrink and swell (Nelson & Miller, 1992)

FACTOR	DESCRIPTION
Clay Mineralogy	The alterations in the volume of soil caused by clay minerals are frequently ascribed to the existence of montmorillonites, vermiculites, and specific mixed-layer minerals. The nonexpansive attitude of illites and kaolinites are widely recognized. However, their particle diameters are extremely small, on the order of a few tenths of a micron or less, and they have the capacity to generate volume changes under certain conditions.
Soil Water Chemistry	The phenomenon of swelling can be mitigated through the augmentation of cation concentration and the amplification of cation valence. An instance of reduced swelling can be observed when Mg^{2+} cations are present in the soil water, as compared to Na^{+} cations.
Soil Suction	Unsaturated soils exhibit a pore pressure that is characterized by a negative value, which can be conceptualized as the manifestation of a self-governing and influential stress parameter referred to as soil suction. The phenomena known as soil suction is subject to the influence of multiple factors, encompassing the saturation level, gravitational force, characteristics of soil pores in terms of size and shape, tension at the surface, and both the electrical and chemical characteristics associated with the soil particles and water content. As the degree of suction grows, there will be an associated augmentation in the swelling potential.
Plasticity	Plasticity is useful as a reliable sign of the soil's capacity to experience volumetric expansion in response to moisture exposure. Soils exhibiting plastic characteristics over a wide range of water content and possessing higher liquid limits tend to display an increased propensity for undergoing swelling and shrinkage.
Soil Structure and Fabric	Clays which are exhibiting flocculated structures typically demonstrate a higher degree of expansion in comparison to clays displaying dispersed structures. The presence of cemented particles has been found to decrease soil swelling. The compaction process at high water content or through remolding leads to modifications in the fabric and structure. Compared to soils statically compacted at lower water contents, kneading-compacted materials have been shown to produce more dispersed structures with less swelling potential.
Dry Density	Increased densities typically provide a reduced distance between particles, which in turn shows the development of stronger repulsive forces among the particles and a higher likelihood of serious swelling.

Table 2.3 Stress State Factors affecting the shrink-swell behavior (Nelson & Miller, 1992)

FACTOR	DESCRIPTION
Initial Moisture Content	A dried expansive soil exhibits a greater attraction to water, or a higher level of suction, compared to the same soil with a higher water content and lower suction. On the other hand, a soil profile that is saturated with water will experience a higher rate of water loss when subjected to drying conditions and will undergo greater shrinkage compared to a soil profile that is initially relatively dry. The assessment of the initial phase soil suction should be undertaken together with the anticipated range of final suction conditions.
Moisture Variations	Heave is primarily determined by fluctuations in water within the active zone near the top portion of the profile. It is within these layers that the most significant variations in moisture content and corresponding volume changes are expected to take place.
Climate	The quantity and diversity of precipitation and evapotranspiration significantly impact the availability of water and the extent of seasonal moisture fluctuations. The phenomenon of greatest seasonal heave is observed in semi-arid environmental conditions characterized by brief periods of precipitation.
Groundwater	Shallow levels of water serve as a significant source of moisture, while the presence of fluctuating water tables contributes to increased volume variation.
Drainage	Surface drainage features, such as the accumulation of water adjacent to a house foundation with inadequate grading, contribute to the presence of water at the ground level. Additionally, the presence of leaking sewage can allow water to penetrate the soil at greater depths.
Vegetation	The process of transpiration, carried out by trees, shrubs, and grasses, results in the extraction of moisture from the soil. Consequently, the soil becomes unevenly saturated in regions with different types of vegetation.
Permeability	Higher permeability in the soil, especially when it's caused by fissures and fractures in the field soil body, makes it possible for water to move through the soil more quickly and encourages quicker rates of swelling.
Temperature	As temperatures rise, moisture will migrate to colder places underneath structures, which will enhance the swelling in those locations.

Table 2.4 Factors in the surrounding environment that might affect swelling or shrinkage (Nelson & Miller, 1992)

FACTOR	DESCRIPTION
Stress History	The degree of expansiveness exhibited by overconsolidated soil is higher in comparison to soil with a comparable void ratio but subjected to normal consolidation scenarios. Research has shown that the amount of swelling experienced under light loads remains consistent regardless of time. However, it has been observed that the swelling pressures of compacted clays can increase over time. It has been found that the process of repeatedly soaking and drying soil has a diminishing influence on the amount of swelling that occurs in the results of laboratory tests.
In situ Conditions	In order to evaluate the possible impacts of soil body loading and/or alterations in moisture levels, it is imperative to conduct an initial estimation of the amount of stress within the soil. The estimation of the initial effective stresses can be achieved through two approaches: sampling from the field and laboratory experiments; or in-situ tests and investigations.
Loading	The level of the surcharge load plays a crucial role in influencing the extent of volumetric changes that occur, given a particular moisture content and density. The utilization of an external load function to mitigate the repulsive interparticle forces and reduce swelling.
Soil Profile	The level of the surcharge load plays a crucial role in influencing the extent of volumetric changes that occur, given a particular moisture content and density. The utilization of an external load function to mitigate the repulsive interparticle forces and reduce swelling. The possible shifts of a system are greatly affected by the overall width and the geographical positioning volumetric change of susceptible sections within the system's profile. The highest degree of displacement will occur within geological layers distinguished by expansive clays that range from the outermost layer to the deepest parts surpassing the active zone. It is anticipated that there will be a decrease in the degree of movement once expansive soil is coated with nonexpansive material or as it is positioned over shallow bedrock.

2.9 Stabilization of Expansive Soils

In some cases, it may be advantageous and cost-effective to modify the soil properties in order to mitigate its expansion potential or stabilize the moisture conditions associated with a structure or pavement. This approach can serve as a viable alternative or complement to the conventional design methods employed for such infrastructural elements. Several methods have been utilized to improve the properties of the soil or provide stable moisture conditions in nearby areas of the foundation or pavement (Nelson et al., 2015). In basic terms, the treatment of expansive soils can be classified into two main categories (Jones, 2017):

(1) Soil Stabilization – removal/replacement; remould and compact; pre-wetting; Surcharge loading; and chemical/cement stabilization.

(2) Water content control methods – horizontal barriers (membranes, asphalt, and rigid barriers); Vertical barriers; electrochemical soil treatment; and heat treatment.

The methods of treatment for expansive soil discussed in this piece of literature can be used individually or in combination to mitigate heave. Nevertheless, it is critical to acknowledge that under any circumstances, the efficacy of one or multiple methods could be compromised due to site-specific conditions. The selection of the methodology to be employed should be evaluated in relation to the following (Nelson & Miller, 1992):

- Aspects pertaining to the economy.
- The comparative assessment of anticipated control over volume fluctuations through the implementation of various treatment alternatives.
- Site-specific factors such as the possibility of volume change, variations in moisture levels, the extent of fissures, permeability, and other related conditions.
- The project's inherent characteristics and properties.
- The requisite strength of the underlying soil for the foundation.
- The temporal duration allocated for treatment.

The objective of this study is to improve or stabilize expansive soils; the water content control methods will not be explained in detail. In addition, since the objective of the thesis is chemically stabilization, other stabilization methods are summarized in Table 2.5.

Table 2.5 Soil Stabilization approaches applied to expansive soils (Nelson & Miller, 1992)

Improvement Approach	Outline of Approach	Advantage	Disadvantage
Removal and Replacement	The expansive soil was excavated and substituted with non-expansive fill material to a sufficient depth in order to mitigate excessive vertical movement. The depth of excavation is determined by its weight, which is necessary to counteract uplift forces and minimize differential movement. According to Chen (1988), it is recommended to have a minimum distance of 1 to 1.3 meters.	The utilization of non-expansive fill has the potential to improve bearing capacities. The proposed task is straightforward and can be easily done, often surpassing alternative methods in terms of time efficiency.	It is advisable to utilize impervious fill material in order to mitigate the entry of water, a measure that can cause significant costs. The required thickness may pose practical challenges. Construction projects may experience failure as a result of the infiltration of water.
Remoulding and Compaction	A reduced level of expansion is observed in soil that is compacted at lower densities above the optimum moisture content (OMC) compared to soil that is compacted at higher densities and below the OMC. Target densities can be obtained through the application of standard compaction techniques and control measurements.	The utilization of clay on the construction site eliminates the need for costly transported fill material. Additionally, this approach allows for the creation of a relatively impermeable fill, which helps to minimize water infiltration. Moreover, the use of compaction can effectively reduce the potential for soil swelling without the introduction of excessive water.	Insufficient compaction density can have a negative impact on the bearing capacity. It is possible that the effectiveness of this approach may be limited in soils with high swelling potential. The implementation needs careful and comprehensive quality control measures.

Table 2.5 (Cont'd)

Improvement Approach	Outline of Approach	Advantage	Disadvantage
Pre-wetting or Ponding	The water content was deliberately increased in order to facilitate heave before starting construction activities. Dykes or berms can be used as means of containing water within inundated regions. In addition, the implementation of trenches and vertical drains may also be utilized as alternative methods for increasing the rate of water infiltration into the soil.	The method has demonstrated efficacy in cases where the soil exhibits adequate permeability, facilitating rapid water infiltration, such as with fissure clays.	It may take several years to get sufficient wetting. The occurrence of strength loss and failure can be observed. The water permeation is restricted to a depth that is shallower than the active zone. The phenomenon of water redistribution can lead to significant changes in the distribution of water resources following construction activities.
Surcharge Loading	Loading expansive clays with enough surcharge to counterbalance projected swell forces can avoid swelling. Only low- to moderate-swelling soils apply. The effectiveness of a surcharge, however, decreases with increasing swell pressures due to the nonlinear behavior of the pressure-swell relationship.	The surcharge approach works best where swell pressures are minimal, and the structure allows for some heaving, such as in a minor highway system. This strategy may work for big projects with high foundation forces and low-to-moderate swell pressures.	A comprehensive both field and lab tests, including a soil testing program, is needed to obtain the depth of the active zone and the maximum swell pressure. Surcharges need careful management of drainage systems. Moisture migrates vertically and horizontally. Swell pressures in many soils exceed typical surcharge loads.

2.9.1 Chemical Additives

Chemical treatment refers to the process of integrating soil with one or more additives, such as powders, slurries, or liquids, with the overall aim of increasing or regulating its tendency to volumetric change, strength, and stress-strain characteristics, water-air movement in the soil, and endurance (Winterkorn & Pamukcu, 1991). The use of chemicals is a frequently employed technique in various geotechnical engineering-related parts of projects, including embankments, roads, highways, and others, with the aim of improving soil properties (Tran et al., 2014). One of the earliest and most commonly employed techniques for enhancing the properties of soil is the application of chemical substances for the purpose of soil stabilization (Chen, 1975).

The chemical additives used for the treatment of expansive soil can be categorized into two distinct groups. The materials used in this context consist of both conventional substances like hydrated lime, portland cement, and fly ash, as well as unconventional compounds like potassium compounds, sulfonated oils, ammonium chloride, and many more (Nelson et al., 2015). The uncommon chemical additives primarily consist of waste from industry or by-products materials that have been chosen based on their significant mineral composition. The primary objective is to enhance the characteristics of expansive soils while simultaneously raising the worth of by-products and waste materials and reducing environmental issues associated with their disposal (Seco et al., 2011). In the past decade, there has been a growing emphasis on the utilization of industrial waste materials as an alternative to industrial products in the stabilization of expansive soils. According to Kamon et al., (1991), the utilization of waste materials results in a reduction in both utilization and storage expenses associated with industrial products. The application of these substances is influenced by multiple considerations, such as the chemical and physical characteristics of the soil at that location, the efficacy of the additive, financial as well as health limitations, and the particular circumstances of the building project (Fang, 1991).

2.9.1.1 Lime Stabilization

Lime has been employed by Chinese people for hundreds of years as a chemical stabilizer. If the shear strength of the chemically treated soil is thought to be insignificant in comparison to other properties, lime has been utilized as a chemical stabilizing agent (Chen, 1975). Lime as a stabilization method has been widely employed globally for an extended period (Chen, 1988). According to Little & Nair, (2009), lime is the stabilizing agent that is most commonly utilized among others.

Many studies have been conducted by various researchers (Bell, 1996; Indraratna et al., 1995) about the use of lime for soil stabilization. Numerous studies have been conducted to investigate the variations linked to the consistency limits values, such as the plastic and liquid limits, as well as the soil characteristics, including volumetric change (e.g., swell pressure, swell potential, heave), shear strength, and the coefficient of permeability in lime-treated expansive soils (Al-Mukhtar et al., 2012). According to Nalbantoglu & Gucbilmez, (2001), the application of lime implementation in fine-content dominant soils typically results in a reduction in plasticity, dispersivity, and tendency to volumetric change, while simultaneously leading to an increase in grain size, permeability, and strength characteristics. Furthermore, the application of lime into the soil results in an increase in soil pH, consequently leading to an increase in the cation exchange capacity (Çokça, 2001).

There are many different kinds of soils, and lime is not always an appropriate treatment. According to the National Lime Association, (2004), clay soils that contain a maximum of 75 retaining percent from the No. 200 sieve and a plasticity index value above 10% are generally regarded as suitable candidates for soil treatment. Certain ingredients found in soil, such as sulfates, organics, and phosphates, tend to trigger reactions that may result in significant detrimental consequences (Nelson et al., 2015).

In most cases, it is common practice to incorporate hydrated lime into the uppermost layers of the soil, typically ranging from 3 to 8% by weight (Nelson & Miller, 1992).

In addition, it is advised that soils that contain a fines content above 50% need to be stabilized using lime in a range of 5 to 10% (Murthy, 2002).

The main factors that influence the strength properties of soil treated using lime are the type of soil, type of lime, percentage of lime, and the conditions under which the soil is cured (Nelson & Miller, 1992). Several factors may affect the reaction rate of lime in the soil, as outlined by (Nelson et al., 2015).

- A soil with a pH value above approximately 7 represents suitable reactivity.
- The presence of organic carbon significantly delays lime-soil reactions.
- It has been observed that soils with poor drainage show a greater degree of lime reactivity compared to soils with good drainage.
- Soils that are rich in calcium (calcareous) have a high degree of reactivity.
- Ettringite-induced heave can occur when lime reacts with soluble sulfate salts present in the soil.

2.9.1.1.1 Lime Stabilization Mechanisms

There is a lot of theory behind the lime reaction that may get complicated (Thompson, 1966, 1968). The lime reacts with other substances through a series of processes; the key ones can be explained by cation exchange, flocculation-agglomeration, lime carbonation, and the pozzolanic reaction (Little, 1995; National Lime Association, 2004; Thompson, 1966, 1968). When lime and clays containing pozzolanic elements are combined in the appearance of water, three fundamental chemical processes take place. These processes are cation exchange and flocculation-agglomeration, cementation (specifically the pozzolanic reaction), and carbonation (Fang, 1991).

2.9.1.1.1.1 Cation Exchange

The initial stage involves the substitution of calcium ions that come from stabilizing agent with the ions existing on the surface of clay particles. The dominant cations that contribute to the formation of the double layer, in conjunction with water molecules, are monovalent cations, specifically sodium (Na^+) and potassium (K^+). Nevertheless, it is possible to easily replace monovalent cations with cations of greater valence, like calcium (Prusinski & Bhattacharja, 1999). The exchangeability of cations can be determined using the lyotropic series, outlined as $Th^{4+} > Al^{3+} > Cu^{2+} > Ba^{2+} = Sr^{2+} > Ca^{2+} > Mg^{2+} > Cs^+ > Rb^+ > NH_4^+ = K^+ > Li^+ > Na^+$ by Cherian & Arnepalli, (2015).

A soil stabilizing agent which is composed of a high amount of calcium is expected to supply an adequate amount of calcium ions, thereby facilitating the exchange of monovalent cations. The process of ion exchange leads to a notable decrease in the thickness of the double layer and a rise in the inter-particle attraction within the soil due to the higher charge density exhibited by di or trivalent ions. The ion exchange procedure is typically characterized by its rapidity, often within a few hours (Mallela et al., 2004; Prusinski & Bhattacharja, 1999), as illustrated in Figure 2.15. A single example of cation exchange has been demonstrated in a study conducted by Sivapullaiah, (2006):

$$Ca^{2+} + Clay \rightarrow Ca^{2+}Clay + (Na^+, K^+) \qquad (Eq. 2.1)$$

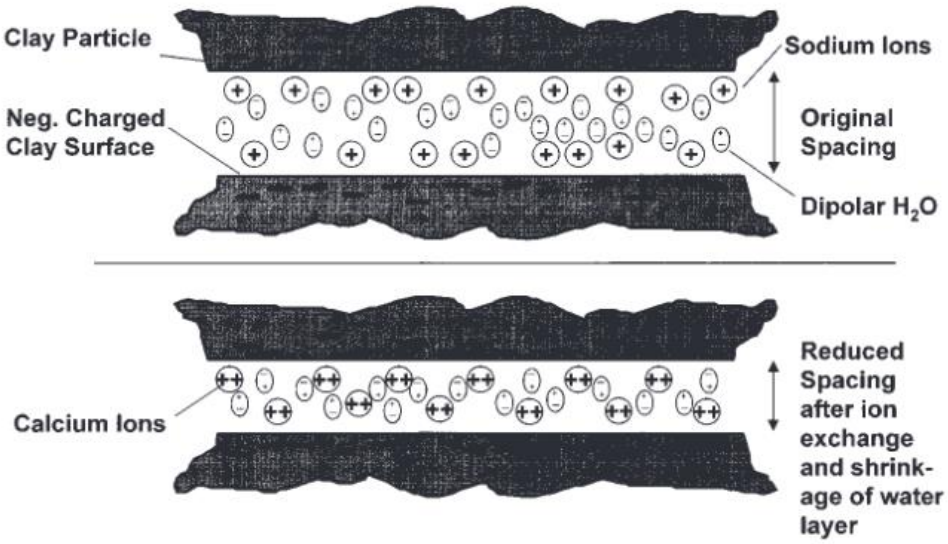

Figure 2.15 Cation exchange (Prusinski & Bhattacharja, 1999)

2.9.1.1.1.2 Flocculation and Agglomeration

Cation exchange responses lead to the flocculation and agglomeration of soil particles, resulting in a decrease in the quantity of clay-sized materials and, consequently, a reduction in soil surface area. Such a decrease in surface area is responsible for the decrease in plasticity, as stated by Terzaghi & Peck, (1967). According to Prusinski & Bhattacharja, (1999), the processes of flocculation and agglomeration result in a transformation of the clay composition, shifting it from a plastic, fine-grained substance to a nonplastic, granular soil.

The phenomenon of flocculation has been linked to several factors, including the presence of a significant amount of electrolytes, a high pH level, and a decrease in the thickness of the double-layer because of cation exchange (Herzog & Mitchell, 1963). The substitution of monovalent ions with calcium ions leads to an augmentation in the interparticle attraction within soil particles (Mallela et al., 2004). Flocs are generated through the process of soil particles being drawn together due to the forces of attraction and cation exchange. The term used to describe this occurrence is known as flocculation (Al-Rawas & Goosen, 2006). According to

Prusinski & Bhattacharja, (1999), flocculation refers to the phenomenon in which clay particles undergo a transformation in their arrangement from a flat and parallel arrangement to a more disordered edge-to-face orientation. The process of clay particles adhering to form flocs results in the development of soil that exhibits improved engineering characteristics, including a more granular arrangement, reduced plasticity, increased permeability, and notably decreased expansivity (Seco et al., 2011).

The occurrence of agglomeration is hypothesized to take place when flocculated clay particles initiate the formation of fragile bonds at the interfaces of the clay particles due to the accumulation of cementitious substances at these interfaces. The process of agglomeration initiates the unification of smaller clay particles, resulting in the formation of bigger aggregates. This process also enhances the overall texture of the clay soil (Prusinski & Bhattacharja, 1999). According to Fang, (1991), the collapsible features of some silts can be neutralized by using an agglomeration process involving lime and soil. The process of flocculation and agglomeration is illustrated in Figure 2.16.

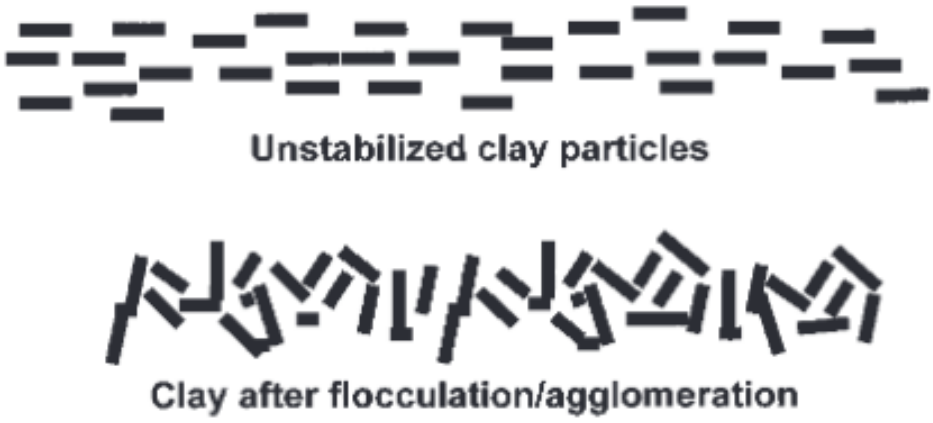

Figure 2.16 Flocculation and agglomeration (Prusinski & Bhattacharja, 1999)

2.9.1.1.1.3 Pozzolanic Reactions

The Pozzolanic reaction, as depicted in Figure 2.17, is a secondary phase utilized in soil treatment. It is valid for both lime- and cement-soil interactions. The alkaline conditions in a calcium-stabilized system augment the solubility and reactivity of silica and alumina, which are constituents of clay particles. The hypothesis suggests that calcium ions react with silica and alumina that are released from the clay lattice, resulting in the formation of supplementary cementitious substances, namely calcium silicate hydrates, CSH, and calcium aluminate hydrates, CAH. This contributes to a better understanding of the process of agglomeration (Prusinski & Bhattacharja, 1999). The cementitious materials consist of calcium silicate hydrates and calcium aluminate hydrates, which are the identical hydrates that are produced within the hydration process of Portland cement application (Terrel et al., 1979). The following straightforward descriptive illustration of soil-lime reactions is given based on the work of Walker, (1992).

$$Ca(OH)_2 \rightarrow Ca^{2+} + 2OH^- \qquad (Eq.\,2.2)$$

$$Ca^{2+} + 2OH^- + SiO_2\ (Clay\ Silica) \rightarrow CSH \qquad (Eq.\,2.3)$$

$$Ca^{2+} + 2OH^- + Al_2O_3\ (Clay\ Alumina) \rightarrow CSH \qquad (Eq.\,2.4)$$

A wide variety of hydrate forms can be obtained, depending on reaction conditions, that is, quantity and type of lime, soil characteristics, curing time, and temperature (Nelson & Miller, 1992).

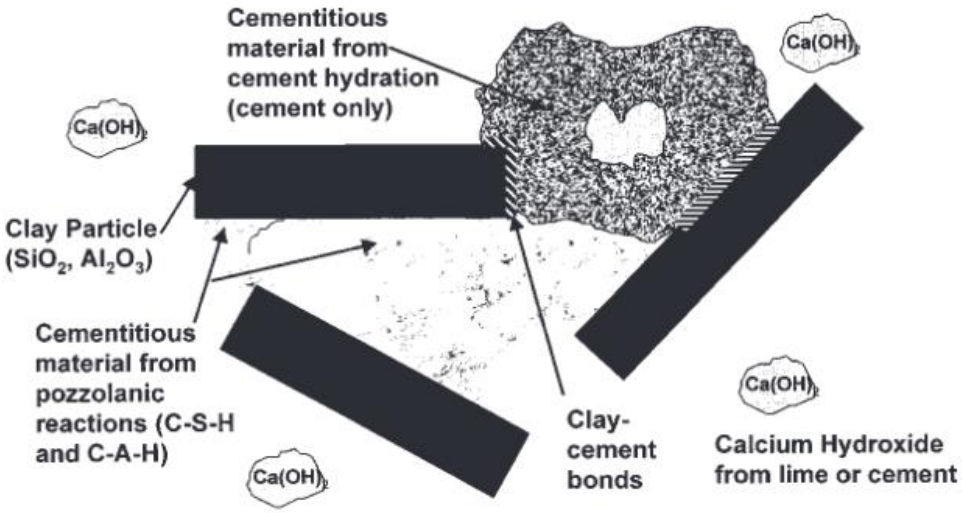

Figure 2.17 Pozzolanic reaction (Prusinski & Bhattacharja, 1999)

2.9.1.1.1.4 Carbonation

When calcium hydroxide comes into contact with carbon dioxide in the atmosphere or when it is dissolved in rainwater, a gradual formation of calcium carbonate occurs, as described by the following reaction:

$$Ca(OH)_2 + CO_2 \rightarrow CaCO_3 + H_2O \qquad (Eq.2.5)$$

The above reaction phenomenon is commonly called carbonation (West & Carder, 1997). The process of lime carbonation is regarded as an unfavorable reaction that can potentially show up in soil-lime combinations. In the aforementioned reaction, the compound lime undergoes a chemical reaction with carbon dioxide, resulting in the formation of calcium carbonate, instead of reacting with clay-silica or clay-alumina to form cementitious compounds known as CAHs and CSHs, as reported by Mallela et al., (2004). Calcium carbonate ($CaCO_3$) is a substance that shows plastic characteristics and has the ability to rise in the plasticity of the soil. Consequently, the usage of excessive lime does not yield beneficial outcomes (Fang, 1991).

2.9.1.2 Silica Fume Stabilization

2.9.1.2.1 Silica Fume Production

Silica fume (SF) is a leftover substance derived from the production process of ferrosilicon or silicon alloy, which represents a significant amount of industrial waste produced during the production procedure (Khalid et al., 2023). According to the American Concrete Institute (ACI) 116R, silica fume is a very fine amorphous silica material that is generated as a byproduct during the production of elemental silicon or silicon-containing alloys in electric arc furnaces (Fattah et al., 2015a). Figure 2.18 illustrates a schematic diagram depicting the production process of a byproduct stated as silica fume. Due to their apparent compatibility, there is occasional confusion between ferrosilicon slag and silica fume. Ferrosilicon slag is a byproduct that is generated as slag during the operation of a blast furnace. Conversely, silica fume is comprised of tiny particles that become released into the air and are subsequently captured through filtration processes (Tangstad, 2013).

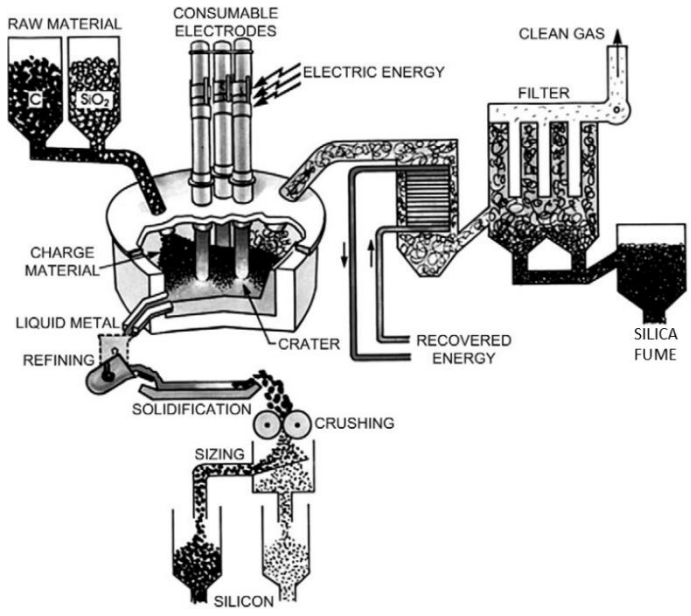

Figure 2.18 The schematic of the silicon melting process results in silica fume (Tangstad, 2013)

2.9.1.2.2 Properties of Silica Fume

Silica fume (SF), alternatively referred to as micro silica, is characterized by its non-crystalline polymorphs and amorphous nature, consisting of silicon dioxide (SiO_2) particles that exhibit a spherical shape (Brescia-Norambuena et al., 2021; Wang et al., 2020). Silicon-based materials, commonly referred to as SF, exhibit a significant surface area ranging from 10 m^2/g to 30 m^2/g and microparticles sizes ranging from approximately 200 to 1100 nm, as reported by Abdel-Gawwad et al., (2021). The SiO_2 content in the SF ranges from approximately 90% to 96%, according to several sources (Billong et al., 2021; Brescia-Norambuena et al., 2021; Ting et al., 2021; Türköz et al., 2021). This SiO_2 is primarily found in the form of quartz. Additionally, the total alkali content in the SF is restricted to 0.17% (Choudhary et al., 2021). According to Negi et al., (2013), silica fume is typically found in a powdered form that seems like ash. Silica fume (SF) is a commonly used material for enhancing problematic soils due to its characteristics of low unit weight, relatively low compactibility, along with significant pozzolanic activity (Goodarzi et al., 2015).

Figures 2.19, 2.20, and 2.21 depict the X-ray diffraction (XRD) pattern, Scanning Electron Microscopy (SEM), and Transmission Electron Microscope (TEM) images of a commercial silica fume, respectively. The X-ray diffraction (XRD) pattern depicted in Figure 2.19 indicates that the structure of silica fume exhibits amorphous characteristics. Figure 2.20 illustrates that the silica fume particle exhibited a fine spherical morphology, characterized by particle size in the range of several hundred nanometers. Figure 2.21 illustrates the formation of agglomerates through the process of melting and solidification of silica fume particles.

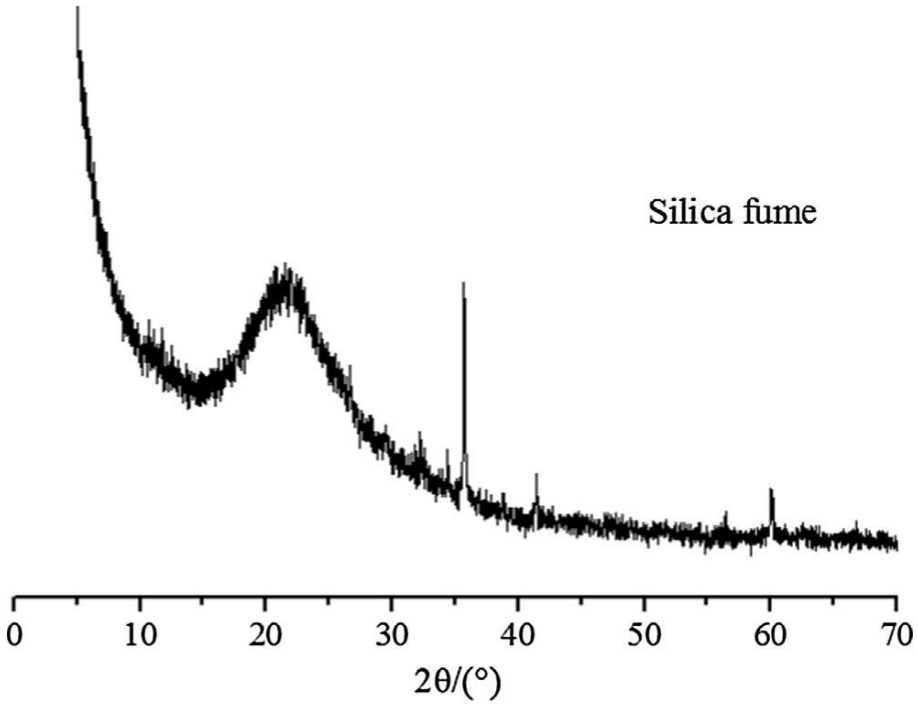

Figure 2.19 X-ray diffraction (XRD) pattern of a commercial silica fume (Wang et al., 2020)

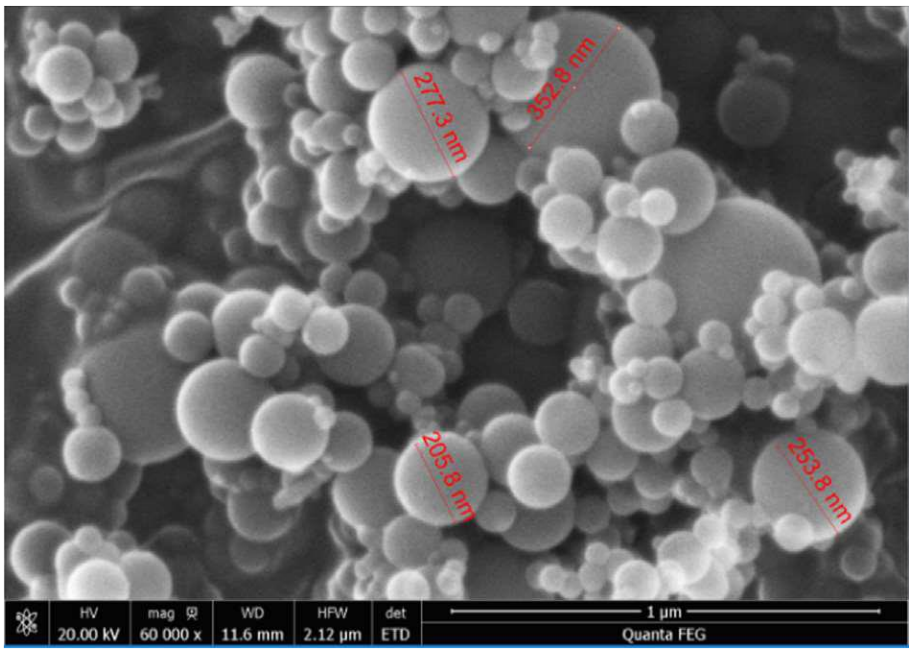

Figure 2.20 Scanning Electron Microscopy (SEM) image of a commercial silica fume (Wang et al., 2020)

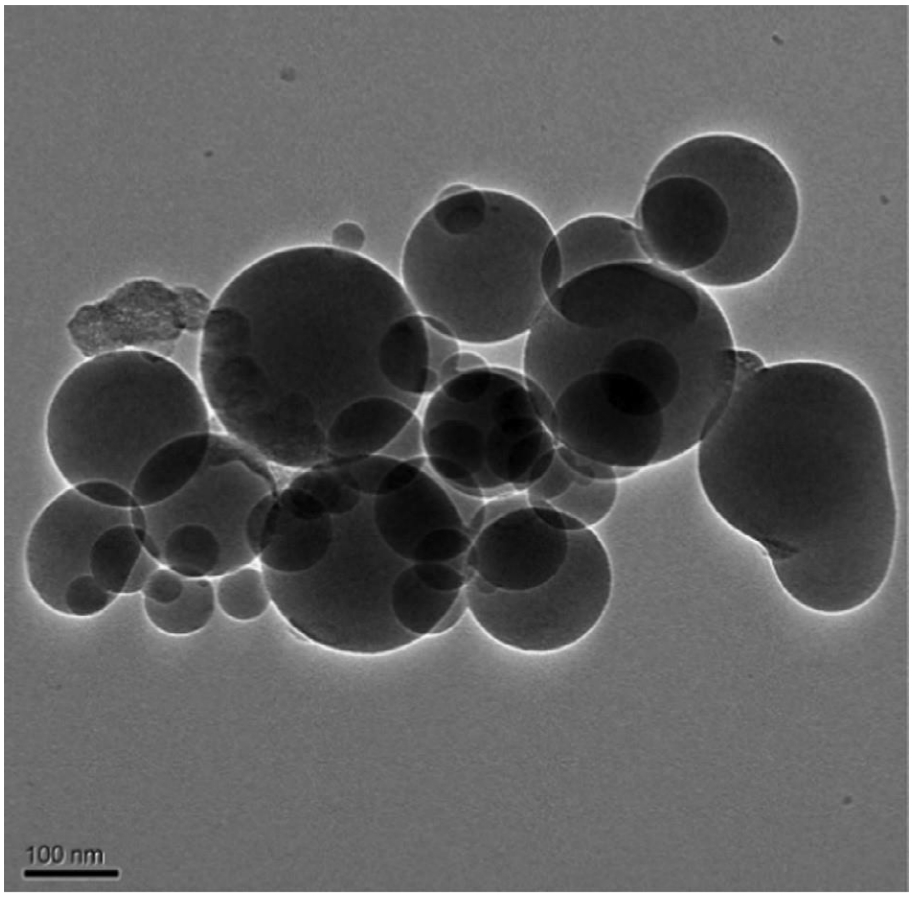

Figure 2.21 Transmission Electron Microscope (TEM) image of a commercial silica fume (Wang et al., 2020)

2.9.1.2.3 Stabilization Mechanism of Silica Fume

The chemical interactions between clay soils and silica fume have not been extensively investigated, thus hindering a precise interpretation of the resulting chemical reactions. Despite the absence of existing research on the interaction between clay and silica fume, an understanding of the chemical composition of silica fume can provide perspectives on potential reactions that may occur when silica fume is introduced into the soil. Amorphous silicon dioxide (SiO_2) is the predominant oxide present in SF, providing it as a pozzolanic agent (Fattah et al., 2015a; Goodarzi et al., 2016).

Since silica fume can be considered a natural pozzolan, there is a potential concern regarding its workability in the absence of additional substances. In order to observe or ascertain that, a study was conducted by Topçuoğlu & Gürocak, (2023) with the objective of identifying the molecular alterations induced by silica fume and some other pozzolanic additives in the microstructure of pure bentonite clay using FT-IR Spectroscopy assessment. This study investigates the effects of various additives, including bentonite clay, silica fume, and other pozzolans. The additive samples were prepared by incorporating these additives into bentonite at different concentrations. Subsequently, the samples were compacted at the optimal water content, cured, and subjected to FT-IR Spectroscopy analysis. In the context of adding silica fume as an additive substance, the FT-IR spectrum exhibited no notable alterations. This can be attributed to the inability of the pozzolanic constituents of silica fume to generate calcium silicate hydrate (CSH) gel, primarily due to the lack or minimal presence of lime within the surrounding environment. Nevertheless, when subjected to water, these substances undergo a reaction with calcium hydroxide under typical conditions, such as at room temperature. This reaction results in the formation of compounds, specifically calcium silicate hydrate and calcium aluminate hydrate, which possess properties that are characteristic of cement. The aforementioned reaction is commonly referred to as a pozzolanic reaction (Chung, 2017).

Calcium hydroxide combines with the active silica to produce calcium silicate hydrate gels ($CaSiO_3.H_2O$). Kalkan & Akbulut, (2004) provide the following equation to describe the fundamental silica fume-calcium interaction in clay:

$$Ca^{2+} + OH^{-} + soluble\ silica \rightarrow calcium\ silicate\ hydrate \qquad (Eq.\ 2.6)$$

It was discovered that the material resulting from the above process enhanced strength and increased brittleness compared to its previous state. There have been previous studies conducted on similar concepts, as evidenced by the works of Bell, (1993) and (Sherwood, 1993). According to Türköz et al., (2018), the inclusion of silica fume triggers a transition in the pattern of clay particles from a dispersed

structure to a flocculated structure. Additionally, this process leads to the formation of fresh cementing compounds. The soil pores are filled to a large extent, and the hydration gels are covered the particle surfaces. Additionally, the flocculated calcium ions (Ca^{+2}) consist mostly of lime and silica dioxide (SiO_2) derived from silica fume. The development of this substance can quickly cover the empty spaces within the soil and effectively bind the clay particles together, leading to a progressive enhancement of the geotechnical characteristics of the soil with increasing additive content (Goodarzi & Salimi, 2015).

2.9.1.2.4 Previous Studies Conducted by Silica Fume

The initial investigations into the application of silica fume as a by-product of silicon metal or ferrosilicon alloy manufacturing, which showed up as an industrial waste, began in Norway during the 1950s with the aim of addressing environmental concerns (Yeğinobalı, 2011). According to Holland et al., (2006), silica fume was initially utilized in various countries throughout the industrial revolution of the mid-twentieth century as a means to mitigate the emission of substances into the atmosphere. Numerous investigations and diverse implementations have been conducted in relation to silica fume, with particular emphasis on its utilization within the construction sector (Al-Mansour et al., 2019). In 1969, an experimental investigation was conducted in Norway to assess the efficacy of adding this specific substance as a cement admixture. This substance, known for its outstanding pozzolanic properties resulting from its fine-grained nature and significant concentration of amorphous silica, was evaluated for its effectiveness in enhancing cement performance. The utilization and investigation of silica fume's behavior in concrete exhibited a slow pace of progress until the early 1980s, primarily concentrated in Scandinavian countries (Yeğinobalı, 2011). The utilization of silica fume in concrete serves to enhance its fundamental features. According to U.S ARMY CORPS OF ENGINEERS, (1999), the utilization of silica fume has been observed to enhance compressive strength, bond strength, and abrasion resistance.

Additionally, it has been noted to decrease permeability, thereby aiding in the preservation of reinforcing steel by reducing the risk of corrosion.

In past decades, the cost of this material was approximately 40% lower compared to Portland cement (Yoder & Witczak, 1975). However, its current price has increased due to its widespread use in the production of concrete (Sadrmomtazi et al., 2018). The silica fume, regardless of being collected as a waste material from industrial processes, has gained significant value as a by-product within the category of pozzolanic materials. This is primarily attributed to its exceptional reactivity and strong pozzolanic characteristics (Atiş et al., 2005). The utilization of this specific pozzolanic substance as a replacement for cement results in enhancements in the features of concrete, particularly in terms of its strength characteristics (Khan & Ali, 2019; Siddique & Chahal, 2011). The integrated use of silica fume as a partial replacement or an additive for cement has been reported in the production of concrete utilized for structural uses (Khan & Ali, 2019; Köksal et al., 2008; Li, 2021; Ortega et al., 2018; Sadrmomtazi et al., 2018; Silva et al., 2020). The study conducted by Liu et al., (2019) demonstrated a notable enhancement in the durability and resistance to freeze-thaw cycles of a pervious concrete lining material when incorporating varying proportions of supplementary cementitious material (SF) as a replacement for cement. A study was carried out by Topçu & Kaval, (2001) to analyze the economic implications of incorporating silica fume in concrete. According to Sezer, 2012), it is recommended to add SF amounts ranging from 5% to 10% in order to mitigate concrete bleeding and enhance resistance against sulfate attacks and chloride ions. Silica fumes have gained significant popularity as a modifier in conventional cement concrete due to its outstanding performance.

Various studies have been carried out in the literature to assess the impact of silica fume on soils with problematic characteristics. The present studies aim to assess the performance of swelling and dispersive soils that have been subjected to treatment with SF. The evaluation primarily focuses on the strength characteristics of these soils, particularly in static conditions, as well as the alterations observed in their geotechnical index features. In their study, Abd El-Aziz et al., (2004) observed that

the incorporation of lime (L) within the soil, ranging from 5% to 9%, along with 10% silica fume, resulted in enhanced engineering characteristics of the soil.

The study conducted by Al-Zairjawi, (2009) investigated the effects of incorporating a cement and silica fume additive on the compaction properties and strength of a high plasticity clay soil. The experimental findings indicate that the addition of an 8% cement and 6% silica fume mixture resulted in a reduction of the maximum dry density from 1.64 to 1.55 g/cm^3. Additionally, this mixture led to a rise in the optimum moisture content from 19 to 23%.

Bharadwaj & Trivedi, (2016) performed a set of laboratory tests involving samples containing varying proportions of silica fume, specifically 0%, 5%, 10%, and 15% by weight of dry soil. The experiment's results indicated a notable alteration in the consistency limits of samples that included silica fume. Furthermore, there was a notable reduction in the differential free swell, which lowered from 48.46% to 9%. This indicates a substantial reduction in the amount of swelling exhibited by the material. The findings of the study indicated that there was a reduction in swelling potential as the percentage of silica fume treatment increased.

In their study, Amina & Rani, (2017) employed hydrated lime and silica fume as waste materials for the purpose of treating dispersive soil. The researchers reached the conclusion that the usage of appropriate additives, such as lime and lime combined with silica fume, resulted in a notable reduction in the dispersive properties of the soil. The experimental results indicated that the addition of 5% L and 2% L + 12% SF led to a reduction in the dispersive properties of the soil.

In a study published by Al-Soudany, (2018), the author examined the effectiveness of enhancing the geotechnical characteristics of soft clay soil through the application of varying proportions of silica fume (0%, 3%, 5%, and 7%). The silica fume-treated soils went through various tests, including classification, determination of specific gravity, evaluation of compaction characteristics and swelling pressure, as well as California bearing ratio (CBR) and unconfined compressive strength (UCS) tests. Consequently, it was found that the plasticity index and liquid limit exhibited a

reduction in response to the increasing content of silica fume. The augmentation of silica fume led to a rise in the optimal water content, whereas the maximum dry unit weight values exhibited a decrease. The utilization of silica fume has been found to enhance the performance of UCS (unconfined compressive strength), CBR (California Bearing Ratio), and swelling pressure. Based on existing literature in the field of soil stabilization, it is commonly observed that silica fume is utilized as a supplementary material, either independently or in conjunction with other additives like lime and cement, with the aim of enhancing the engineering characteristics of expansive soils.

In a study done by Fattah et al., (2015b), it was observed that the bearing capacity of a square foundation constructed on soft clay soil, which had been treated with a combination of lime and silica fume, exhibited a notable increase. The study involved varying amounts of lime, specifically 2%, 4%, and 6%, in combination with different amounts of silica fume, specifically 2.5%, 5%, and 10%. Through experimentation, the optimal percentage of silica fume was obtained and subsequently mixed with the corresponding lime percentages. The slurry mixture was pumped into the surrounding area of the foundation at various depths and distances. An enhancement in the bearing capacity ranging from 6.58% to 88%, was achieved through the implementation of injection techniques away from 0.5 times the width of the foundation (B) around the foundation.

The study carried out by Goodarzi et al., (2016) investigated the potential application and efficacy of utilizing a combination of cement and silica fume (CSF) for stabilizing expansive clay. A clay sample was subjected to two separate additions of cement, and CSF blends with a 10% replacement of cement. Subsequently, a range of macro and micro-level tests were conducted under different curing conditions to assess the reactions to these modifications. The experimental results involving CSF demonstrate a notable increase in strength (approximately 35%) and a decrease in compression index (an increase of approximately 50%) when compared to the performance of single usage of the cement. The utilization of supplementary materials such as SF in cement has been observed to result in a decrease in both the

amount of binder required and the time needed for curing in the treatment of expansive clay. This finding is significant as it highlights the potential of SF in contributing to waste recycling efforts.

Kalkan, (2009) found that the usage of silica fume admixture had a significant impact on mitigating desiccation cracks in expansive clays. In a separate study done by Kalkan, (2011), the impact of wetting-drying cycles on the swelling characteristics of clay soil that had been treated with varying proportions of silica fume (10%, 20%, 25%, and 30%) was examined. The samples prepared with silica fume amounts ranging from 25% to 30% exhibited a noticeable improvement in both swell percentage and swell pressure of the modified soil.

In a study made by Tiwari & Satyam, 2019), an experimental investigation was carried out to assess the impact of polypropylene fiber on the swelling pressure and expansion characteristics of clay soil treated with silica fume. The research was conducted in a tripartite manner, resulting in the assessment of the impact of various combinations consisting of varying amounts of fiber (0.25%, 0.50%, and 1.00%) and silica fume (2%, 4%, and 8%) in together. The soil's expansive behavior was enhanced, resulting in a transition from a soil classification that is characterized by high plasticity clay (CH) to one characterized by low plasticity clay (CL), as evidenced by reductions in both the plasticity index and liquid limit values. The research findings indicate that silica fume possesses significant potential for modifying the properties of expansive clay. This is attributed to the reaction between silica and calcium, resulting in the formation of calcium silicate hydrate (CSH) gel.

The objective of the study conducted by Zaini & Hasan, (2023) is to investigate the potential of using silica fume at amounts ranging from 4% and 6%, along with lime at addition levels of 3%, 5%, 7%, and 9%, for the purpose of stabilizing kaolin soil. The optimal percentages of SF and lime for achieving maximum shear strength are 4% and 7%, respectively. The addition of SF and lime to kaolin resulted in increased unconfined compressive strength and friction angle compared to kaolin treated separately with SF and lime. This improvement can be attributed to the enhanced

effectiveness of pozzolanic reactions between SF and lime in conjunction with soil particles. Upon the addition of silica fume to the mixture of lime and kaolin, it initially exhibits inactive behavior. Upon the beginning of the reaction between lime and water in the mixture, the formation of Calcium Silicate Hydrate (CSH) and calcium hydroxide occurs. These compounds play a crucial role in the crystallization process that contributes to the development of strength. The pozzolanic reaction is a chemical process that takes place between silica fume and calcium hydroxide, resulting in the formation of additional calcium silicate hydrate (CSH) within the voids surrounding the hydrated particles.

In a study handled by Khalid et al., (2023), a new approach is suggested for the stabilization of highly expansive soils. This approach involves the integration of milled wheat straw (WS) with minimal screening and silica fume (SF) in a manner of a composite binary admixture (CBA). The mechanical properties of soil treated with CBA were evaluated using unconfined compression, direct shear, and flexural tests. The results indicated that adding 16% of CBA and a curing period of 28 days led to a significant increase in unconfined compressive strength (q_u), cohesion (c), and flexural strength (f) by 94.3%, 65.7%, and 90.7% accordingly. In addition, the evaluation of volumetric change variations is done by the examination of ID ? consolidation and swelling tests. The results indicated a significant reduction in various parameters, including the compression index (C_c), recompression index (C_r), swell potential, free swell index (FSI), and swell pressure. Specifically, the addition of 16% CBA in the soil and a curing period of 28 days resulted in reductions of 72.5%, 47.7%, 59%, 35.8%, and 65% for C_c, C_r, swell potential, FSI, and swell pressure, respectively. Furthermore, the wetting-drying (W-D) cycle tests provided evidence to support the notion that soil treated with CBA exhibited a reduced susceptibility to the effects of wetting-drying seasons in contrast to soil that was not subject to treatment. The mineralogical and microstructural examinations demonstrated that the presence of CBA in the soil matrix establishes a well-balanced Ca:Si and Ca:Al environment. This environment leads to the formation of cementing compounds, namely CSH and CAH, which contribute to the development of strong

bonds and enhance the aggregation of expansive soil particles. Consequently, the mechanical properties of the soil are improved.

CHAPTER 3

EXPERIMENTAL STUDY

3.1 Purpose

The experimental study aims to examine the effects of the addition of silica fume with lime on grain size distribution, consistency limits, swell percentage, and unconfined compressive strength; and to investigate the effect of curing on swelling percentage and unconfined compressive strength on an expansive soil treated with silica fume and lime.

3.2 Materials

Kaolinite: The Kalemaden Endüstriyel Hammaddeler Sanayi, ve Ticaret A.Ş. from Çanakkale, Turkey, sent Kaolinite as gravel-sized grains. Those grains were crumbled, sieved from the No. 40 sieve, and dried in a 40^{o} C oven before the study (Figure 3.1).

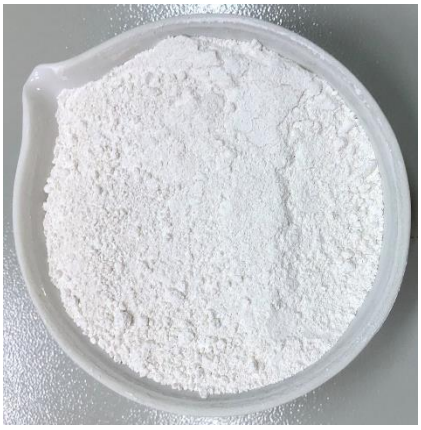

Figure 3.1 Kaolinite

Bentonite: The bentonite type was Na-Bentonite, provided by the Karakaya Bentonit Sanayi ve Ticaret A.Ş. Ankara, Turkey. The bentonite was sieved from the No. 40 sieve and dried in a 40^{o} C oven before the study (Figure 3.2).

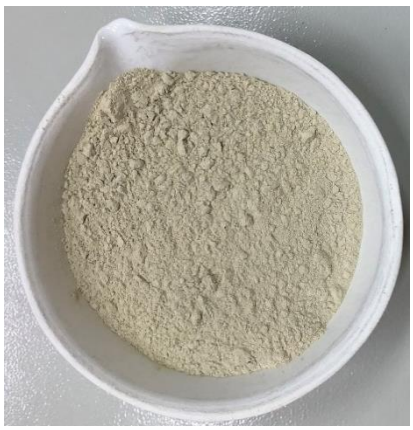

Figure 3.2 Bentonite

Lime: A hydrated lime produced by Baştaş Kireç Fabrikası in accordance with the TS EN 459-1 CL 70-S regulations provided. The lime was sieved from the No. 40 sieve and dried in a 40^{o} C oven before the study (Figure 3.3).

Figure 3.3 Hydrated Lime

Silica Fume: The silica fume was taken from Antalya Elektrometalurji A.Ş, obtained by special-filtered dust holders in the ferrosilicon (FeSi) and ferrochrome silicon (SiFeCr) furnaces. The silica fume was sieved from the No. 40 sieve and dried in a 40^{o} C oven before the study (Figure 3.4).

Figure 3.4 Silica Fume

The chemical compositions of the kaolinite, bentonite, lime, and silica fume used in experiments are obtained from their suppliers and given in Table 3.1.

Table 3.1 Chemical Compositions of Kaolinite, Bentonite, Lime, and Silica Fume

Composition (%)	Kaolinite	Bentonite	Lime	Silica Fume
SiO_2	47.89	61.28	<0.10	85-95
Fe_2O_3	*	3.01	<0.10	0.5-1.0
Al_2O_3	36.75	17.79	<0.10	1.0-3.0
MgO	0.09	2.1	0.9	1.0-2.0
CaO	0.39	4.54	95.55	0.8-1.2
Na_2O	0.01	2.7	*	*
K2O	0.75	1.24	*	*
SO_4	0.37	*	*	*
TiO_2	0.61	*	*	*
C	*	*	*	0.5-1.0
S	*	*	*	0.1-0.3
Loss of Ignition	12.73	*	3.2	0.5-1.0

*Not determined

3.3 Preparation of the Samples

Expansive soils are prevalent in nature. At the same time, it may be impossible to demonstrate the stabilizers' true stabilization mechanisms due to the potential inhomogeneity or degradation of these types of soils. So, the expansive soil sample used in this research was artificially made in the laboratory. The prepared expansive soil sample (No-Additive sample) consists of 85% of kaolinite and 15% bentonite by dry mass.

At the beginning of the preliminary studies, the silica fume effect was pretested, and the outcomes showed that using silica fume with lime decreased the swelling percentage by a sufficient amount. Then, two sets of samples are constituted, with 11 samples. During these processes, the relative amounts of kaolinite and bentonite remained constant. The additive percentages of each constituted sample are given in Table 3.2.

Initially, all ingredients, bentonite, kaolinite, lime, and silica fume, were held in a 50 ^{o}C oven for at least two nights to dry without evaporating the waters between the sheets. Then, each was crushed to pass from the No. 40 sieve with a trowel and plastic hammer. The required amounts of oven-dried and No. 40-sieved components were weighed and put into the sample combinations, which will be analyzed. Then, the resulting dry mixtures are run through a No. 10 for eight times to achieve as much as possible homogeneity.

After mixing the dry components, each sample was subjected to a standard proctor test. Each sample's maximum dry density and optimum moisture content were obtained after the tests. And then, each of the samples was mixed with optimum water content to achieve maximum dry density. The samples were then sealed in ceramic containers and left in a desiccator for at least two nights to avoid heterogeneous water distribution (Figure 3.5).

The same method was followed to prepare the specimens for the tests in which the samples were cured. The samples were left to cure for 7 or 28 days at 22 °C and 70% humidity rate following mixing and compacting procedures.

Table 3.2 Percent Additive in Each Sample

Name	Kaolinite + Bentonite (%)	Lime (%)	Silica Fume (%)
No-Additive	100	-	-
3% L	97	3	-
3% L + 5% SF	92	3	5
3% L + 10% SF	87	3	10
3% L + 15% SF	82	3	15
3% L + 20% SF	77	3	20
5% L	95	5	-
5% L + 5% SF	90	5	5
5% L + 10% SF	85	5	10
5% L + 15% SF	80	5	15
5% L + 20% SF	75	5	20

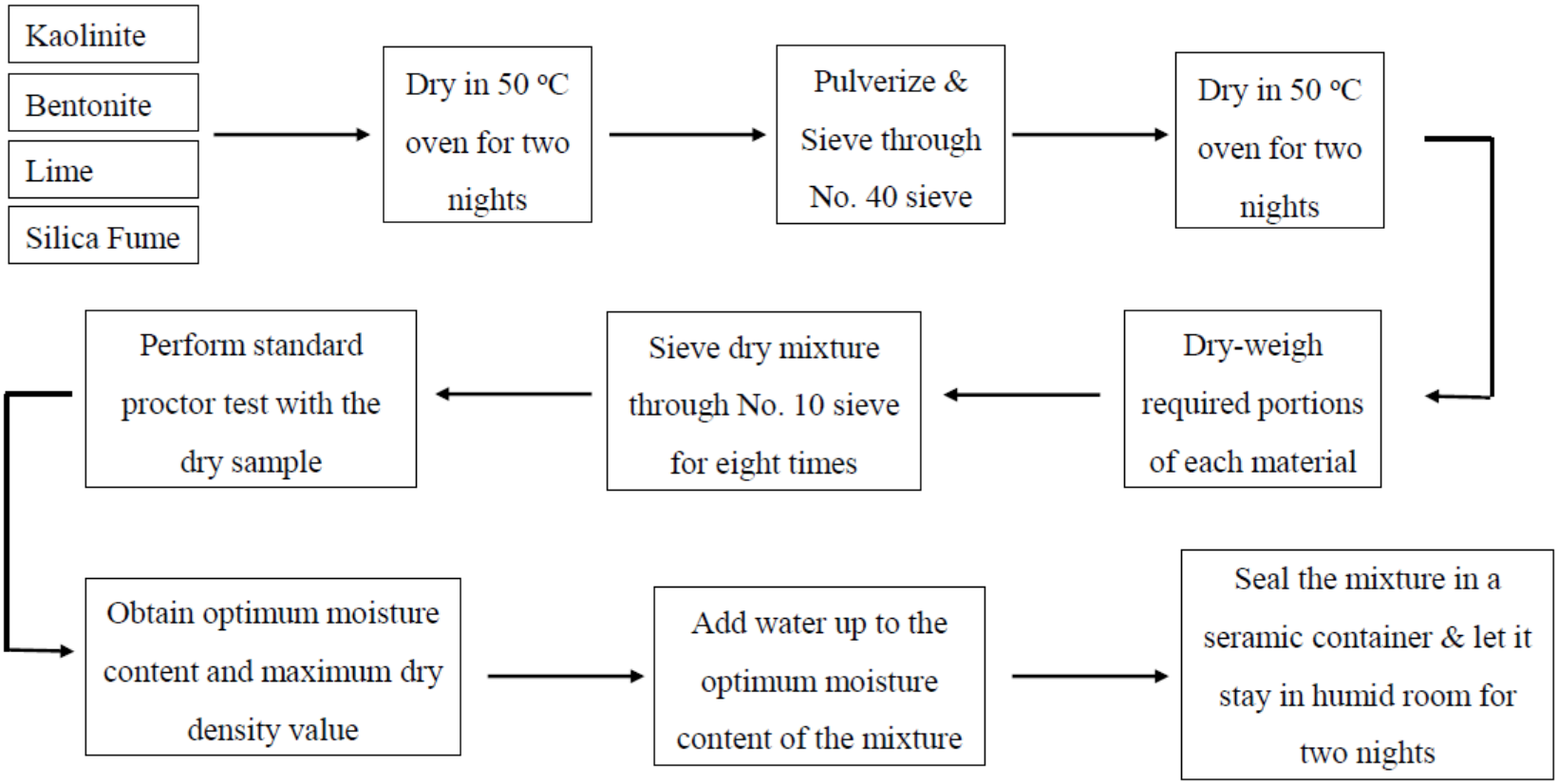

Figure 3.5 Sample Preparation Procedure

3.4 Sample Properties

Standard proctor tests, hydrometer tests, consistency limit tests, and specific gravity tests were applied to each sample as basic index tests. Moreover, each test was carried out in line with the relevant standards. As an important note, it should be stated that all of the basic index tests have conducted without the effect of pozzolanic reactions.

Standard proctor tests were applied to obtain compaction curves. ASTM D698 standard procedures were used while doing the tests. The mixtures were first dry-weighted and mixed roughly, and then the dry mixture passed from the No. 10 sieve eight times to have a high homogeneity. The experiment started with approximately 15% water content and increased by approximately 5% each time. The compaction curves of untreated and treated with 3% lime with varying percentages of silica fume samples are shown in Figure 3.6, and 5% lime with varying percentages of silica fume samples are given in Figure 3.7. In addition, the saturation values at the maximum dry density state of the treated and No-Additive sample are given in Table 3.3.

Grain size distribution curves of each sample were obtained by hydrometer test, done according to ASTM D7928. Since lime is a water-soluble substance, there was a need for a lime correction for ten out of eleven samples. This adjustment was made by adding the necessary amount of lime to the water-sodium hexametaphosphate solution. Then, the readings were used while calculating the value of the $\Delta\rho_{agent}$ term. The grain size distribution curves of two different lime-containing sets are shown in Figures 3.8 and 3.9.

Consistency limits tests were done in line with ASTM D4318. Before performing the tests, dry mixtures were blended with an eyeball-estimated amount of water, then placed in a humidity cabinet for one night to let water for absorption. Each of the liquid limit and plastic limit tests were repeated three times. The samples were

classified (Figure 3.10) by Unified Soil Classification System (USCS), with the results of consistency limit tests.

Specific gravity tests of the sample could not be done as mixtures. The reasons for this were; having hydrated lime that is soluble in water, becoming swollen and sticky due to relatively high percentages of bentonite, and having pozzolanic reactions. Then, each of the materials that were used in the samples was tested separately. ASTM D854 was followed while conducting specific gravity tests of kaolinite, bentonite, and silica fume. ASTM C188-14 was done to get the specific gravity value of lime. The procedure for ASTM C188-14 is as follows:

1. Make ready 50 gr of oven-dried soil sample.
2. Fill the Le Chatelier bottle with kerosene to a 0 to 1 mL scale at the stem.
3. Put the Le Chatelier bottle in a water bath set for a temperature between 23 ± 2 ^{o}C.
4. Let the Le Chatelier bottle in a water bath for at least an hour.
5. Take the bottle out of the water bath, and get the initial volume measurement, V_1.
6. Pour the prepared sample into the bottle without missing any particles using a glass funnel and close the flask with a stopper.
7. Either rotate the bottle while it is in a tilted position or carefully shake it in a horizontal plane.
8. Immerse the flask in a constant-temperature water bath for long enough to prevent differences in the temperature of more than 0.2 ^{o}C between the first and last readings.
9. Take the bottle out of the water bath, and get the final volume measurement, V_2.
10. Do this test at least two times to achieve less standard deviation than 0.10.

$$Density\ of\ the\ Sample, \qquad \rho = \frac{m}{(V_2 - V_1)} \qquad (Eq.3.1)$$

where m: Mass of the sample (gram)

V_1: First read volume (cm^3)

V_2: Last read volume (cm^3)

After obtaining every material's specific gravity value, each of the samples' specific gravity values is calculated by using the percentages of them from Table 3.1. Furthermore, the change in specific gravity due to the effect of additives is shown in Figure 3.11.

The variation in the liquid limit, plastic limit, and plasticity index are given in Figures 3.12, 3.13, and 3.14, respectively.

The activity values are calculated using the results of the hydrometer and Atterberg limit tests. In addition, the swelling potential is determined from the classification chart Seed et al., (1962) suggested. Figure 3.15 shows the provided chart, which contains each sample.

The properties of samples are tabulated in Table 3.4.

Table 3.3 Saturation Values at Maximum Dry Density State

Name	Saturation (%)
No-Additive	90.10
3% L	83.15
3% L + 5% SF	97.27
3% L + 10% SF	93.40
3% L + 15% SF	89.89
3% L + 20% SF	95.35
5% L	83.98
5% L + 5% SF	91.96
5% L + 10% SF	91.71
5% L + 15% SF	89.67
5% L + 20% SF	82.88

Table 3.4 Sample Properties

Name	% Clay	% Silt	LL	PL	PI	Activity %	USCS Name	G_s	Maximum Dry Density [g/cm^3]	Optimum Water Content [%]	Swelling Potential (Seed et al., 1962)
No-Additive	56.79	43.21	106	31	75	1.321	CH	2.631	1.4564	27.62	Very High
3% L	52.41	47.59	90	33	57	1.088	CH	2.625	1.4453	25.85	Very High
3% L + 5% SF	53.49	46.51	99	32	67	1.253	CH	2.614	1.3261	36.14	Very High
3% L + 10% SF	52.40	47.60	101	36	65	1.240	CH	2.604	1.3409	33.78	Very High
3% L + 15% SF	50.63	49.37	97	35	62	1.225	CH	2.593	1.3695	30.97	Very High
3% L + 20% SF	55.17	44.83	93	38	55	0.997	CH	2.582	1.3099	35.87	Very High
5% L	50.45	49.55	90	33	57	1.130	CH	2.620	1.4366	26.41	Very High
5% L + 5% SF	53.54	46.46	91	35	56	1.046	CH	2.610	1.3336	33.72	Very High
5% L + 10% SF	53.95	46.05	95	38	57	1.057	CH	2.599	1.3359	33.37	Very High
5% L + 15% SF	54.38	45.62	103	40	63	1.159	CH	2.589	1.3568	31.45	Very High
5% L + 20% SF	52.44	47.56	104	43	61	1.163	CH	2.578	1.2971	31.75	Very High

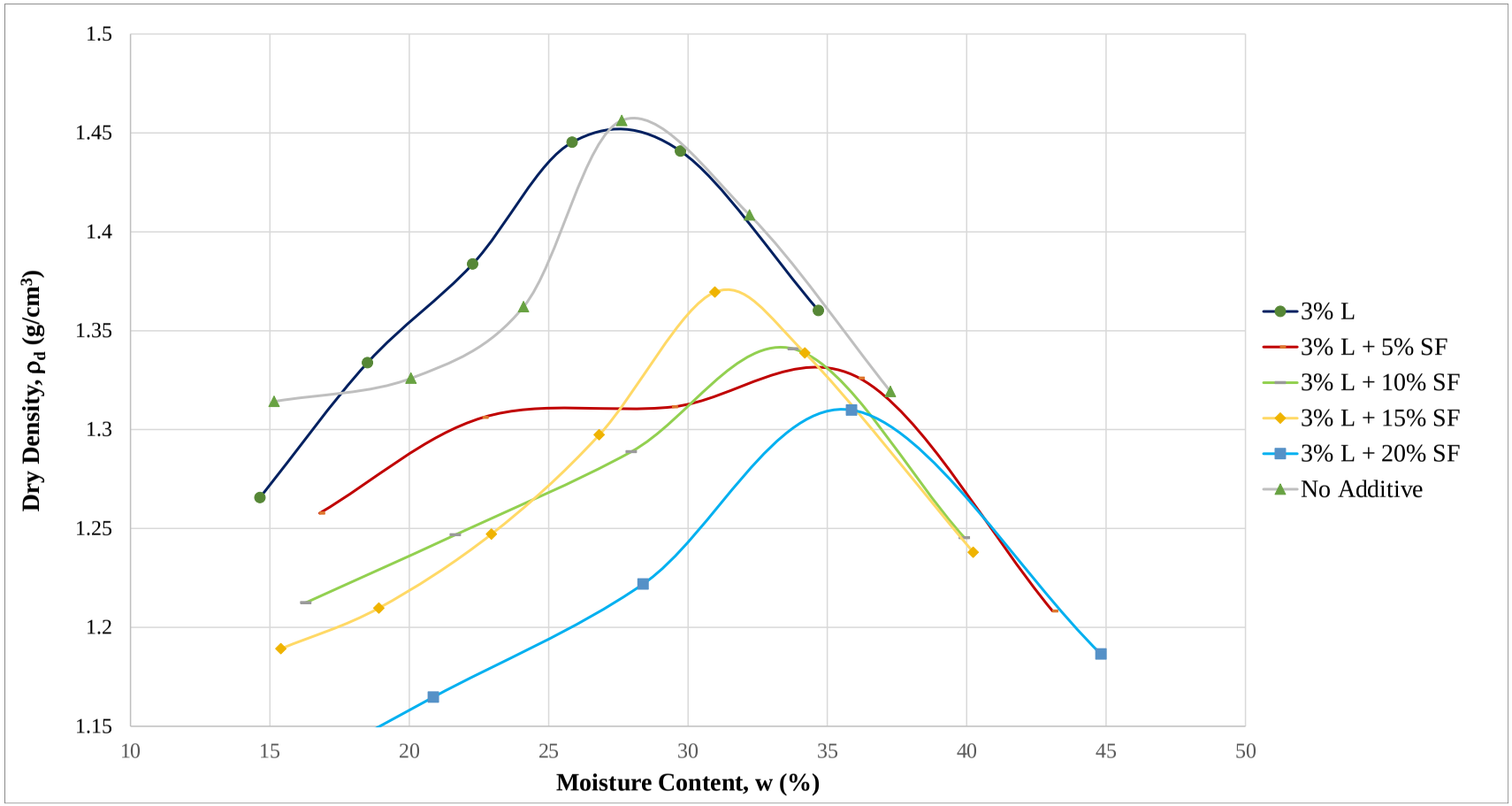

Figure 3.6 Compaction Curves of 3% Lime-Added Set

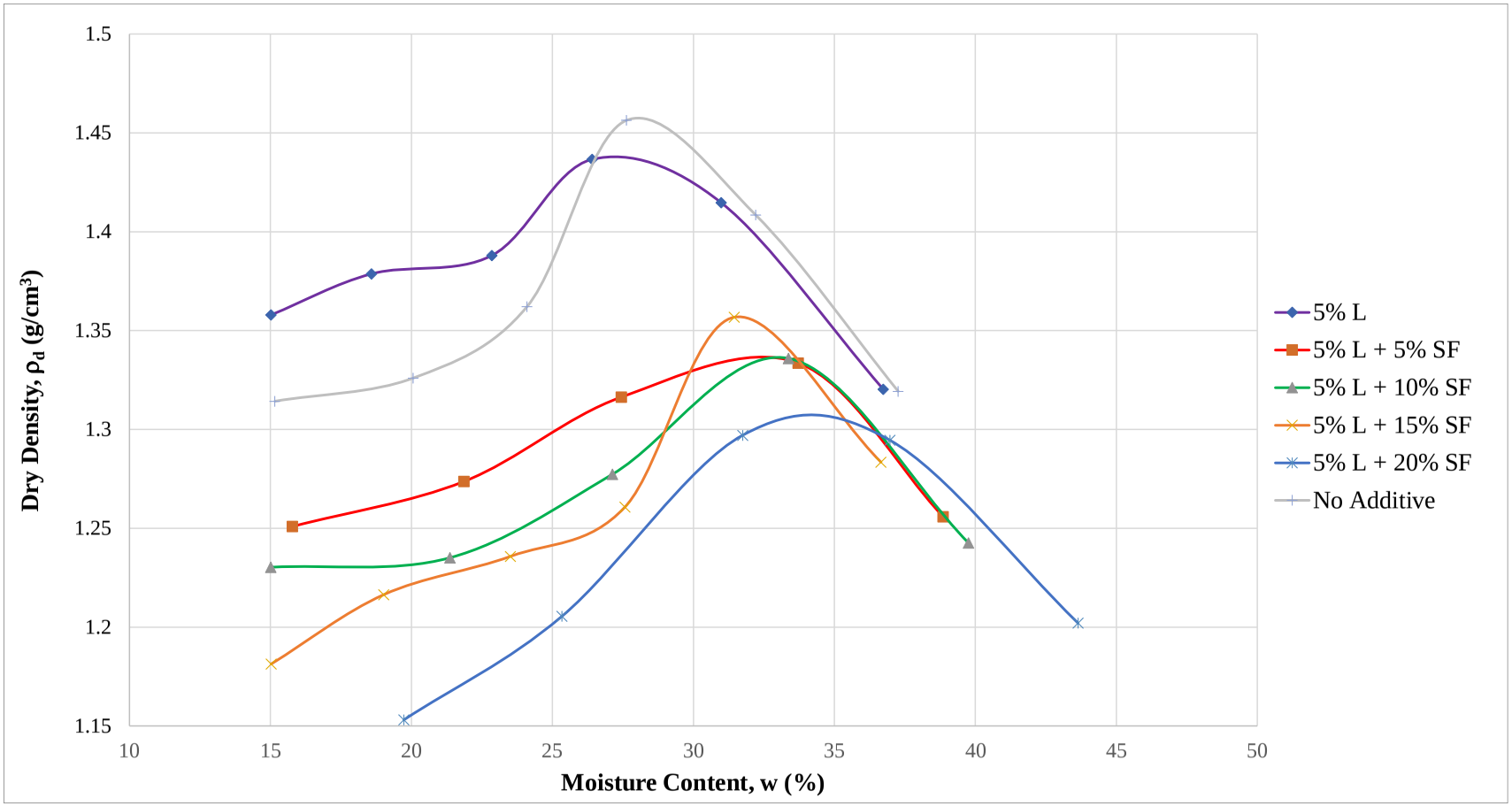

Figure 3.7 Compaction Curves of 5% Lime-Added Set

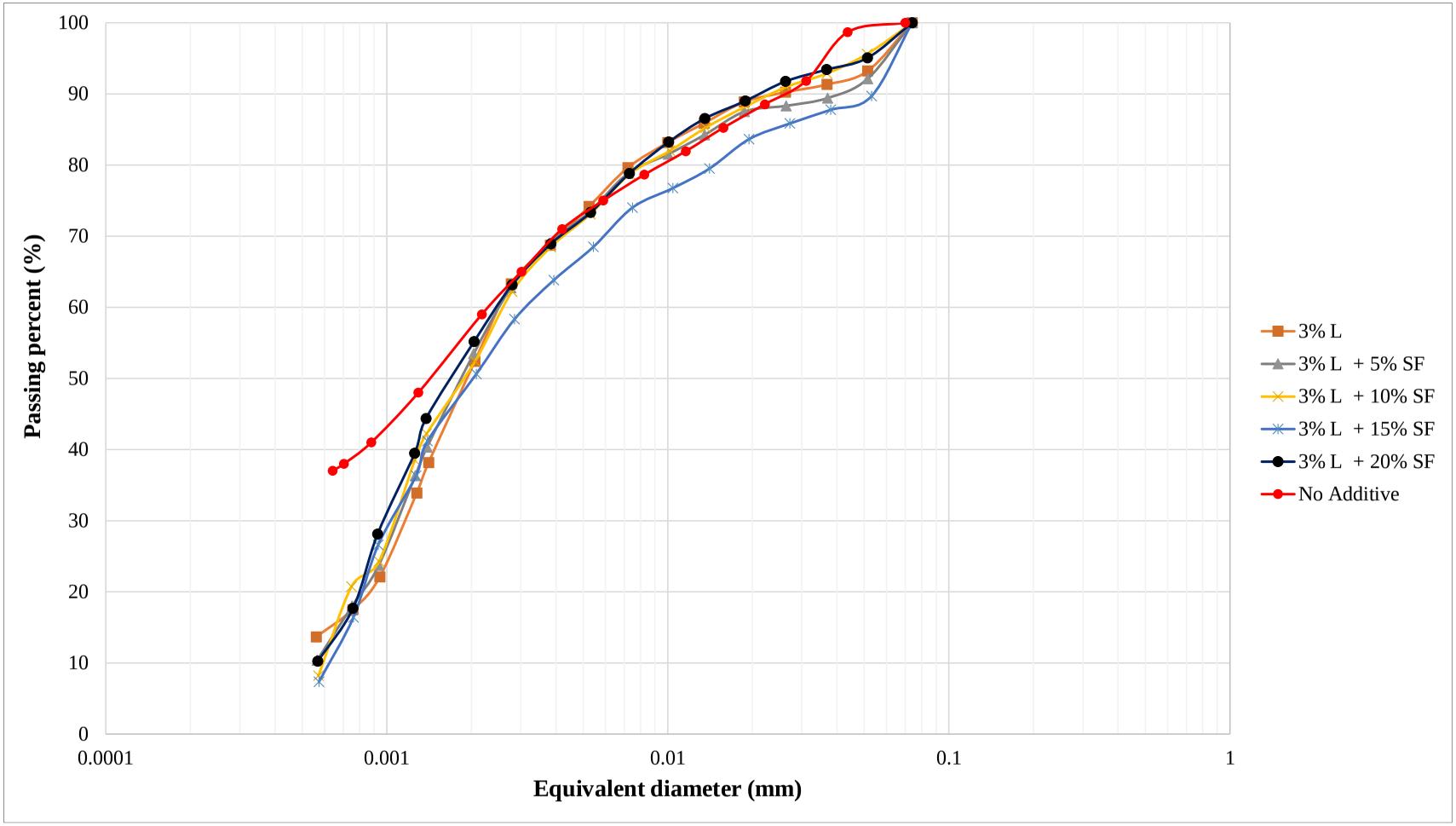

Figure 3.8 Grain Size Distribution Curves of 3% Lime-Added Set

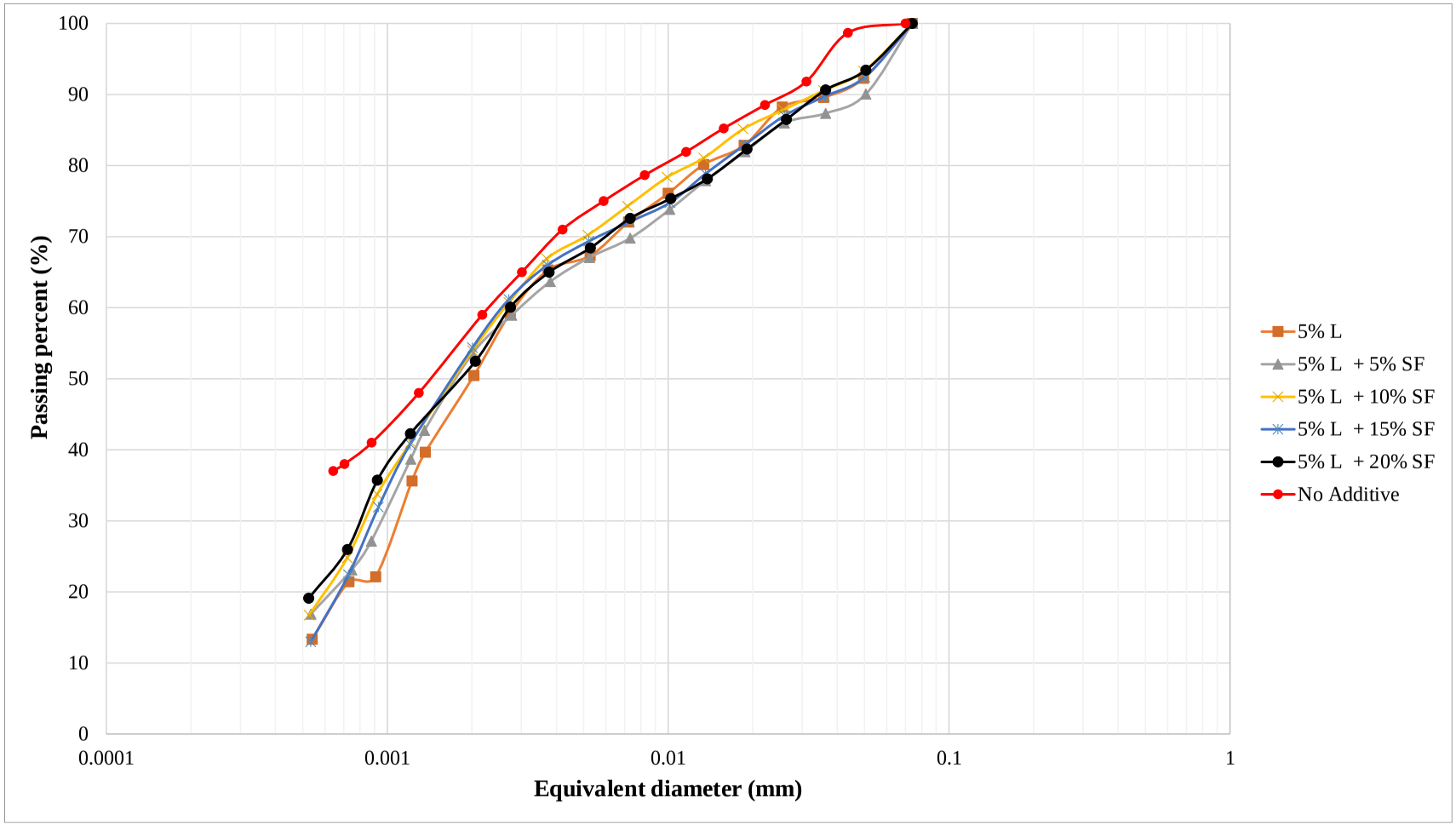

Figure 3.9 Grain Size Distribution Curves of 5% Lime-Added Set

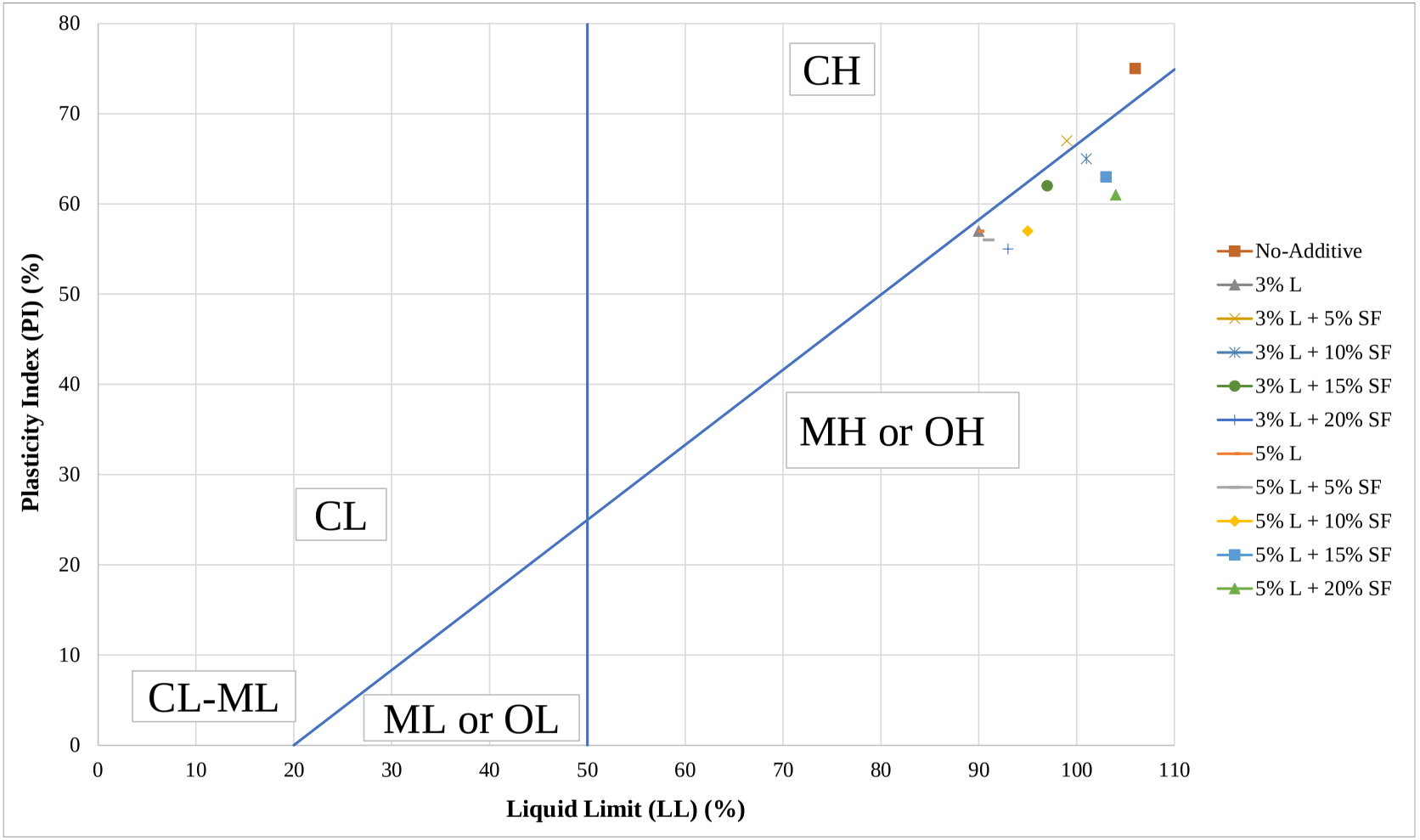

Figure 3.10 Plasticity Chart (USCS)

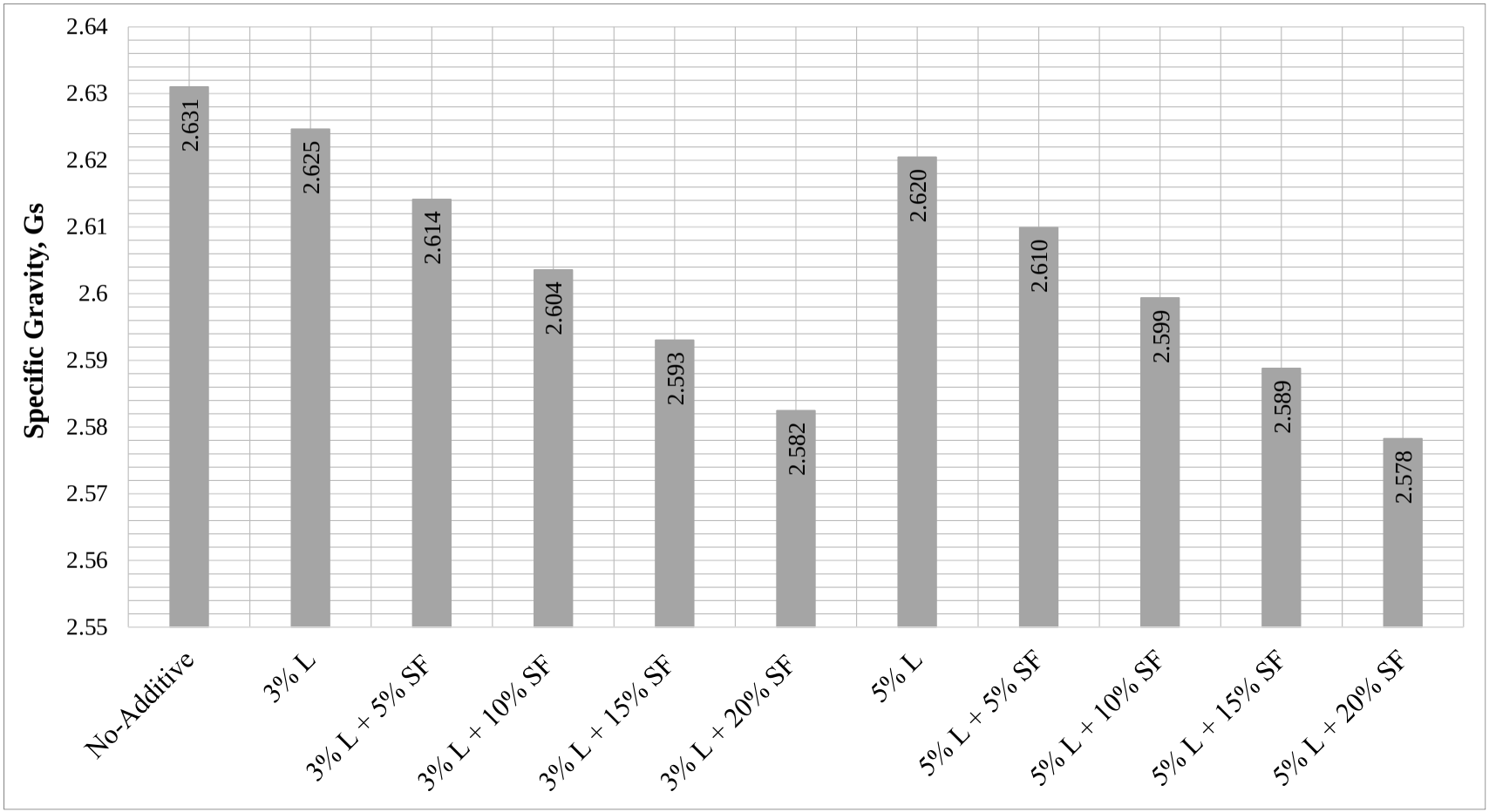

Figure 3.11 Effect of Addition of Lime and Silica Fume on Specific Gravity

Figure 3.12 Effect of Addition of Lime and Silica Fume on Liquid Limit (LL)

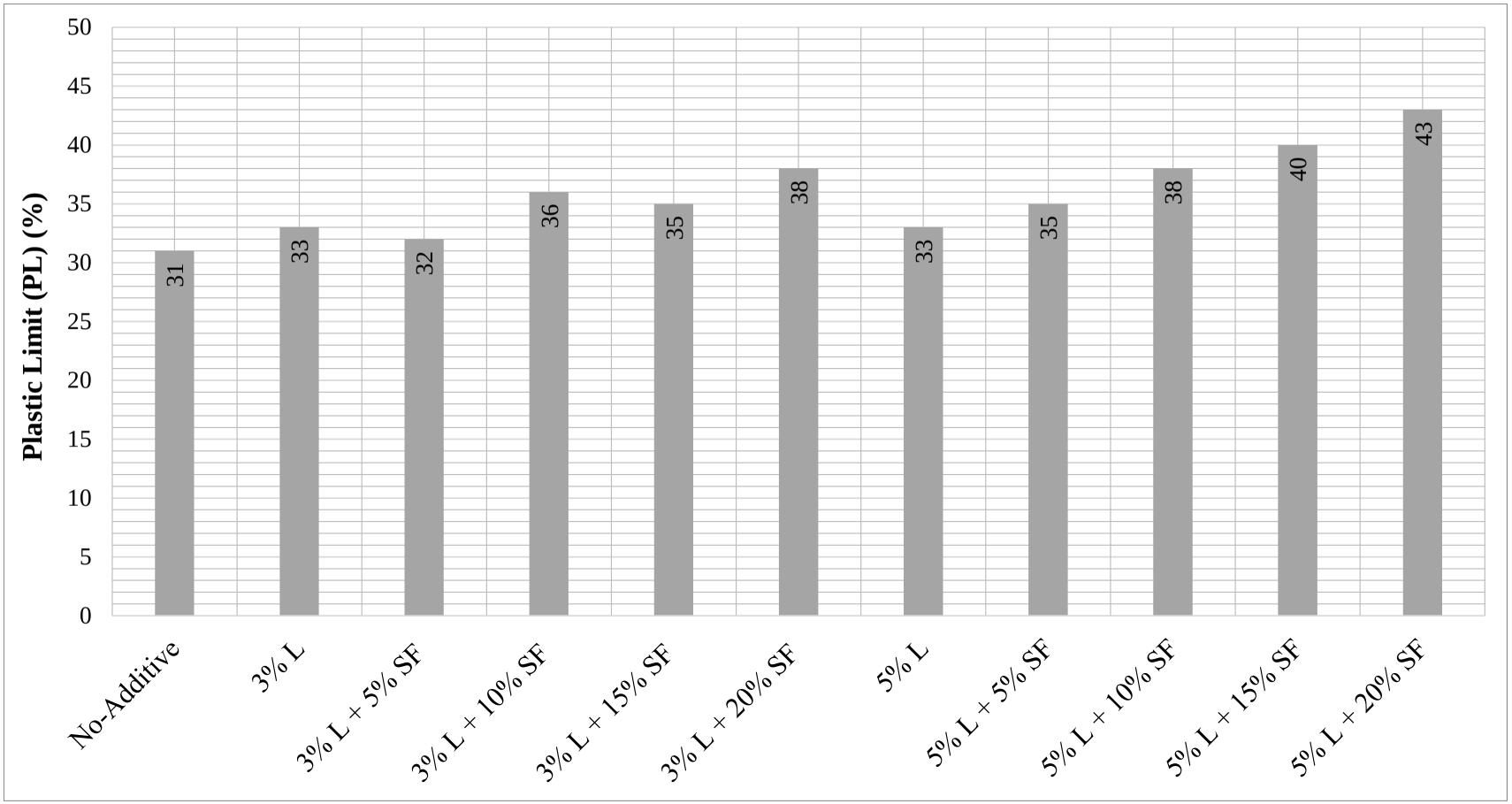

Figure 3.13 Effect of Addition of Lime and Silica Fume on Plastic Limit (PL)

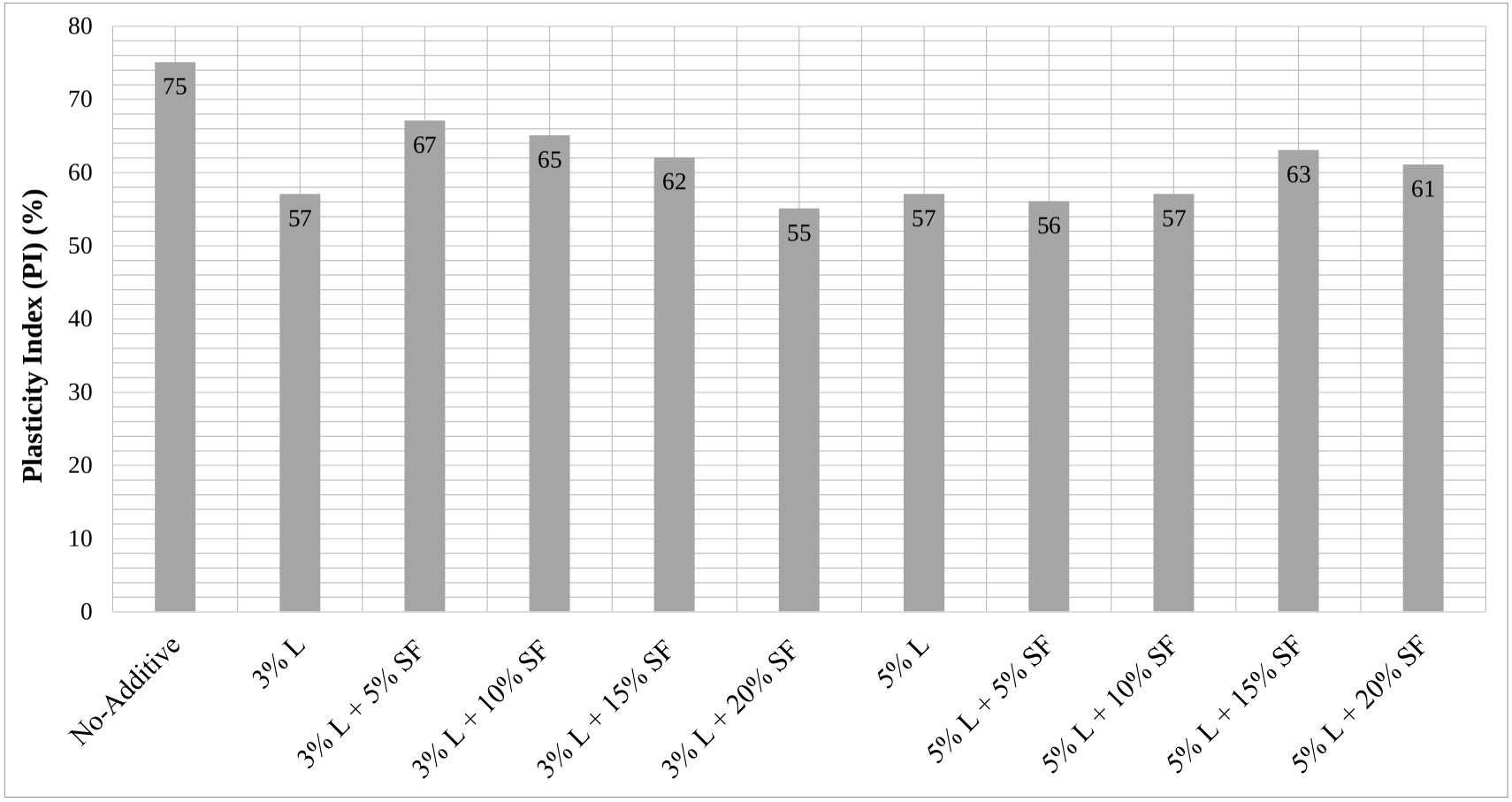

Figure 3.14 Effect of Addition of Lime and Silica Fume on Plasticity Index (PI)

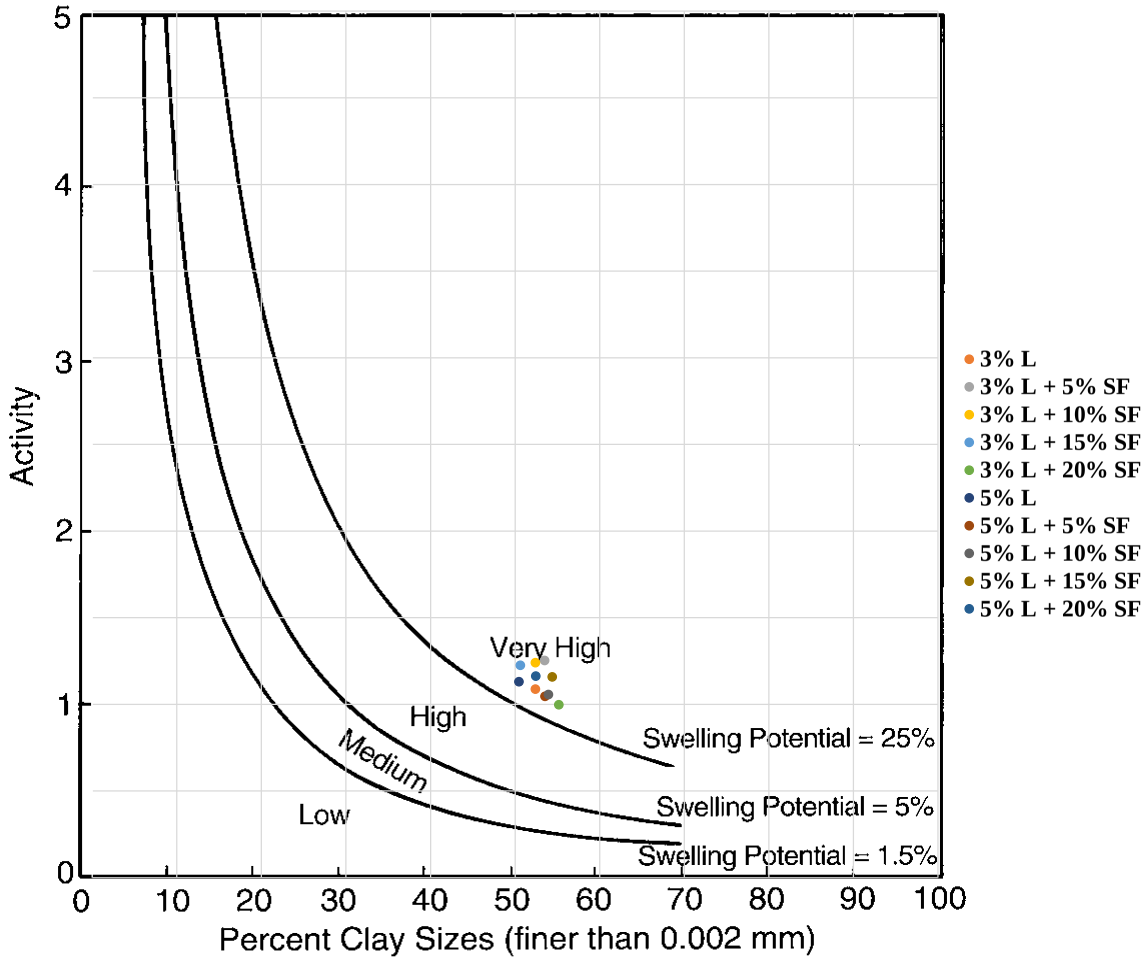

Figure 3.15 Classification Chart for Swelling Potential (After Seed et al., (1962))

3.5 Test Procedures

3.5.1 Free Swell Test

3.5.1.1 Preparing the Specimen

The specimens were prepared as reconstituted samples. The dry samples were mixed with their optimum water content amount and left in a humid room for two nights for evenly distributed water. One day desiccator-waited bulk samples were compacted for their maximum dry density values, as stated in Table 3.2. The procedure was done by statically compacting the bulk samples in a cutting ring with 18.9 mm height and 63 mm diameter (Figure 3.16) using a hydraulic jack (Figure 3.17). In addition, the three-layered under-compaction method was used to have more homogeneously compacted specimens.

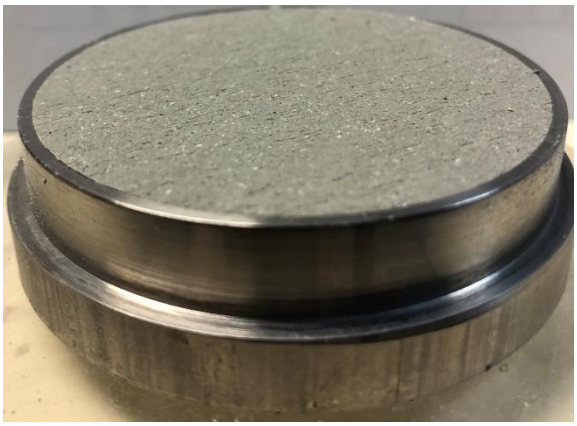

Figure 3.16 A View of the Specimen Compacted into the Cutting Ring

3.5.1.2 Test Procedure

The free swell test method was used to determine the swelling percent of the specimens, which were compacted in the cutting ring as previously described. ASTM D4829 was followed while conducting the free swell test. All of the free swell tests

were done by using the Bishop apparatus (Figure 3.17). The following procedure is applied for the free swell test:

1. Put porous stone with filter paper on top of it at the base of the oedometer cell.
2. Place the cutting ring that has the compacted specimen on filter paper.
3. Put another filter paper over the top of the cutting ring surface.
4. Fix the cutting ring, and place the top cap on the upper filter paper.
5. Place and adjust the loading frame and arm.
6. Apply a small surcharge (7 kPa) without inundating the cell for 10 minutes to let it compress under the surcharge.
7. Adjust the dial gauge to zero after 10 minutes of applying the surcharge load.
8. Pour distilled water until the cell is full of water.
9. Start the chronometer when the dial gauge readings start to increase.
10. Take readings at specific intervals (0.5 min, 1 min, 2 min, 4 min, 15 min, 30 min, 1 hour, 2 hours, one day, two days) until the change between the two readings becomes less than 0.005 times specimen height.

The obtained data were used to calculate each of the specimen's free swell percentages as follows:

$$Swell\ Percent = \left(\frac{H_f - H_i}{H_i}\right) \times 100 \qquad (Eq.3.2)$$

Where H_i = Initial height of the sample

H_f = Final height of the sample

The time vs. swell percentage graphs were plotted by using the Taylor method.

The stabilization percentages are calculated by below equation.

$$Stabilization\ Percent = \left(\frac{Untreated\ Swell\ - Treated\ Swell}{Untreated\ Swell}\right) \times 100 (Eq.3.3)$$

Since there will be both the effects of silica fume + lime application and replacing some amount of expansive soil with unexpansive soil had a part in reducing the No-

Additive samples swelling percent value in treated samples, there could be a correction application. Within this concept the “net swell” values can be calculated for each treated sample by simply:

$$Net\ Swell = Untreated\ Swell\ x\ (100 - Total\ Percent\ of\ Additive)\ (Eq.3.4)$$

With the calculated net swell values, the net swell stabilization percentages are calculated for each specimen.

Although, it can be stated that the collected datas can be used to check the rate of swell, there is just one theory about the rate of swell estimation in the literature. According to Basma & Tuncer, (1991), it is proposed that the swell rate might be determined by measuring an amount of time equivalent to fifty percent of the final swell value.

For studies on cured specimens, the cutting ring-compacted samples were allowed to cure without wrapping around in a desiccator in a humidity room. The specimens were cured for periods of 7 and 28 days.

Figure 3.17 Bishop Apparatus

3.5.1.3 Results

At least two tests were done for every sample to decide whether they have done correctly. When reporting test results, two values close enough to each other were taken, their average was taken and reported.

The percent swell vs. time graph for No-Additive sample is shown in Figure 3.18.

The percent swell vs. time graph of the lime plus silica fume added samples are shown in Appendix A.

Since swell rate estimation is just based on a single suggestion, the swell rate results were not detailed and considered due to that. However, a graph in Appendix C shows swell percent vs. percent additive results with 0-7-28 days of curing for each treated sample.

Swelling percentage by percent additive graph of No-Additive sample and lime plus silica fume treated without curing samples are shown in Figure 3.19.

Swelling percentage by percent additive graph of No-Additive sample and lime plus silica fume treated with 7 days of curing samples are shown in Figure 3.20.

Swelling percentage by percent additive graph of No-Additive sample and lime plus silica fume treated with 28 days of curing samples are shown in Figure 3.21.

The net swell percentage vs. percent additive graph of the lime plus silica fume added samples are shown in Appendix D. And also, stabilization percentages in net swell percentages by changing additive percentages are given in Appendix D.

In order to clearly observe the influence of the additives and the effect of curing, the swelling percentage of No-Additive sample was presented in all swell percentages by percent additive figures.

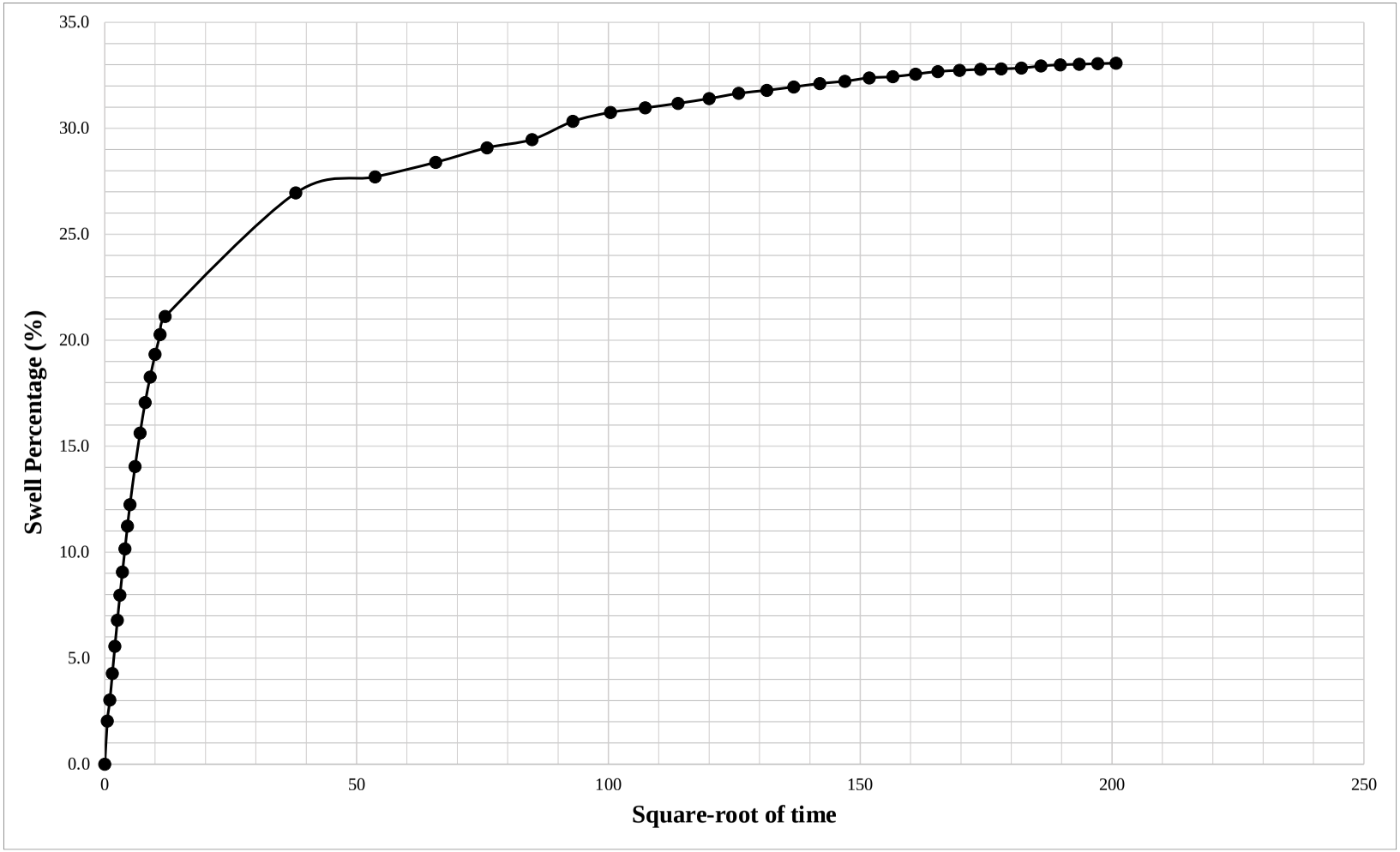

Figure 3.18 Percent Swell vs Square-Root of Time relationship for No-Additive Sample

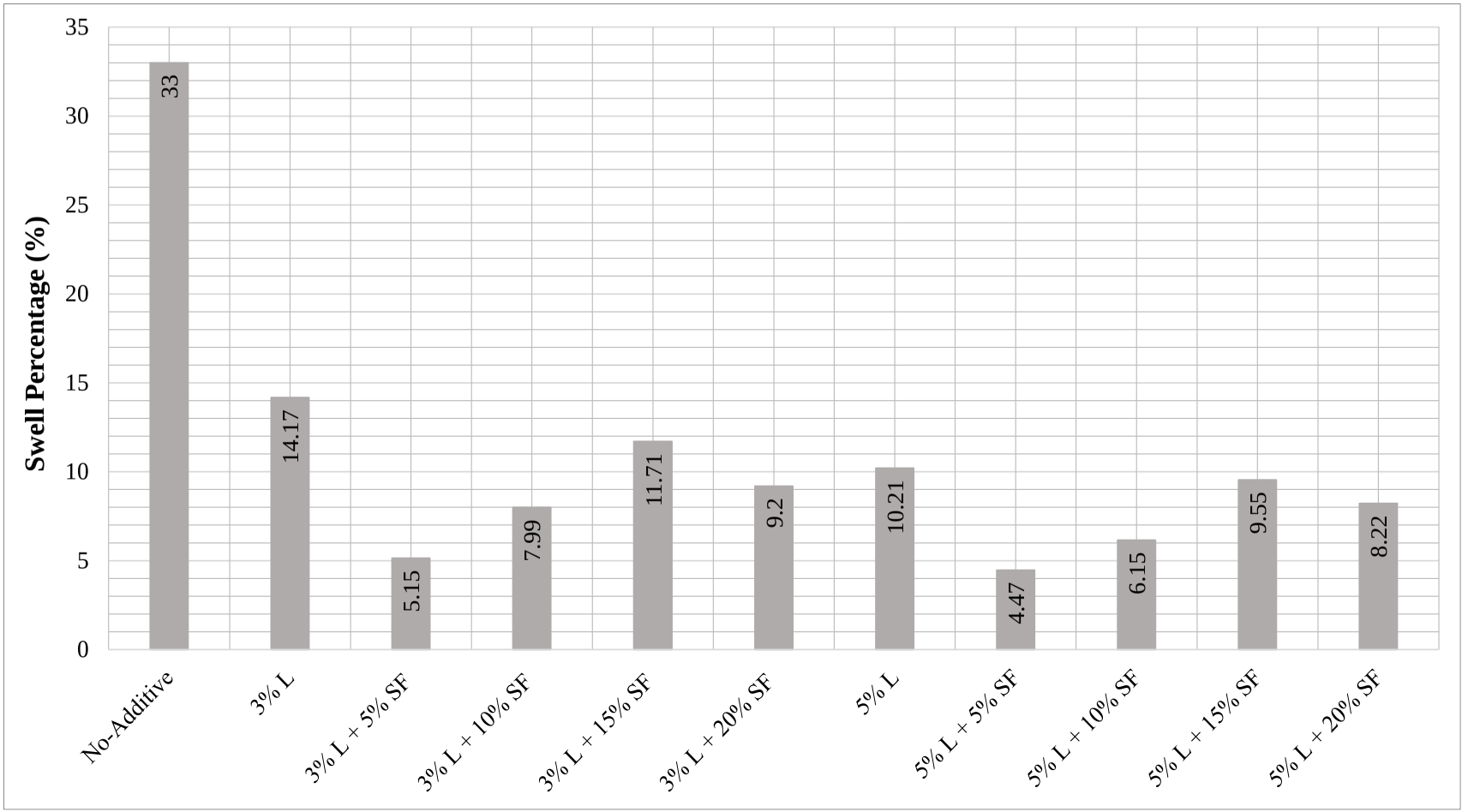

Figure 3.19 Effect of Addition of Lime and Silica Fume on Swelling Percent without Curing

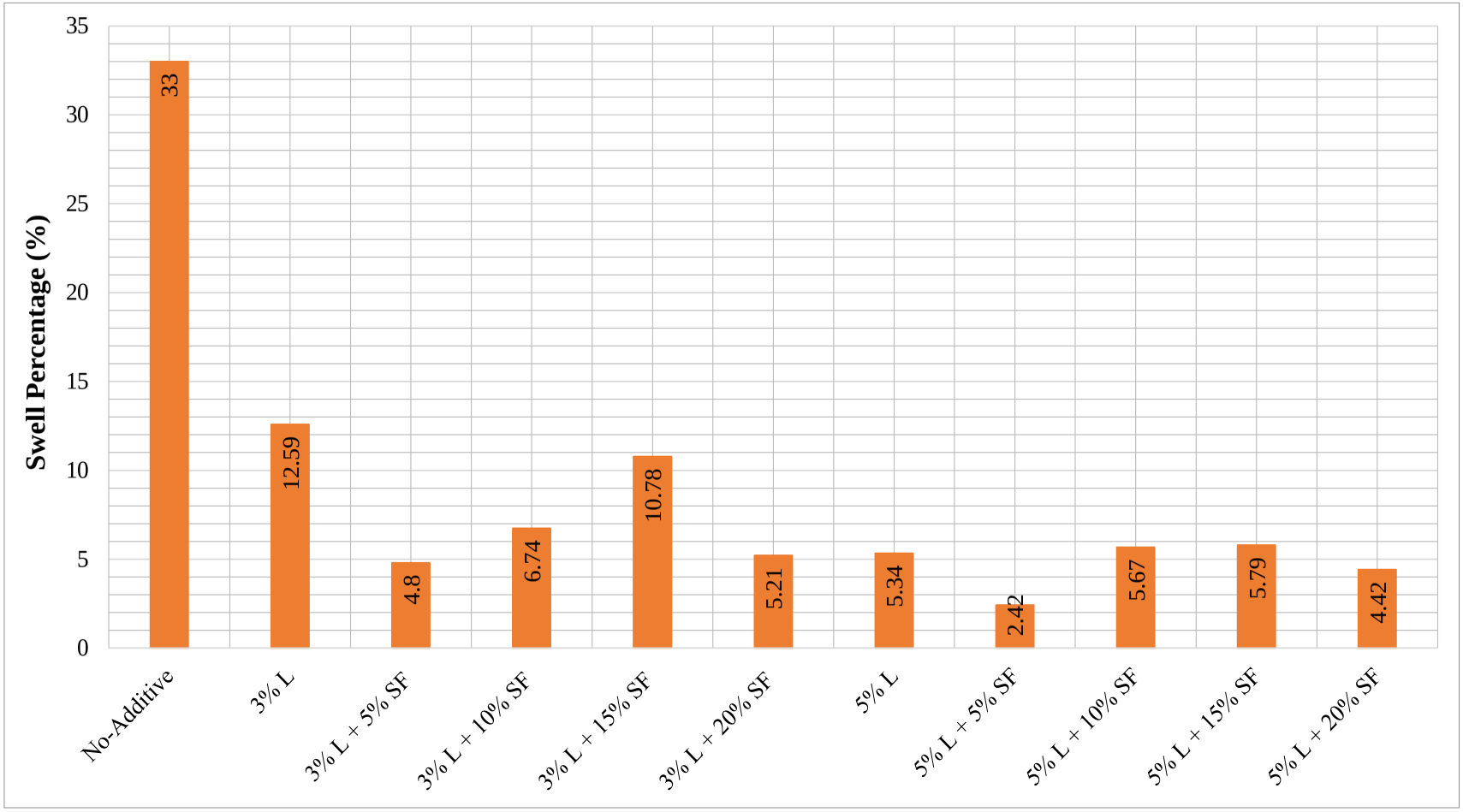

Figure 3.20 Effect of Addition of Lime and Silica Fume on Swelling Percent with 7 Days of Curing

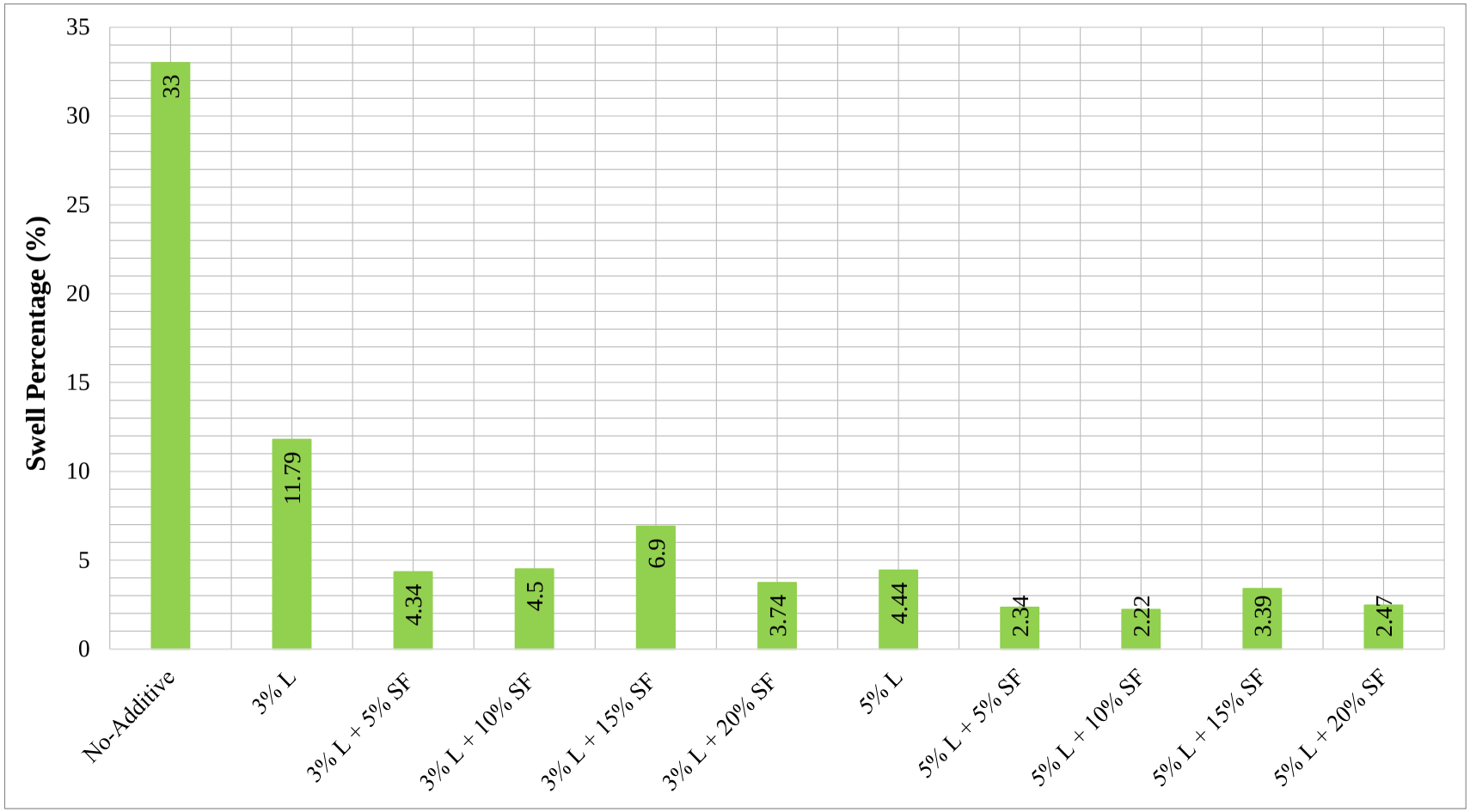

Figure 3.21 Effect of Addition of Lime and Silica Fume on Swelling Percent with 28 Days of Curing

3.5.2 Unconfined Compression Test

3.5.2.1 Preparing The Specimen

The specimens were prepared as explained in section 3.3, except the dimensions of the specimens were 36 mm diameter and 72 mm height. In Figure 3.22, the used equipment that was used to get appropriate dimensioned specimens is shown. In addition, a view from static compaction done by hydraulic jack is given in Figure 3.23. While compacting the samples, the procedure is used as follows:

1. Put filter paper not to lose any particles.
2. Place the compaction mold and its extender over the filter paper.
3. Pour soil into the mold with the help of a funnel.
4. Statically compact the sample with the long part of the piston.
5. Remove the extender and turn the mold upside down to have a uniform density.
6. Compress the sample with the short part of the piston.
7. Put another mold with a larger diameter than the specimen to remove the sample from the compaction mold without any disturbance.

Take the specimen from the mold in the reverse direction they were compacted.

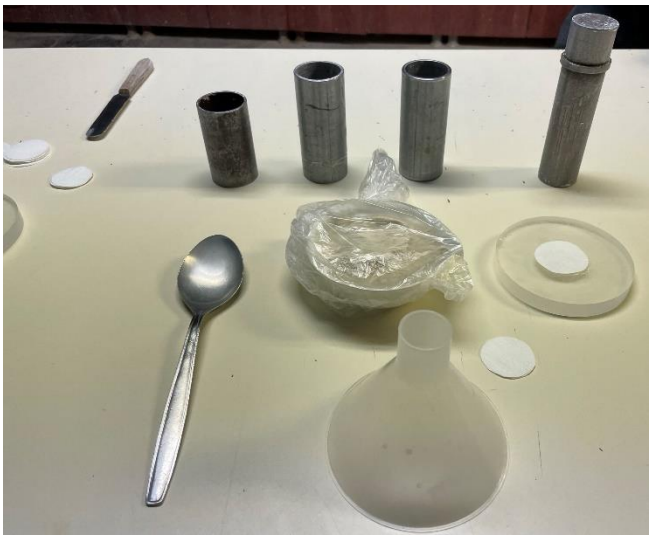

Figure 3.22 Equipments for Specimen Compaction for Unconfined Compressive Strength Test

Figure 3.23 A View of Static Compaction Done by Hydraulic Jack

3.5.2.2 Test Procedure

The unconfined compressive strength tests were done with Wykeham Farrance Tritech ID 10 kN compression test machine (Figure 3.24) according to ASTM D2166. Three commonly prepared specimens were tested for each of the samples. The steps were followed:

1. Place the soil between the greased plates.
2. The ASTM D2166 is stated that the strain rate could be between 0.5 to 2 percent per mm/min. In this study, a 1% strain rate is used, which equals 0.72 mm/min. And this strain rate was maintained for all of the UCS tests.
3. Move the bottom until the loading frame touches the specimen (can be identified by observing one to two division changes in the axial load dial gage)
4. Start the test and move the bottom plate until one failure condition is observed.
    - If an apparent failure plane is observed,
    - If the axial load drops by 25%,
    - If the specimen has reached 15% strain,
    - When the specimen has reached 5% strain after the peak strength,
5. After the test, take diameter measurements to check the cylindrical assumption.
6. Take water content measurements.

The deformation modulus which can be called as E_{50} value is obtained by drawing a secant line to c_u value.

The prepared specimens were left to cure in the absence of any coverings in a desiccator which was also in a humidity cabinet for testing the cured specimens. The curing periods of 7 and 28 days were obtained.

Figure 3.24 Uniaxial Compression Test Device

3.5.2.3 Results

At least two tests were done for every sample to decide whether they have done correctly. When reporting test results, two values close enough to each other were taken, their average was taken and reported.

The stress vs. strain graphs for No-Additive sample is shown in Figure 3.25.

The stress vs. strain graphs of the lime plus silica fume added samples are shown in Appendix A.

Unconfined compressive strength by percent additive graph of No-Additive sample and lime plus silica fume treated without curing samples are shown in Figure 3.26.

Unconfined compressive strength by percent additive graph of No-Additive sample and lime plus silica fume treated with seven days of curing samples are shown in Figure 3.27.

Unconfined compressive strength by percent additive graph of No-Additive sample and lime plus silica fume treated with 28 days of curing samples are shown in Figure 3.28.

In order to observe the influence of the additives and the effect of curing, the unconfined compressive strength of No-Additive sample was presented in all unconfined compressive strength by percent additive figures.

Deformation modulus, E_{50} by percent additive graph of No-Additive sample and lime plus silica fume treated without curing samples are shown in Figure 3.29.

Deformation modulus, E_{50} by percent additive graph of No-Additive sample and lime plus silica fume treated with seven days of curing samples are shown in Figure 3.30.

Deformation modulus, E_{50} by percent additive graph of No-Additive sample and lime plus silica fume treated with 28 days of curing samples are shown in Figure 3.31.

In order to observe the influence of the additives and the effect of curing, the unconfined compressive strength of No-Additive sample was presented in all deformation modulus, E_{50} by percent additive figures.

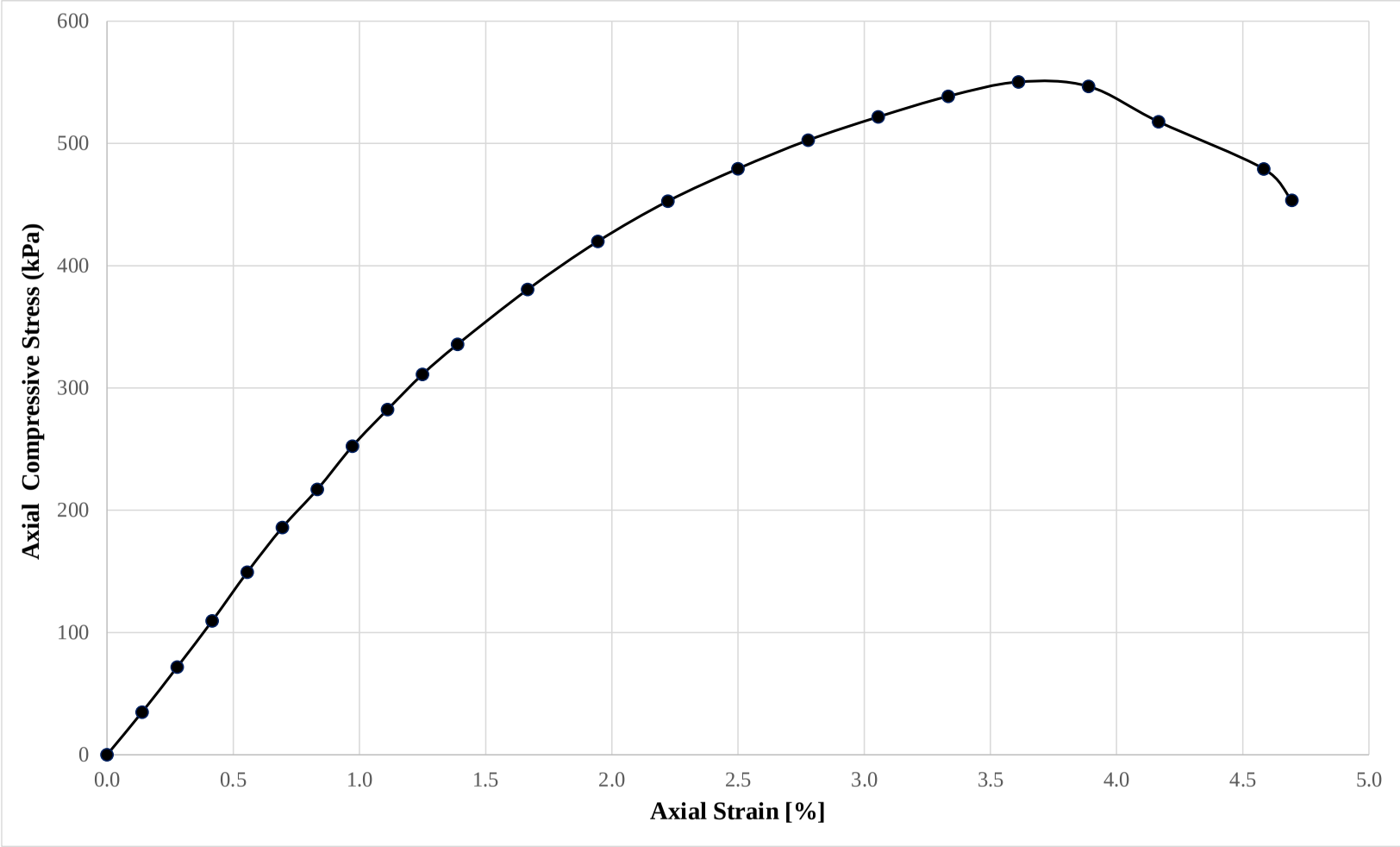

Figure 3.25 Axial Compressive Stress vs Axial Strain Relationships for No-Additive Sample

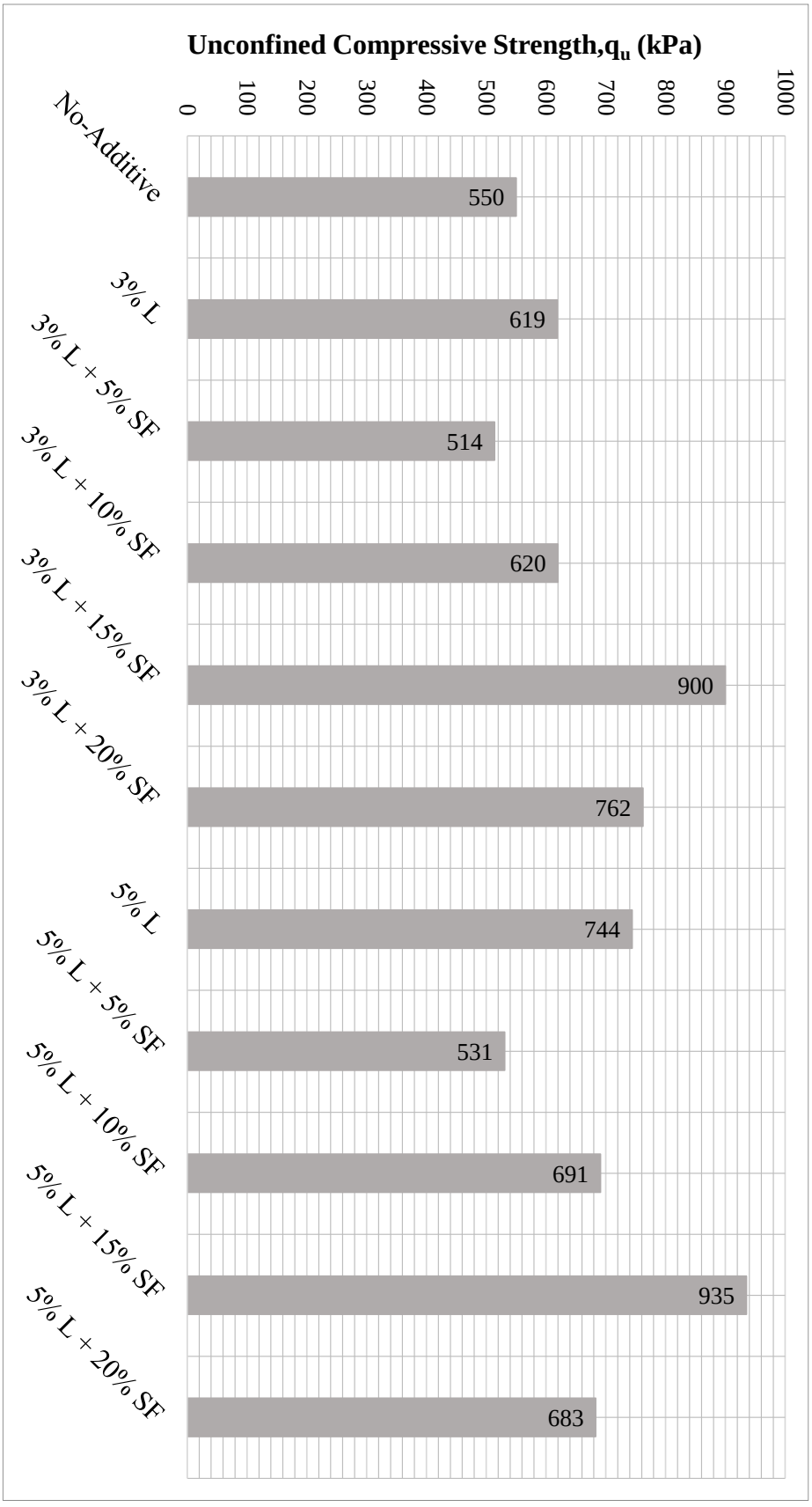

Figure 3.26 Effect of Addition of Lime and Silica Fume on Unconfined Compressive Strength without Curing

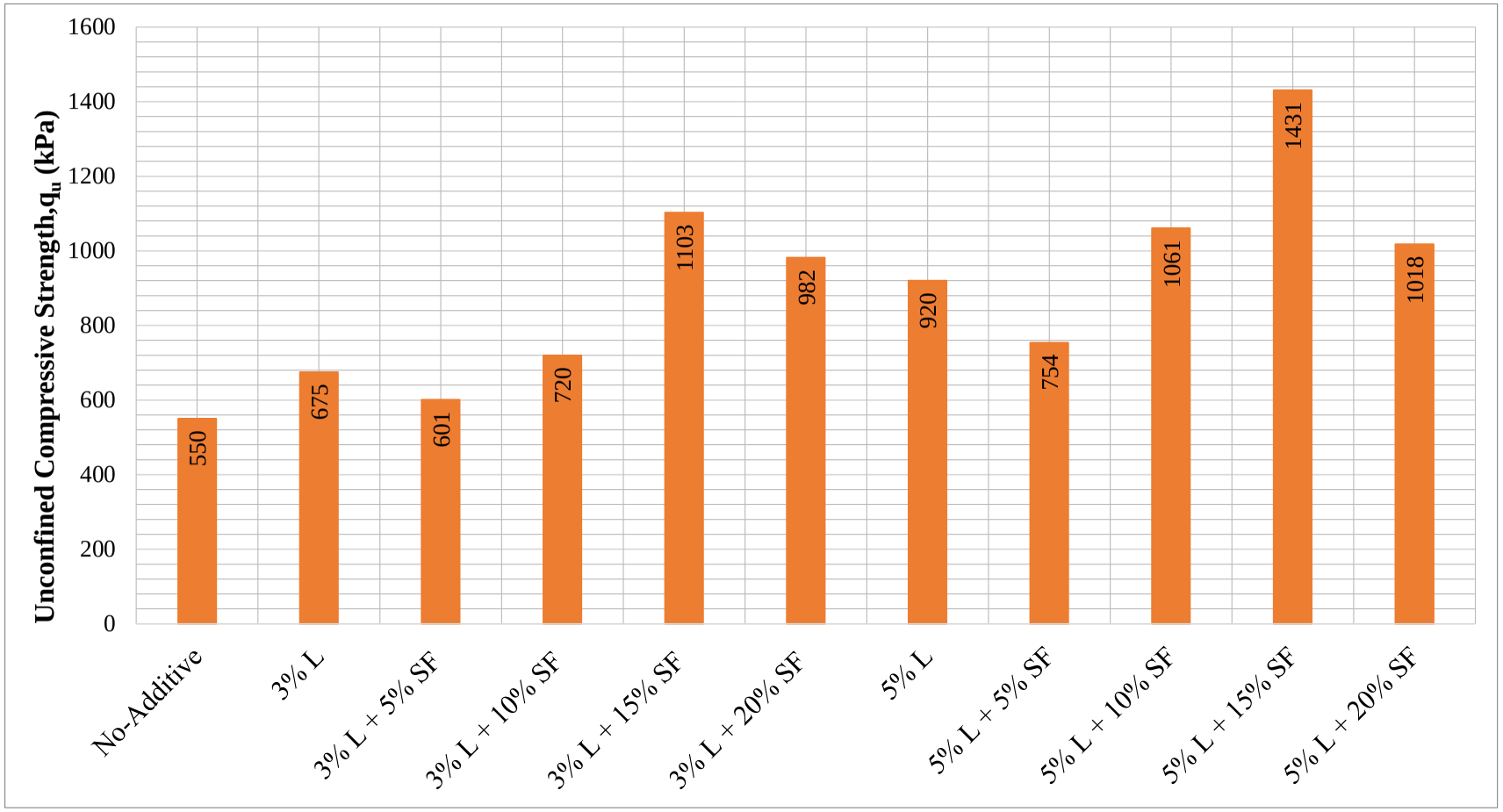

Figure 3.27 Effect of Addition of Lime and Silica Fume on Unconfined Compressive Strength with 7 Days of Curing

Figure 3.28 Effect of Addition of Lime and Silica Fume on Unconfined Compressive Strength with 28 Days of Curing

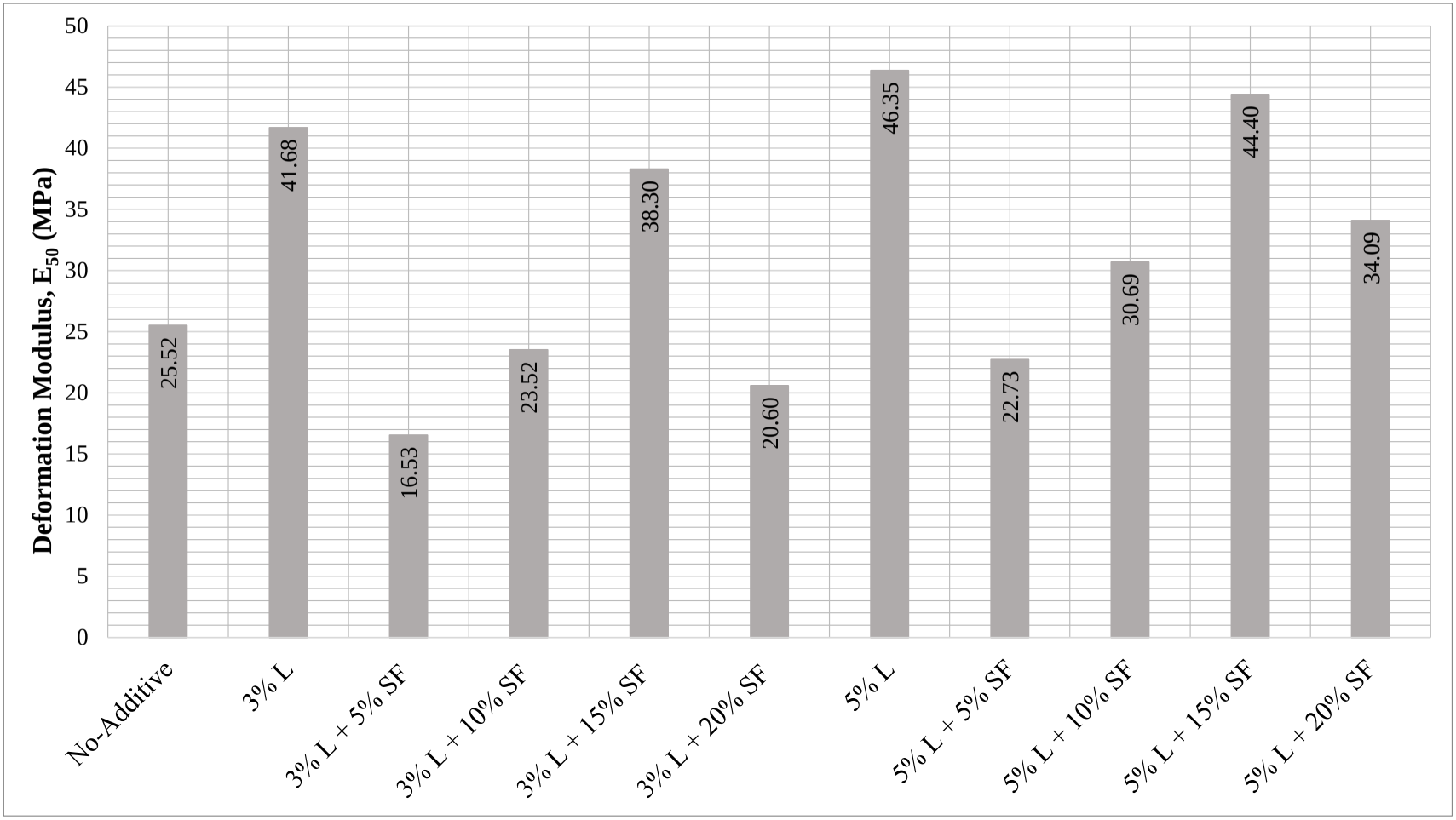

Figure 3.29 Effect of Addition of Lime and Silica Fume on Deformation Modulus, E_{50} without Curing

Figure 3.30 Effect of Addition of Lime and Silica Fume on Deformation Modulus, E_{50} with 7 Days of Curing

Figure 3.31 Effect of Addition of Lime and Silica Fume on Deformation Modulus, E50 with 28 Days of Curing

CHAPTER 4

DISCUSSION OF RESULTS

4.1 Effect of Stabilizers on Specific Gravity, Gs

Specific gravity values for kaolinite, bentonite, lime, and silica fume were 2.61, 2.75, 2.41, and 2.41, respectively. The specific gravity of No-Additive sample was determined to be 2.63. Lime and silica fume's specific gravity is less than No-Additive sample's. As a result, the samples created by adding lime and silica fume had a lower specific gravity than No-Additive sample (Figure 3.11).

4.2 Effect of Stabilizers on Grain Size Distribution

The addition of stabilizers altered No-Additive sample's grain size distribution curve to the coarser side (Figures 3.8, 3.9). Furthermore, according to Table 3.3, for the 3% lime-added set, the 3% L + 15% SF sample showed the maximum stabilization with the maximum increase in silt percentage. Also, the 5% L sample had the maximum stability with the maximum change in silt percentage for the 5% lime-added group. Since sodium hexametaphosphate was used during the hydrometer tests, the percent change in silt value can not be related to the flocculation resulting from pozzolanic reactions. Finally, the changing of grain size distribution curves was caused mainly by adding coarser material to No-Additive sample.

Furthermore, the present findings are consistent with the results reported by Kumar et al., (2012), which demonstrated that a rise in lime amount is associated with a noticeable decrease in clay content and a simultaneous increase in the proportion of coarser particles.

4.3 Effect of Stabilizers on Maximum Dry Density, $\rho_{dry,max}$ and Optimum Moisture Content, w_{opt}

The effect of additives on the optimum water content (w_{opt}) and maximum dry density values ($\rho_{dry,max}$) obtained from the compaction tests performed with standard proctor energy on the samples are shown in Figures 4.1 and 4.2. As shown in Figure 4.1, the maximum dry density, $\rho_{dry,max}$ values decrease with the addition of lime and silica fume. As seen in Figure 4.2, the optimum water content, w_{opt} values increase with the addition of lime and silica fume together; however, the optimum water content values decrease with just lime.

As stated by ,Sharma et al. (2012), the particles coat the clay surfaces, leading to the formation of larger particles with additional gaps, consequently causing a decrease in density. The stabilizing agent is used to fill the voids in the modified soil samples (Yarbaşı et al., 2007). The reduction in the overall surface area occurs when the soils are covered and interconnected by SF and numerous lime particles through coagulation and aggregation. This is due to the increased demand for water in the pozzolanic reaction of the free radicals of lime. Consequently, this process requires an increased quantity of water, resulting in an increase in the Optimum Moisture Content (OMC) (Zaini & Hasan, 2023). Yarbaşı et al., (2007) reported that altering the particle size and porous structure of clayey specimens treated with silica fume resulted in an elevation of the optimum moisture content (OMC). In addition, the inclusion of silica fume can lead to a decrease in the amount of free clay, leading to a material that is coarser and possesses a larger surface area. According to the findings of Harichane et al., 2011a), it is evident that this particular technique necessitates a greater amount of energy, thereby implying that an increased quantity of water is required for the compression of the specimens. Furthermore, the slight decline in the optimum moisture content (OMC) can be explained by the research conducted by Harichane, et al., (2011b). This decrease is mainly due to the substitution of soil with natural pozzolana, which possesses a comparatively lower specific gravity.

Figure 4.1 Effect of Addition of Lime and Silica Fume on Maximum Dry Density

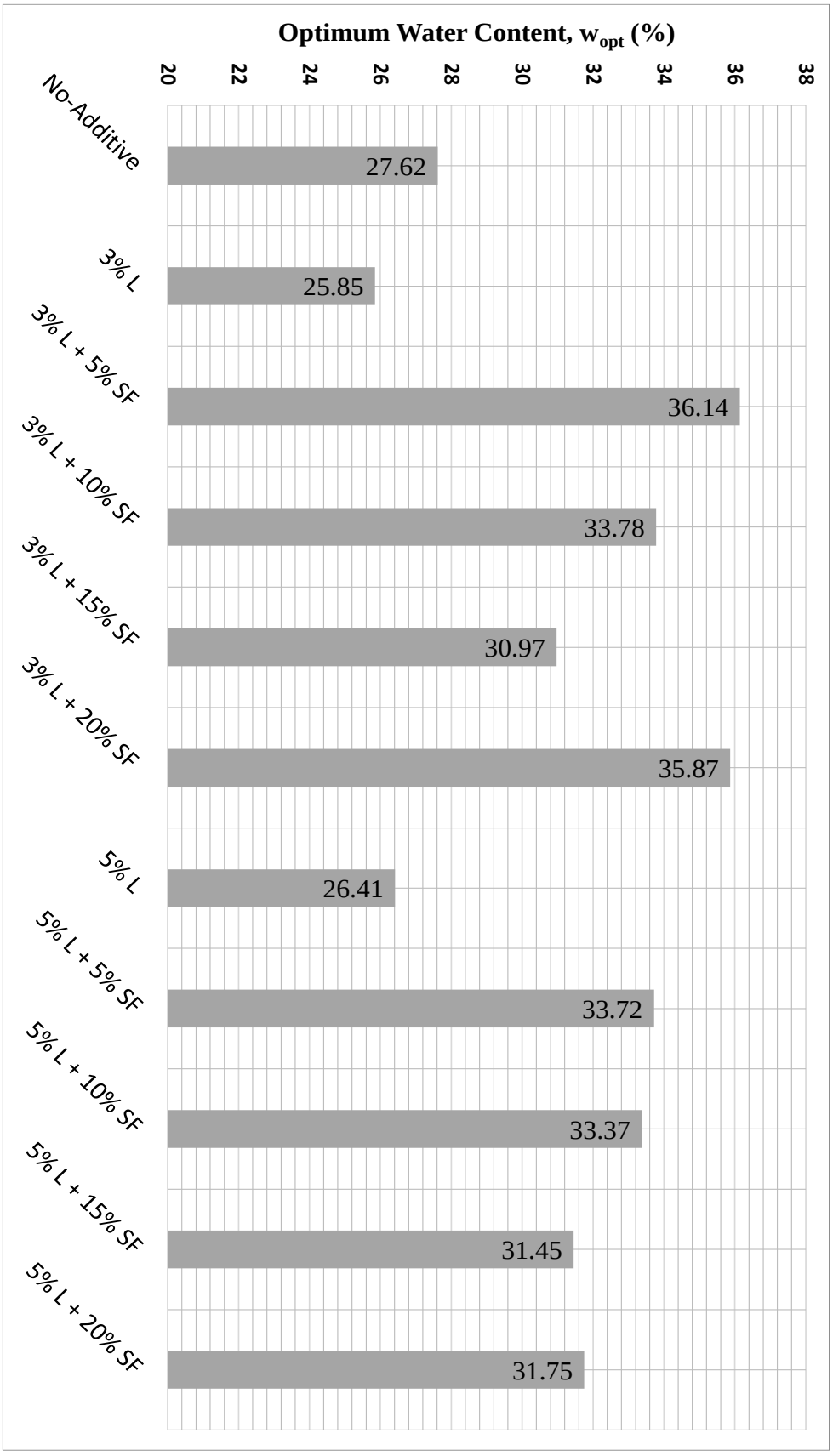

Figure 4.2 Effect of Addition of Lime and Silica Fume on Optimum Water Content

4.4 Effect of Stabilizers on Consistency Limits

The liquid limit of No-Additive sample was found as 106%, and it decreased with the addition of stabilizers (Figure 3.12). The liquid limit values increase with increasing silica fume content, keeping 5% lime content constant. On the other hand, there is no such trend in the 3% lime added set. The minimum liquid limit is 90% in both 3% and 5% lime-added samples without the addition of silica fume.

The plastic limit values for all samples ranged from 31% to 43%. No-Additive sample had the lowest plastic limit (31%), indicating that the mixture of all stabilizers increased the plastic limit of No-Additive sample (Figure 3.13). The plastic limit values increase as the silica fume percentage increases while the 5% lime content remains constant. Nevertheless, the 3% lime added set shows no such tendency. The maximum plastic limit is 43% in 5% lime plus 20% silica fume added sample.

The samples' plasticity index values are derived using the plastic and liquid limit values obtained from the Atterberg Limit Tests. With the addition of stabilizers, the plasticity index was reduced because the liquid limit decreased and the plastic limit increased (Figure 3.14). No-Additive sample's plasticity index was calculated to be 75%. On the other hand, there is not any trend obtained by changing the percent additives.

The decrease in the soil specimen's plasticity characteristics can be linked to the substitution of clay particles with nonexpansive silica fume particles, which possess lower plasticity. Furthermore, as noted by Abd El-Aziz et al., (2004), the application of SF results in the coating and binding of clay particles that have limited cementitious properties, as well as the formation of a pozzolanic reaction between SF and aluminous materials. This process ultimately leads to a reduction in the liquid limit and plasticity index. Al-Soudany, (2018; Harichane et al., (2018; Kalkan, (2011; Phanikumar et al., (2020) documented comparable results in their studies.

4.5 Effect of Stabilizers on Activity, A_c

With the addition of lime plus silica fume, the activity of No-Additive sample reduced. In addition, there is no such similar trends obtained in 3% and 5% lime-added sets (Figure 4.3).

Figure 4.3 Effect of Addition of Lime and Silica Fume on Activity

4.6 Effect of Stabilizers on Swell Percentage

The inclusion of stabilizers reduced sample swell percentages. Percent differences in swelling percentages by changing additive percentages are shown in Figure 4.4. As can be seen, in both 3% and 5% lime added sets, the trend in the variation of the swell percentages in between the changing silica fume percentages was the same. Hence, in comparison to lime solely, the lime-silica fume mixture demonstrates superior efficacy in mitigating the swelling tendency of expansive soil and exhibits a reduced time requirement to achieve maximum volumetric change resulting from swelling. The observed behavior can be attributed to the occurrence of the pozzolanic reaction between lime and silica subsequent to the decomposition of silica from clay minerals. This process requires a significant duration for the development of pozzolanic compounds and the following binding of particles. Conversely, the introduction of a greater concentration of silica into the soil with the addition of silica fume leads to an accelerated reaction between calcium ions (Ca^{2+}) from lime and silicon dioxide (SiO_2) from silica fume. As a result, the CSH compound quickly starts the process of coating and adhering to the LSF-treated specimens, in contrast to the lime-treated specimens. The addition of silica fume has been observed to accelerate the occurrence of the pozzolanic reaction within a reduced timeframe (GhavamShirazi & Bilsel, 2021).

Furthermore, the exceptional fineness of SF particles, characterized by their nearly perfect spherical shape and diameters ranging from 20 to 500 nm, makes them highly effective as fillers. The process described above leads to a decrease in the size of larger soil pores, which likely facilitates the even distribution of newly formed cementing crystalline components within the available area. Consequently, this results in the development of a more uniform and dense microstructure (Goodarzi et al., 2016). The behavior above tends to reduce the water adsorption capacity of clay surfaces (Kalkan, 2011; Ouhadi et al., 2010), thereby decreasing their swelling potential. Moreover, it can be observed that the swell percentage values in the absence of the additive took a longer duration to reach their ultimate value,

supporting the statements made above. The inclusion of additives accelerates the getting of the end results for these variables. It can be argued that such behavior could offer a significant advantage in terms of usage. The rapid stabilization of fillings, particularly those constructed through layer compression, can be considered a superior characteristic (Türköz et al., 2018).

In the samples where 3% and 5% lime additives were kept constant, with the addition of 5% and 10% silica fume, the maximum levels were reached in reducing swelling percentage without a cure. Nevertheless, the samples containing 15% and 20% silica fume showed a higher swelling potential than the ones with 10%. So, adding more than 10% silica fume did not impact the swelling potential. The reason for this situation has been evaluated such that silica fume is a pozzolanic substance and that there is no sufficient amount of lime to activate a binding feature of silica with increasing silica fume percentages (Türköz et al., 2018). Furthermore, addition of 5% lime plus silica fume level of 5% is the optimum percentage without curing in swelling aspect.

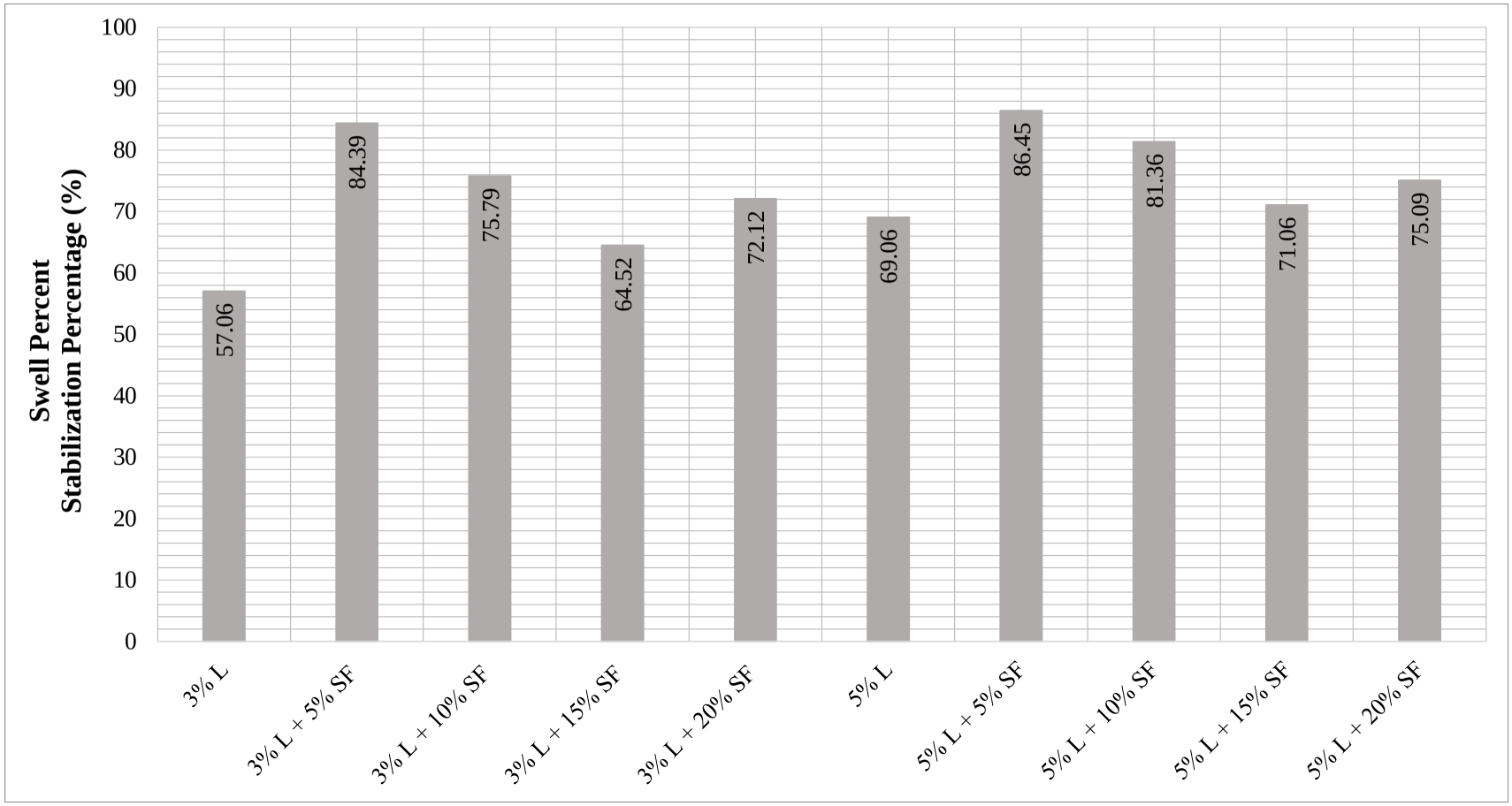

Figure 4.4 Effect of Addition of Lime and Silica Fume on Stabilization Percentage of Swelling Percent without Curing

4.7 Effect of Cure on Swell Percentage

In this part of the study, materials were kept in the curing chamber for 7 and 28 days at 70% moisture and 22°C. The swelling percentages of the samples were significantly reduced after 7 and 28 days of cure. Since pozzolanic reactions took place over a relatively long time to result in cemented soil matrix that decreases the swelling potential of the expansive soils, then each stabilizer addition gradually reduced the swelling potential by curing. The drop in swelling over time during the curing process can be linked to the progression of clay-pozzolana reactions and the creation of novel cementitious substances that consistently unite the clay aggregates, resulting in a decrease in their hydration and consequently, a drop in their capacity to swell (Celik & Nalbantoglu, 2013). The change in percent swell value of each sample between No-Additive sample was the highest for 28 days of curing and lowest for no curing (Figure 4.5). In addition, the obtained trends for 3% and 5% lime-included sets were the same, with no curing results. Furthermore, mixture of 5% silica fume plus 5% lime is the optimum percentage with both 7 and 28 days of curing in swelling aspect.

Figure 4.5 Effect of Addition of Lime and Silica Fume on Stabilization Percentage of Swelling Percent with 7 and 28 Days of Curing

4.8 Effect of Stabilizers on Unconfined Compressive Strength

The expectation was that adding stabilizers to No-Additive sample would increase No-Additive sample's unconfined compressive strength value. However, the percent change in unconfined compressive test results on 5 % silica fume-added samples between No-Additive sample showed the opposite in both sets (Figure 4.6). This situation could be due to having the least amount of silica fume between silica fume-added samples, which may lead to not effectively starting chemical interactions at initial state. Other than 5% silica fume-added samples, it can be observed that the pattern in the change of the unconfined compressive between the varying silica fume percentages was the same in both 3% and 5% lime-added sets. In addition, it was also expected that the unconfined compressive strength values should increase with the increasing silica fume content, yet, the 15% silica fume added sample's strength change due to No-Additive sample is more than the 20% silica fume added sample. This situation is due to the 15% silica fume added samples having the highest dry density in the samples containing silica fume in the mixture. The observed significant rise in the unconfined compressive strength of the stabilized specimens correlates with the formation of a cementitious gel as a consequence of a chemical interaction between SF and the expansive soil. This phenomenon can be attributed to the presence of SiO_2, Al_2O_3, and CaO as the predominant oxides in these materials. The oxides mentioned have the ability to produce a cementitious gel, specifically calcium silicate hydrate (CSH) and calcium aluminate hydrate (CAH) when they undergo a reaction (Chew et al., 2004; Qing et al., 2020). The production of calcium silicate hydrate (CSH) and calcium aluminate hydrate (CAH) within the soil matrix enhances its strength. It facilitates the cohesion of soil particles through the formation of a cementation gel (Khalid et al., 2023). As a result, it can be seen that the maximum increase is observed in 15% silica fume plus 5% lime added sample without curing in compressive strength aspect.

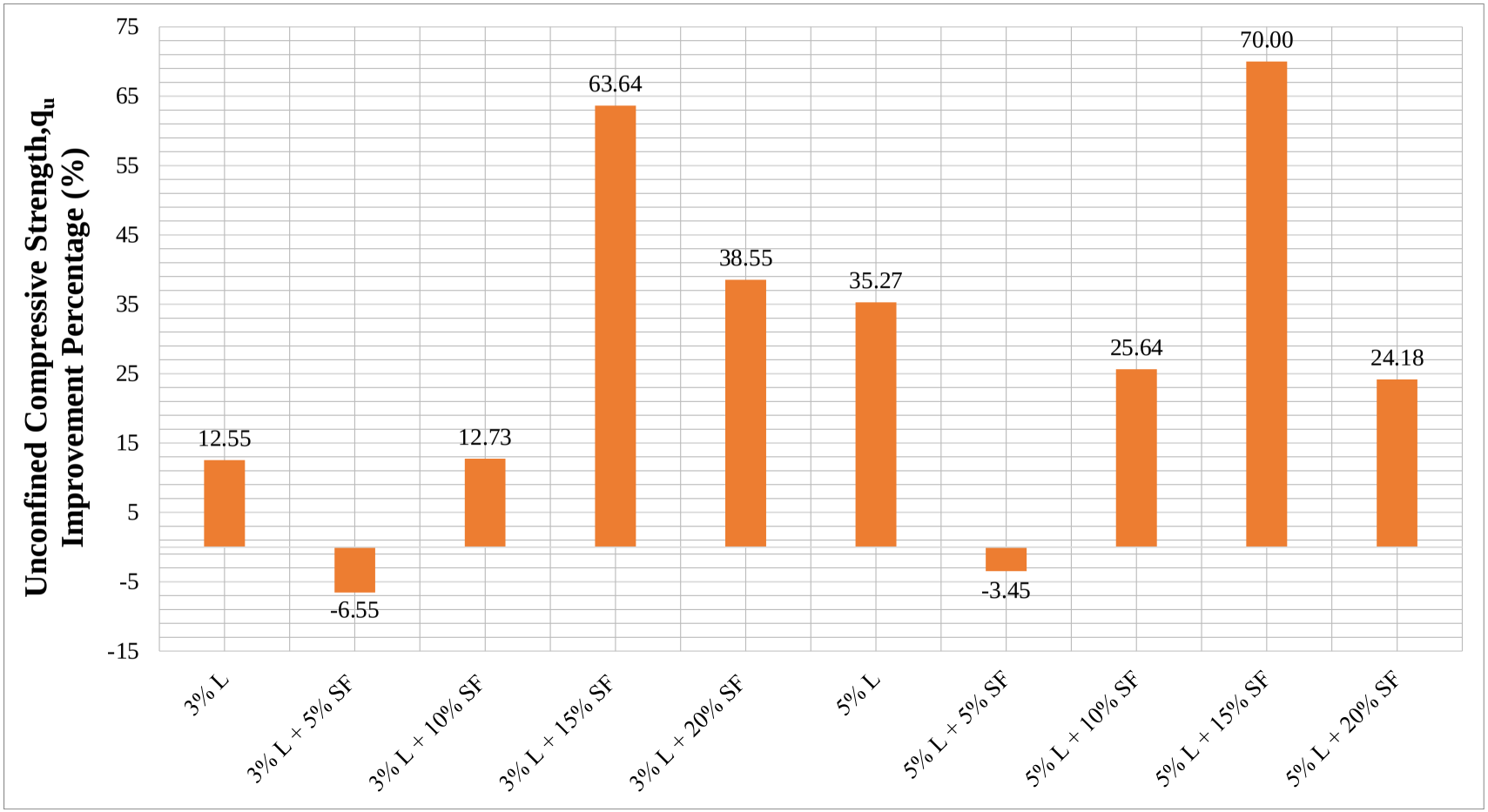

Figure 4.6 Effect of Addition of Lime and Silica Fume on Stabilization Percentage of Unconfined Compressive Strength without Curing

4.9 Effect of Cure on Unconfined Compressive Strength

Specimens were stored in a desiccator in a humidity room for 7 and 28 days at 70% moisture and 22°C for this study phase. According to Turkoz & Vural, (2013) study, the duration of curing was found to have a significant impact on strength enhancement, particularly in clays exhibiting high plasticity. Each sample's unconfined compressive strength improved considerably after 7 and 28 days of the curing process. As pozzolanic reactions require a long time to produce flocculated soil formations that harden the soil body, which increases the unconfined compressive strength of the soils, each stabilizer addition progressively improves the unconfined compressive strength by hardening as a result of curing. And also, while the strengths of the specimens increasing the specimens will be more brittle than their previous states, as stated by the researches of Bell, (1993) and (Sherwood, 1993). This situation can be seen in the Table 4.1.

The difference in unconfined compressive strength values between No-Additive sample and additive-used samples was highest after 28 days of curing and lowest without any curing period (Figure 4.7). According to the research conducted by Latifi et al. (2016), the process of curing within the initial seven days was found to be of considerable significance in promoting strength enhancement for clays characterized by high plasticity. The observed outcome can be attributed to the occurrence of the pozzolanic reaction between lime and silica fume, which has been found to be particularly efficient when interacting with soil particles (Alrubaye et al., 2017). Furthermore, the trends observed for 3% and 5% lime-included sets were the same, with no curing outcomes. As a result, addition of 5% lime plus silica fume level of 15% is the optimum percentage with both 7 and 28 days of curing in compressive strength aspect.

Table 4.1 Strain Values at Peak and Failure Unconfined Compressive Strength Values

Name	%Strain @$q_{u,peak}$	%Strain @$q_{u,failure}$
No-Additive	3.61	4.59
3% L - NC	2.23	3.06
3% L - 7D	1.94	2.49
3% L - 28D	1.67	2.09
3% L + 5% SF - NC	10	12.5
3% L + 5% SF - 7D	10.41	12.5
3% L + 5% SF - 28D	5.42	6.25
3% L + 10% SF - NC	6.29	8.93
3% L + 10% SF - 7D	4.57	5.82
3% L + 10% SF - 28D	3.34	3.63
3% L + 15% SF - NC	4.14	4.14
3% L + 15% SF - 7D	3.46	3.87
3% L + 15% SF - 28D	3.03	3.03
3% L + 20% SF - NC	6.67	8.33
3% L + 20% SF - 7D	4.58	5.83
3% L + 20% SF - 28D	3.3	3.58
5% L - NC	2.5	2.78
5% L - 7D	1.95	2.23
5% L - 28D	1.39	1.53
5% L + 5% SF - NC	5.83	7.92
5% L + 5% SF - 7D	2.51	3.07
5% L + 5% SF - 28D	1.67	2.23
5% L + 10% SF - NC	4.2	5.46
5% L + 10% SF - 7D	2.91	3.05
5% L + 10% SF - 28D	1.94	1.94
5% L + 15% SF - NC	3.3	3.58
5% L + 15% SF - 7D	2.21	2.21
5% L + 15% SF - 28D	1.93	1.93
5% L + 20% SF - NC	3.06	3.62
5% L + 20% SF - 7D	1.67	1.67
5% L + 20% SF - 28D	1.53	1.53

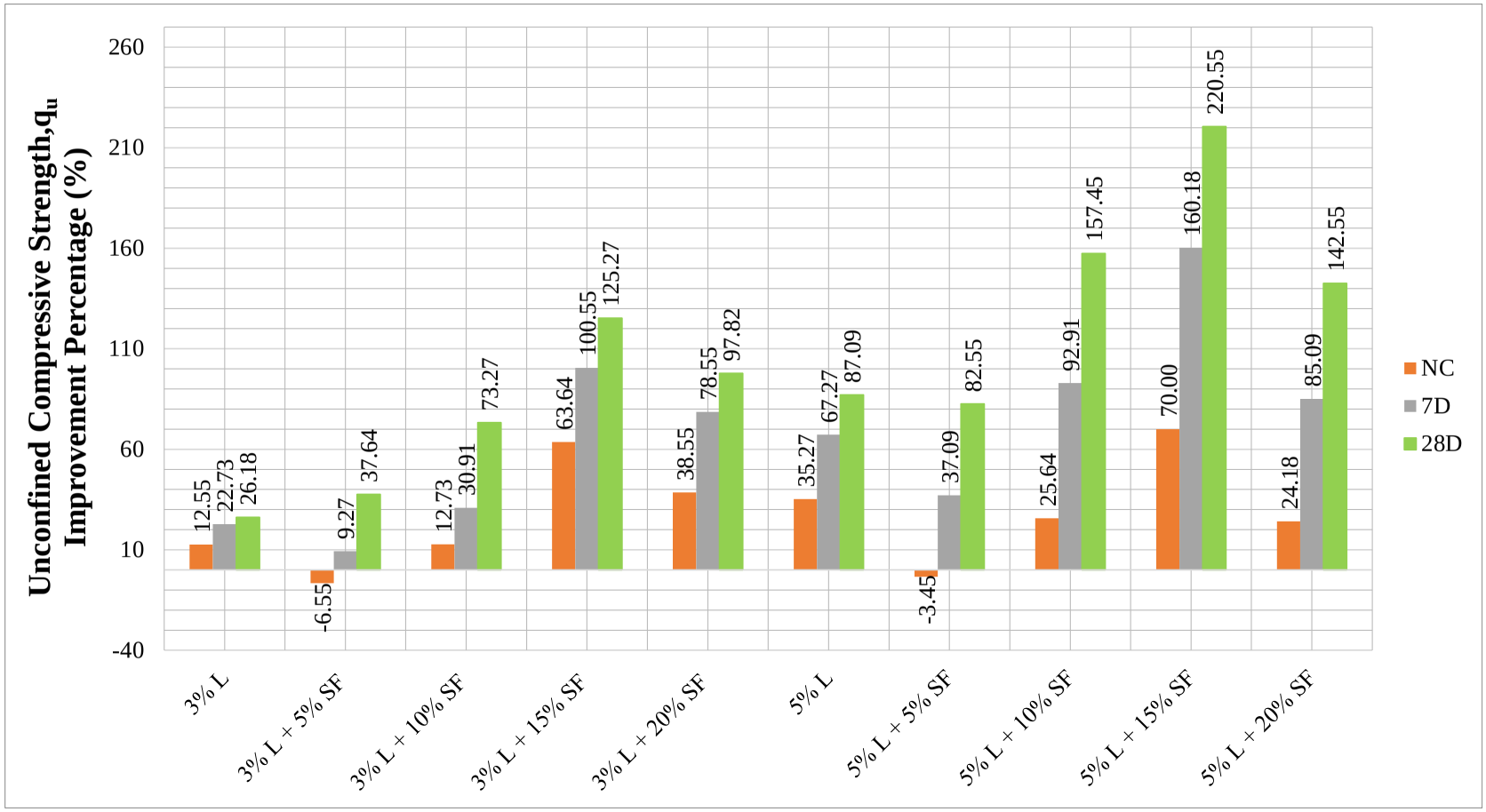

Figure 4.7 Effect of Addition of Lime and Silica Fume on Stabilization Percentage of Unconfined Compressive Strength with 7 and 28 Days of Curing

4.10 Effect of Stabilizers on Deformation Modulus, E_{50}

The E_{50} variable is a crucial mechanical characteristic used to quantify the specimen's ability to resist elastic-plastic deformation (Rehman et al., 2021). The deformation modulus, E_{50} was utilized to evaluate the stiffness of both stabilized and unstabilized specimens. The determination of the deformation modulus involves the assessment of the slope of the axial compressive stress versus the axial strain plot at a point corresponding to half of the maximum compressive stress.

It was expected that the inclusion of stabilizers into the No-Additive sample would result in an elevation of its deformation modulus value. Nevertheless, the percentage change in deformation modulus for samples with different additive compositions, such as 3% L + 5% SF, 3% L + 10% SF, 3% L + 20% SF, and 5% L + 5% SF, exhibited contrasting results compared to the No-Additive sample (Figure 4.8). This scenario may be attributed to having much more ductile behavior than No-Additive sample of those samples. Yet, the samples with the same percentage of silica fume included in the 5% L set do not exhibit the same pattern as the samples in the 3% L included set. This phenomenon may be attributed to the superior effectiveness of chemical reactions in compensating for the decrease in density. Furthermore, it was anticipated that the deformation modulus values would exhibit an increase as the silica fume content increased. However, it is noteworthy that the change in deformation modulus for the sample with 15% silica fume addition, in comparison to the No-Additive sample, is greater than that of the sample with 20% silica fume addition. The observed outcome can be linked to the fact that the samples containing 15% silica fume exhibited the highest dry density among the samples incorporating silica fume in the mixture. Consequently, it is evident that the sample containing 5% lime and 15% silica fume, without any curing process, exhibits the highest level of increase. The observed enhancement in the E_{50} values could potentially be attributed to the pozzolanic activity and self-cementitious properties exhibited by the lime-soil mixture.

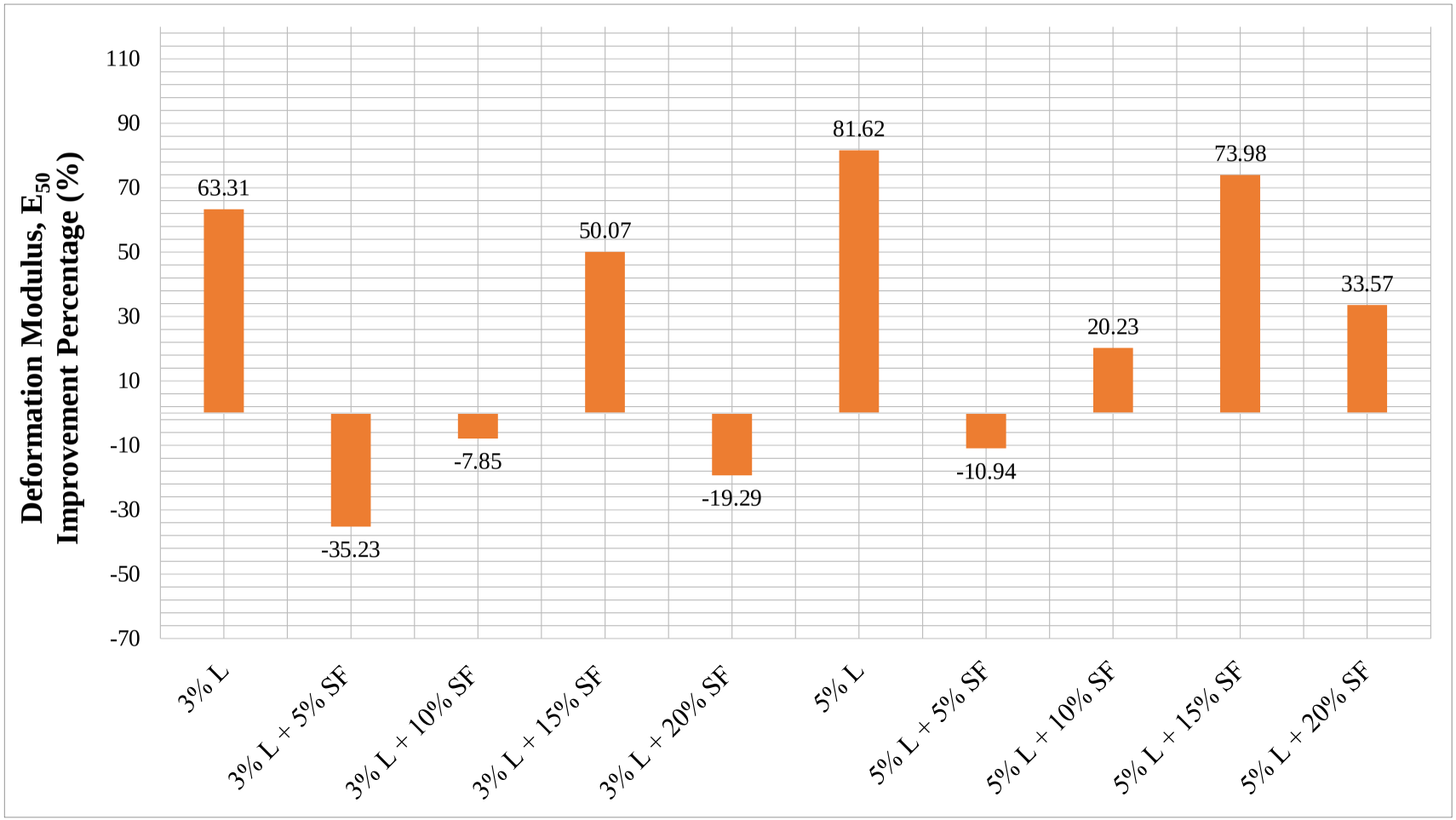

Figure 4.8 Effect of Addition of Lime and Silica Fume on Stabilization Percentage of Deformation Modulus, E_{50} without Curing

4.11 Effect of Cure on Deformation Modulus, E_{50}

The specimens were placed in a desiccator inside a humidity-controlled room for 7 and 28 days. The humidity level was maintained at 70%, and the temperature was set at 22°C. This experimental phase was conducted to investigate the effects of these specific conditions on the specimens. The deformation modulus values of each sample exhibited significant improvement following the curing periods of 7 and 28 days. Pozzolanic reactions demand a significant duration to generate flocculated soil structures that enhance the stiffness of the soil mass, thereby augmenting its deformation modulus. Consequently, the inclusion of stabilizers progressively enhances the deformation modulus through a hardening process facilitated by the curing mechanism. The variation in deformation modulus values between untreated and treated samples was greatest in the 28-day curing period, while it was the smallest in the absence of any curing process (see Figure 4.9). In addition, it was noticed that the trends for the sets containing 3% and 5% lime were identical, with no curing results. Consequently, it can be concluded that a silica fume content of 15% plus 5% lime combination is the most favorable percentage in terms of the deformation modulus aspect for both the 7-day and 28-day curing periods.

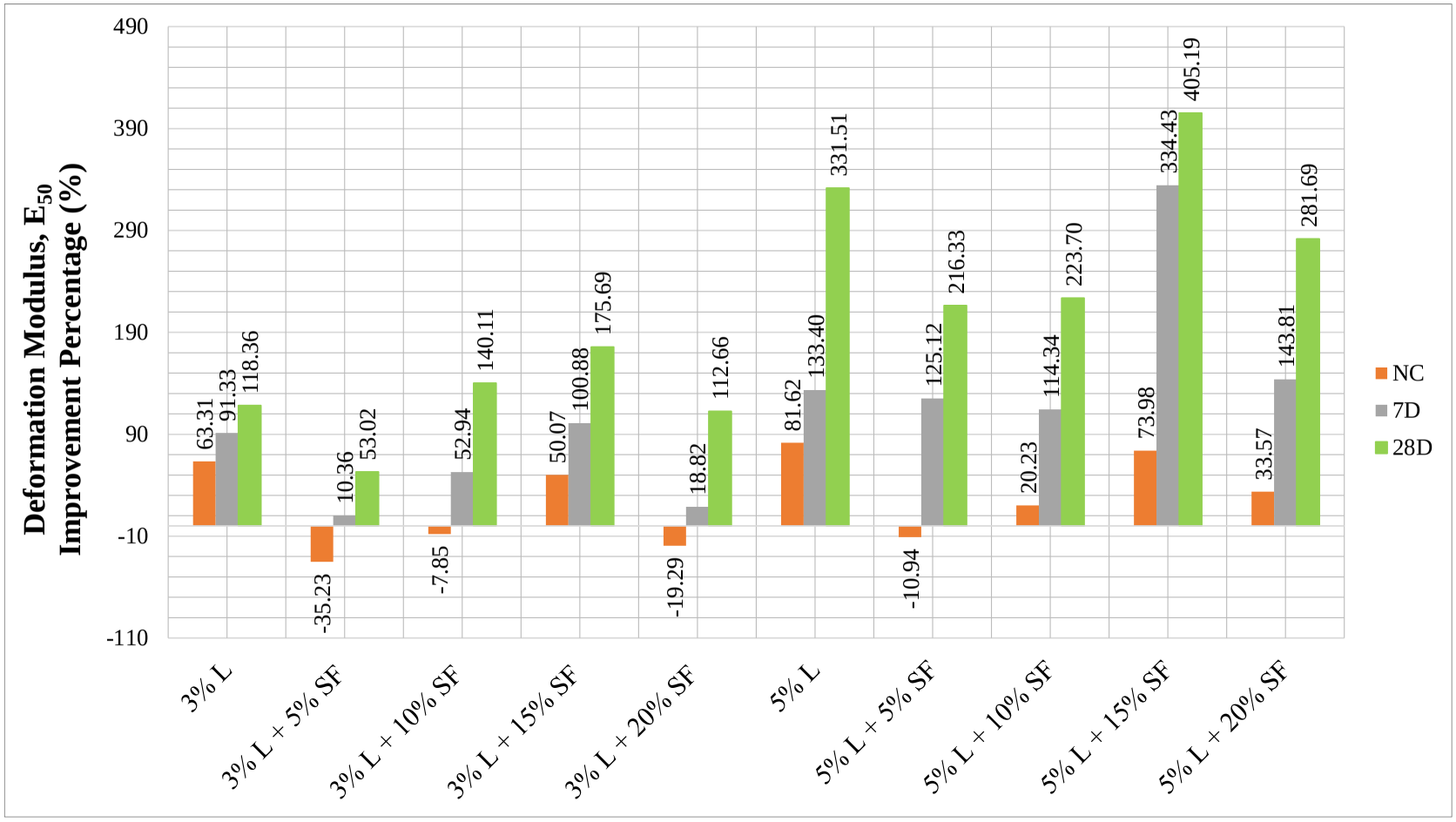

Figure 4.9 Effect of Addition of Lime and Silica Fume on Stabilization Percentage of Deformation Modulus, E50 with 7 and 28 Days of Curing

CHAPTER 5

CONCLUSIONS

This study aimed to examine the impact of combining silica fume and lime on expansive soils', which is named as No-Additive sample and also consist of 85% kaolinite plus 15% sodium-bentonite, swelling and strength characteristics. Furthermore, an investigation is conducted to examine the impact of curing on these properties by comparing the non-cured samples with those cured for **7** days and 28 days. Based on the findings obtained from the performed experiments, the resulting conclusions have been stated as follows:

1. The utilization of activity values is beneficial in assessing the soil's tendency for swelling. Based on the computed activity outcome, it is evident that the No-additive sample exhibits a significantly higher level of activity. The calculations of activity may not be appropriate for stabilized soil samples. Although the stabilized samples' activity is lowered compared to the No-additive sample, the classification remains unchanged.
2. The addition of stabilizers resulted in a decrease in the percentage of swelling. The observed trend in the variation of swell percentages between different silica fume percentages remained consistent in the 3% and 5% lime-added sets. In the experimental conditions where lime additives were maintained at fixed concentrations of 3% and 5%, the introduction of silica fume at levels of 5% and 10% resulted in reaching the level of maximum reductions in swelling percentage in the absence of any curing process. However, it was observed that the samples containing 15% and 20% silica fume exhibited a higher tendency for swelling than those with 10%. Moreover, it has been determined that a 5% silica fume plus 5% lime combination is the most favorable proportion to stabilize No-Additive sample in the absence of curing.

3. The obtained percentages of swelling in the samples exhibited a significant decrease following a curing period of 7 and 28 days. The spotted trends for the sets containing 3% and 5% lime were identical to those obtained without curing. The percent variation in swell value for each sample was found to be highest after 28 days of curing and lowest when no curing was applied. In addition, it has been determined that a 5% silica fume plus 5% lime mixture is the optimal proportion for achieving desirable results to stabilize No-Additive sample during both the 7-day and 28-day curing periods.
4. The hypothesis was that the inclusion of stabilizers in the No-Additive sample would result in an increase in its unconfined compressive strength value. However, the percentage change in unconfined compressive test results for samples 5% silica fume included additive exhibited a contrasting trend compared to the No-Additive sample. In addition to the samples with 5% silica fume, it is evident that the trend in the alteration of the unconfined compressive strength among the different percentages of silica fume was consistent in both sets with 3% and 5% lime addition. Furthermore, it was anticipated that the undrained strength values would exhibit an upward trend as the silica fume content increased. However, it is notable that the strength variation of the sample with 15% silica fume addition, compared to the No-Additive sample, was greater than that of the sample with 20% silica fume addition. Consequently, in the absence of curing, the sample with 15% silica fume plus 5% lime addition shows the greatest gain in compressive strength of No-Additive sample.
5. The unconfined compressive strength of each sample showed significant improvement following a curing period of 7 and 28 days. The variation in unconfined compressive strength values between the sample without any additives and the samples with additives was greatest in the 28-day curing period. At the same time, it was least significant in the absence of any curing period. Additionally, the observed trends for the sets containing 3% and 5% lime were found to be identical, with no curing results. Moreover, it has been

determined that a 15% silica fume plus 5% lime is the most favorable proportion in terms of compressive strength for both 7 and 28 days of curing to stabilize No-Additive sample.

6. The deformation modulus values, E_{50}, obtained from the UCS test data show a parallel relationship with the unconfined compressive strength results, both in the absence and presence of curing conditions. The percentage of 15% silica fume plus 5% lime is determined to be optimal combination to stabilize No-Additive sample for curing periods of 0 days, 7 days, and 28 days.
7. When all's said and done, the mixture of 5% L + 5% SF is the most suitable combination for improving a very expansive soil sample's swelling characteristics. Since the main object of this study was to decrease the swelling percent from very high to very low, the 5% L + 5% SF has provided the maximum improvement by being much more effective than just using 5% L. Then, the strength aspect is considered, and it is seen that the 5% L + 5% SF combination doubled the UCS value of untreated samples and tripled the deformation modulus value of untreated samples. After it was understood that the recommended combination was sufficient for both criteria, the swell rate values were also checked. Then, it is observed that the swell rate value of the untreated sample has decreased by 1/4 of its original value with the recommended combination.

In addition, the optimum additive combinations can be seen for each case in Table 5.1.

Table 5.1 Optimum Additive Combinations for Each Aspect

Aspects / Curing Periods	Swell Percentage	Swell Rate	Unconfined Compressive Strength	Deformation Modulus
No Curing	5% L + 5% SF	5% L + 20% SF	5% L + 15% SF	5% L
7 Days of Curing	5% L + 5% SF	5% L + 5% SF	5% L + 15% SF	5% L + 15% SF
28 Days of Curing	5% L + 10% SF	5% L + 15% SF	5% L + 15% SF	5% L + 15% SF

In conclusion, combining silica fume and lime proved encouraging outcomes in stabilizing expansive soil. Various tests have shown that the interaction between calcium ions (Ca^{2+}) derived from lime and silicon dioxide (SiO_2) present in silica fume leads to the creation of a cementitious pozzolanic compound. This compound plays a crucial role in the cohesive binding of clay particles. Hence, using silica fume combined with lime for soil stabilization accelerates the occurrence of the pozzolanic reaction. Adding silica fume improves the engineering characteristics of expansive clay and offers a means of recycling this waste material.

Recommendations for Future Researches:

While the conducted tests are deemed reliable, it is advisable to conduct supplementary examinations, such as SEM and XRD studies, to thoroughly analyze the microfabric and mineralogical properties of both treated and untreated samples. This comprehensive approach will enable an improved evaluation of the specimens.

The application methodology of silica fume in combination with lime can be assessed by several different approaches to see the application effects on the test results. Besides selecting the appropriate utilization methodology for silica fume + lime, large-scale application of silica fume with lime could be helpful to compare the laboratory test versus field-gathered specimens' laboratory test results. In the meantime, the leachate performance can be evaluated by both laboratory and field test results. In addition, some field tests can also be performed after the large-scale application to see the effects of the used combination. In order to see the effect of silica fume + lime utilization on other aspects, for instance, the compressibility characteristics (such as consolidation behavior) or permeability characteristics can be evaluated by performing necessary laboratory and field tests. After all these studies, the optimum additive combination with the adequate application methodology and the stabilization approach can be used for different soils in chemical and mineralogical aspects.

REFERENCES

Abd El-Aziz, M. A., Abo-Hashema, M. A., & El-Shourbagy, M. (2004). The effect of lime-silica fume stabilizer on engineering properties of clayey subgrade. *Engineering Conference, Faculty of Engineering, Mansoura University, Paper*, *96*, 1–18.

Abdel-Gawwad, H. A., Rashad, A. M., Mohammed, M. S., & Tawfik, T. A. (2021). The potential application of cement kiln dust-red clay brick waste-silica fume composites as unfired building bricks with outstanding properties and high ability to CO2-capture. *Journal of Building Engineering*, *42*, 102479. https://doi.org/https://doi.org/10.1016/j.jobe.2021.102479

Abiddin Erguler, Z., & Ulusay, R. (2003). A simple test and predictive models for assessing swell potential of Ankara (Turkey) Clay. *Engineering Geology*, *67*(3), 331–352. https://doi.org/https://doi.org/10.1016/S0013-7952(02)00205-3

Aldaood, A., Bouasker, M., & Al-Mukhtar, M. (2014). Free swell potential of lime-treated gypseous soil. *Applied Clay Science*, *102*, 93–103. https://doi.org/https://doi.org/10.1016/j.clay.2014.10.015

Al-Mansour, A., Chow, C. L., Feo, L., Penna, R., & Lau, D. (2019). Green Concrete: By-Products Utilization and Advanced Approaches. *Sustainability*, *11*(19). https://doi.org/10.3390/su11195145

Al-Mukhtar, M., Khattab, S., & Alcover, J.-F. (2012). Microstructure and geotechnical properties of lime-treated expansive clayey soil. *Engineering Geology*, *139–140*, 17–27. https://doi.org/https://doi.org/10.1016/j.enggeo.2012.04.004

Al-Rawas, A. A., & Goosen, M. F. A. (2006). *Expansive soils: recent advances in characterization and treatment*.

Al-Rawas, A. A., Taha, R., Nelson, J. D., Al-Shab, B. T., & Al-Siyabi, H. (2002). A comparative evaluation of various additives used in the stabilization of expansive soils. *Geotechnical Testing Journal*, *25*(2), 199–209.

Alrubaye, A. J., Hasan, M., & Fattah, M. Y. (2017). Stabilization of soft kaolin clay with silica fume and lime. *International Journal of Geotechnical Engineering*, *11*(1), 90–96. https://doi.org/10.1080/19386362.2016.1187884

Al-Soudany, K. Y. (2018). Improvement of expansive soil by using silica fume. *Kufa J Eng*, *9*(1), 222–239.

Al-Zairjawi, K. M. (2009). Effect Of Adding Cement And Silica Fume With Cement On Compaction Properties And Shear Strength Of Clayey Soil. *Al-Qadisiyah Journal for Engineering Sciences*, *2*(2), 253–261.

Amina, S. M., & Rani, V. (2017). Control of dispersivity of soil using lime and silica fume. *International Journal for Research in Applied Science and Engineering Technology*, *5*(5), 386–391.

Arnold, M. (1984). The genesis, mineralogy and identification of expansive soils. *Fifth International Conference on Expansive Soils 1984: Preprints of Papers*, 32–36.

Atiş, C. D., Özcan, F., Kılıç, A., Karahan, O., Bilim, C., & Severcan, M. H. (2005). Influence of dry and wet curing conditions on compressive strength of silica fume concrete. *Building and Environment*, *40*(12), 1678–1683. https://doi.org/https://doi.org/10.1016/j.buildenv.2004.12.005

Baghdadi, Z. A., Fatani, M. N., & Sabban, N. A. (1995). Soil Modification by Cement Kiln Dust. *Journal of Materials in Civil Engineering*, *7*(4), 218–222. https://doi.org/10.1061/(ASCE)0899-1561(1995)7:4(218)

Barton, C. D., & Karathanasis, A. D. (2002). Clay minerals. In *Encyclopedia of soil science* (Vol. 10). Marcel Dekker: New York.

Basma, A. A., Al-Homoud, A. S., Husein Malkawi, A. I., & Al-Bashabsheh, M. A. (1996). Swelling-shrinkage behavior of natural expansive clays. *Applied Clay Science*, *11*(2), 211–227. https://doi.org/https://doi.org/10.1016/S0169-1317(96)00009-9

Basma, A. A., Al-Homoud, A. S., Husein Malkawi, A. I., & Al-Bashabsheh, M. A. (1996). Swelling-shrinkage behavior of natural expansive clays. *Applied Clay Science*, *11*(2), 211–227. https://doi.org/https://doi.org/10.1016/S0169-1317(96)00009-9

Bell, F. G. (1993). Engineering treatment of soils, published by E and FN Spon, an imprint of Chapmen and Hall. *Boundary Row, London*.

Bell, F. G. (1996). Lime stabilization of clay minerals and soils. *Engineering Geology*, *42*(4), 223–237. https://doi.org/https://doi.org/10.1016/0013-7952(96)00028-2

Bharadwaj, S., & Trivedi, M. K. (2016). Impact of micro silica fume on engineering properties of expansive soil. *Int J Sci Technol Eng*, *2*(12), 435e40.

Billong, N., Oti, J., & Kinuthia, J. (2021). Using silica fume based activator in sustainable geopolymer binder for building application. *Construction and Building Materials*, *275*, 122177. https://doi.org/https://doi.org/10.1016/j.conbuildmat.2020.122177

Bohn, H. L., McNeal, B. L., & O'Connor, G. A. (1985). *Soil Chemistry*. Wiley. https://books.google.com.tr/books?id=VXNRAAAAMAAJ

Brescia-Norambuena, L., González, M., Avudaiappan, S., Saavedra Flores, E. I., & Grasley, Z. (2021). Improving concrete underground mining pavements performance through the synergic effect of silica fume, nanosilica, and polypropylene fibers. *Construction and Building Materials*, *285*, 122895. https://doi.org/https://doi.org/10.1016/j.conbuildmat.2021.122895

Celik, E., & Nalbantoglu, Z. (2013). Effects of ground granulated blastfurnace slag (GGBS) on the swelling properties of lime-stabilized sulfate-bearing soils. *Engineering Geology*, *163*, 20–25. https://doi.org/https://doi.org/10.1016/j.enggeo.2013.05.016

Charlie, W. A., Osman, M. A., & Ali, E. M. (1984). Construction on expansive soils in Sudan. *Journal of Construction Engineering and Management*, *110*(3), 359–374.

Chen, F. H. (1975). *Foundations on expansive soils* (Vol. 12). Elsevier Scientific Pub. Co.

Chen, F. H. (Fu H. (1988). *Foundations on expansive soils / F.H. Chen*. Elsevier ; Distributors for the U.S. and Canada, Elsevier Science Pub. Co.

Cherian, C., & Arnepalli, D. N. (2015). A Critical Appraisal of the Role of Clay Mineralogy in Lime Stabilization. *International Journal of Geosynthetics and Ground Engineering*, *1*(1), 8. https://doi.org/10.1007/s40891-015-0009-3

Chew, S. H., Kamruzzaman, A. H. M., & Lee, F. H. (2004). Physicochemical and Engineering Behavior of Cement Treated Clays. *Journal of Geotechnical and Geoenvironmental Engineering*, *130*(7), 696–706. https://doi.org/10.1061/(ASCE)1090-0241(2004)130:7(696)

Chindris, L., Stefanescuu, D. P., Radermacher, L., Radeanu, C., & Popa, C. (2017). Expansive soil stabilization-general considerations. *17th International Multidisciplinary Scientific Geoconference SGEM 2017*, 247–256.

Chittoori, B. C. S. (2009). *Clay Mineralogy Effects On Long-term Performance Of Chemically Treated Expansive Clays*.

Choudhary, R., Gupta, R., Alomayri, T., Jain, A., & Nagar, R. (2021). Permeation, corrosion, and drying shrinkage assessment of self-compacting high strength concrete comprising waste marble slurry and fly ash, with silica fume. *Structures*, *33*, 971–985. https://doi.org/https://doi.org/10.1016/j.istruc.2021.05.008

Chung, D. D. L. (2017). 6 - Cement-Matrix Composites. In D. D. L. Chung (Ed.), *Carbon Composites (Second Edition)* (pp. 333–386). Butterworth-Heinemann. https://doi.org/https://doi.org/10.1016/B978-0-12-804459-9.00006-3

Çokça, E. (2001). Use of Class C Fly Ashes for the Stabilizationof an Expansive Soil. *Journal of Geotechnical and Geoenvironmental Engineering*, *127*(7), 568–573. https://doi.org/10.1061/(ASCE)1090-0241(2001)127:7(568)

Das, B. M. (2016). *Principles of foundation engineering* (Eighth SI). Cengage Learning.

Ebailila, M., Kinuthia, J., Oti, J., & Al-Waked, Q. (2022). Sulfate soil stabilisation with binary blends of lime–silica fume and lime–ground granulated blast furnace slag. *Transportation Geotechnics*, *37*, 100888. https://doi.org/https://doi.org/10.1016/j.trgeo.2022.100888

Fang, H.-Y. (1991). *Foundation engineering handbook* (2nd ed.). Van Nostrand Reinhold.

Fattah, M. Y., Al-Saidi, A. A., & Jaber, M. M. (2015a). Characteristics of Clays Stabilized with Lime-Silica Fume Mix. *Bollettino Della Societa Geologica Italiana*, *134*, 104–113.

Fattah, M. Y., Al-Saidi, A. A., & Jaber, M. M. (2015b). Improvement of bearing capacity of footing on soft clay grouted with lime-silica fume mix. *Geomechanics & Engineering*, *8*(1), 113–132. https://scienceon.kisti.re.kr/srch/selectPORSrchArticle.do?cn=JAKO201511742735320

Foster, M. D., & Survey, U. S. G. (1955). The relation between composition and swelling in clays. In *Open-File Report*. https://doi.org/10.3133/ofr5491

GhavamShirazi, S., & Bilsel, H. (2021). Characterization of volume change and strength behavior of micro-silica and lime-stabilized Cyprus clay. *Acta Geotechnica*, *16*(3), 827–840. https://doi.org/10.1007/s11440-020-01060-1

Goodarzi, A. R., Akbari, H. R., & Salimi, M. (2016). Enhanced stabilization of highly expansive clays by mixing cement and silica fume. *Applied Clay Science*, *132–133*, 675–684. https://doi.org/https://doi.org/10.1016/j.clay.2016.08.023

Goodarzi, A. R., Goodarzi, S. H., & Akbari, H. R. (2015). Assessing geo-mechanical and micro-structural performance of modified expansive clayey soil by silica fume as industrial waste. *Iranian Journal of Science and Technology Transactions of Civil Engineering*, *39*(C2), 333–350.

Goodarzi, A. R., & Salimi, M. (2015). Stabilization treatment of a dispersive clayey soil using granulated blast furnace slag and basic oxygen furnace slag. *Applied Clay Science*, *108*, 61–69. https://doi.org/https://doi.org/10.1016/j.clay.2015.02.024

Grim, R. E. (1942). Modern concepts of clay materials. *The Journal of Geology*, *50*(3), 225–275.

Harichane, K., Ghrici, M., & Kenai, S. (2018). Stabilization of Algerian Clayey Soils with Natural Pozzolana and Lime. *Periodica Polytechnica Civil Engineering*, *62*(1), 1–10. https://doi.org/10.3311/PPci.9229

Harichane, K., Ghrici, M., Kenai, S., & Grine, K. (2011). Use of Natural Pozzolana and Lime for Stabilization of Cohesive Soils. *Geotechnical and Geological Engineering*, *29*(5), 759–769. https://doi.org/10.1007/s10706-011-9415-z

Harichane, K., Ghrici, M., & Missoum, H. (2011). Influence of natural pozzolana and lime additives on the temporal variation of soil compaction and shear strength. *Frontiers of Earth Science*, *5*(2), 162–169. https://doi.org/10.1007/s11707-011-0166-1

Hausmann, M. R. (1990). *Engineering Principles of Ground Modification* (2nd Edition). McGraw-Hill. https://books.google.com.tr/books?id=ElV-AAAACAAJ

Herzog, A., & Mitchell, J. K. (1963). Reactions accompanying stabilization of clay with cement. *Highway Research Record*, *36*.

Holland, T. C., Detwiler, R., Aïtcin, P.-C., Hulshizer, A. J., Ozyildirim, H. C., Arney, D. O., & Pistilli, M. F. (2006). Guide for the use of silica fume in concrete. *ACI Committee Report: Farmington Hills, MI, USA*, 63.

Indraratna, A. S., Balasubramanian, A. K., & Khan, M. J. (1995). Effect of fly ash with lime and cement on the behavior of a soft clay. *Quarterly Journal of Engineering Geology*, *28*(2), 131–142. https://doi.org/10.1144/GSL.QJEGH.1995.028.P2.04

Jones, L. (2017). Expansive Soils. In P. Bobrowsky & B. Marker (Eds.), *Encyclopedia of Engineering Geology* (pp. 1–7). Springer International Publishing. https://doi.org/10.1007/978-3-319-12127-7_118-1

Kalantari, B., Prasad, A., & Huat, B. B. K. (2011). Stabilising peat soil with cement and silica fume. *Proceedings of the Institution of Civil Engineers - Geotechnical Engineering*, *164*(1), 33–39. https://doi.org/10.1680/geng.900044

Kalkan, E. (2009). Influence of silica fume on the desiccation cracks of compacted clayey soils. *Applied Clay Science*, *43*(3), 296–302. https://doi.org/https://doi.org/10.1016/j.clay.2008.09.002

Kalkan, E. (2011). Impact of wetting–drying cycles on swelling behavior of clayey soils modified by silica fume. *Applied Clay Science*, *52*(4), 345–352. https://doi.org/https://doi.org/10.1016/j.clay.2011.03.014

Kalkan, E. (2013). Preparation of scrap tire rubber fiber–silica fume mixtures for modification of clayey soils. *Applied Clay Science*, *80–81*, 117–125. https://doi.org/https://doi.org/10.1016/j.clay.2013.06.014

Kalkan, E., & Akbulut, S. (2004). The positive effects of silica fume on the permeability, swelling pressure and compressive strength of natural clay liners. *Engineering Geology*, *73*(1), 145–156. https://doi.org/https://doi.org/10.1016/j.enggeo.2004.01.001

Kamon, M., Montananandh, S., & Katsumi, T. (1991). Utilization of industrial wastes by solidification. *Zairyo*, *40*(459), 1538–1544.

Khalid, U., Rehman, Z. Ijaz, N., Khan, I., & Junaid, M. F. (2023). Integrating wheat straw and silica fume as a balanced mechanical ameliorator for expansive soil: a novel agri-industrial waste solution. *Environmental Science and Pollution Research*, *30*(29), 73570–73589. https://doi.org/10.1007/s11356-023-27538-5

Khan, M., & Ali, M. (2019). Improvement in concrete behavior with fly ash, silica-fume and coconut fibres. *Construction and Building Materials*, *203*, 174–187. https://doi.org/https://doi.org/10.1016/j.conbuildmat.2019.01.103

Knappett, J., & Craig, R. F. (2012). *Craig's soil mechanics* (8th ed.). Spon Press.

Köksal, F., Altun, F., Yiğit, İ., & Şahin, Y. (2008). Combined effect of silica fume and steel fiber on the mechanical properties of high strength concretes. *Construction and Building Materials*, *22*(8), 1874–1880. https://doi.org/https://doi.org/10.1016/j.conbuildmat.2007.04.017

Kumar, N. S., Swain, S. K., & Sahoo, U. C. (2012). Stabilization of a Clayey Soil with Fly Ash and Lime: A Micro Level Investigation. *Geotechnical and*

Geological Engineering, *30*(5), 1197–1205. https://doi.org/10.1007/s10706-012-9532-3

Kumar Verma, S., Sheikhar Singla, C., Nadda, G., & Kumar, R. (2020). Development of sustainable concrete using silica fume and stone dust. *Materials Today: Proceedings*, *32*, 882–887. https://doi.org/https://doi.org/10.1016/j.matpr.2020.04.364

Lambe, T. W. (1958). The structure of compacted clay. *Proc. ASCE*, *84*(2), 1–34.

Li, Y. (2021). Effect of post-fire curing and silica fume on permeability of ultra-high performance concrete. *Construction and Building Materials*, *290*, 123175. https://doi.org/https://doi.org/10.1016/j.conbuildmat.2021.123175

Little, D. N. (1995). *Stabilization of pavement subgrades and base courses with lime*.

Little, D. N., & Nair, S. (2009). *Recommended practice for stabilization for sulfate rich subgrade soils*. National Highway Cooperative Research Program, Transportation Research Board ….

Liu, H., Luo, G., Wang, L., Wang, W., Li, W., & Gong, Y. (2019). Laboratory Evaluation of Eco-Friendly Pervious Concrete Pavement Material Containing Silica Fume. *Applied Sciences*, *9*(1). https://doi.org/10.3390/app9010073

Mallela, J., Quintus, H. Von, & Smith, K. (2004). Consideration of lime-stabilized layers in mechanistic-empirical pavement design. *The National Lime Association*, *200*(1), 1–40.

Mishra, A. K., Dhawan, S., & Rao, S. M. (2008). Analysis of Swelling and Shrinkage Behavior of Compacted Clays. *Geotechnical and Geological Engineering*, *26*(3), 289–298. https://doi.org/10.1007/s10706-007-9165-0

Mitchell, J. K. (1976). *Fundamentals of Soil Behavior*. Wiley. https://books.google.com.tr/books?id=R_ZRAAAAMAAJ

Mitchell, J. K., & Soga, K. (2005). *Fundamentals of soil behavior* (3rd ed.). John Wiley & Sons.

Murray, H. H. (2006). *Applied Clay Mineralogy: Occurrences, Processing and Applications of Kaolins, Bentonites, Palygorskitesepiolite, and Common Clays: Vol. v.Volume 2*. Elsevier Science.

Murthy, V. N. S. (2002). *Geotechnical engineering: principles and practices of soil mechanics and foundation engineering*. CRC press.

Nalbantoglu, Z., & Gucbilmez, E. (2001). Improvement of calcareous expansive soils in semi-arid environments. *Journal of Arid Environments*, *47*(4), 453–463. https://doi.org/https://doi.org/10.1006/jare.2000.0726

National Lime Association. (2004). Lime-treated soil construction manual lime stabilization & lime modification. *Published by National Lime Association, USA, Bulletin*, *326*.

Negi, C., Yadav, R. K., & Singhai, A. K. (2013). Effect of silica fume on engineering properties of black cotton soil. *Int. J. Comput. Eng. Res.(IJCER)*, *83*.

Nelson, J. D., Chao, K. C., Overton, D. D., & Nelson, E. J. (2015). *Foundation engineering for expansive soils*. WILEY.

Nelson, J. D., & Miller, D. J. (1992). *Expansive soils: problems and practice in foundation and pavement engineering*. J. Wiley.

Nidzam, R. M., & Kinuthia, J. M. (2010). Sustainable soil stabilisation with blastfurnace slag – a review. *Proceedings of the Institution of Civil Engineers - Construction Materials*, *163*(3), 157–165. https://doi.org/10.1680/coma.2010.163.3.157

Ortega, J. M., Esteban, M. D., Williams, M., Sánchez, I., & Climent, M. Á. (2018). Short-Term Performance of Sustainable Silica Fume Mortars Exposed to Sulfate Attack. *Sustainability*, *10*(7). https://doi.org/10.3390/su10072517

Oti, J. E., Kinuthia, J. M., & Bai, J. (2009). Unfired clay bricks: from laboratory to industrial production. *Proceedings of the Institution of Civil Engineers - Engineering Sustainability*, *162*(4), 229–237. https://doi.org/10.1680/ensu.2009.162.4.229

Ouhadi, V. R., Yong, R. N., Goodarzi, A. R., & Safari-Zanjani, M. (2010). Effect of temperature on the re-structuring of the microstructure and geo-environmental behaviour of smectite. *Applied Clay Science*, *47*(1), 2–9. https://doi.org/https://doi.org/10.1016/j.clay.2008.08.008

Oweis, I. S., & Khera, R. P. (1998). *Geotechnology of waste management* (2nd ed.). PWS Publishing.

Phanikumar, B. R., m, J. R., & e, R. R. (2020). Silica fume stabilization of an expansive clay subgrade and the effect of silica fume-stabilised soil cushion on its CBR. *Geomechanics and Geoengineering*, *15*(1), 64–77. https://doi.org/10.1080/17486025.2019.1620348

Popescu, M. E. (1986). A comparison between the behaviour of swelling and of collapsing soils. *Engineering Geology*, *23*(2), 145–163. https://doi.org/https://doi.org/10.1016/0013-7952(86)90036-0

Prusinski, J. R., & Bhattacharja, S. (1999). Effectiveness of Portland Cement and Lime in Stabilizing Clay Soils. *Transportation Research Record*, *1652*(1), 215–227. https://doi.org/10.3141/1652-28

Puppala, A. J. (2016). Advances in ground modification with chemical additives: From theory to practice. *Transportation Geotechnics*, *9*, 123–138. https://doi.org/https://doi.org/10.1016/j.trgeo.2016.08.004

Qi, S., & Vanapalli, S. K. (2015). Hydro-mechanical coupling effect on surficial layer stability of unsaturated expansive soil slopes. *Computers and Geotechnics*, *70*, 68–82. https://doi.org/https://doi.org/10.1016/j.compgeo.2015.07.006

Qing, Y., Chuanxin, D., Jinli, Z., & Gang, Y. (2020). Influence of Silica Fume and Additives on Unconfined Compressive Strength of Cement-Stabilized Marine Soft Clay. *Journal of Materials in Civil Engineering*, *32*(2), 04019346. https://doi.org/10.1061/(ASCE)MT.1943-5533.0003010

Rehman, Z., Farooq, K., Mujtaba, H., & Khalid, U. (2021). Unified evaluation of consolidation parameters for low to high plastic range of cohesive soils. *Mehran University Research Journal Of Engineering & Technology*, *40*(1), 93–103. https://search.informit.org/doi/10.3316/informit.751672711687837

Sadrmomtazi, A., Tahmouresi, B., & Saradar, A. (2018). Effects of silica fume on mechanical strength and microstructure of basalt fiber reinforced cementitious composites (BFRCC). *Construction and Building Materials*, *162*, 321–333. https://doi.org/https://doi.org/10.1016/j.conbuildmat.2017.11.159

Seco, A., Ramírez, F., Miqueleiz, L., & García, B. (2011). Stabilization of expansive soils for use in construction. *Applied Clay Science*, *51*(3), 348–352. https://doi.org/https://doi.org/10.1016/j.clay.2010.12.027

Seed, H. B., J, W. R., & Lundgren, R. (1962). Prediction of Swelling Potential for Compacted Clays. *Journal of the Soil Mechanics and Foundations Division*, *88*(3), 53–87. https://doi.org/10.1061/JSFEAQ.0000431

Sezer, İ. G. (2012). Compressive strength and sulfate resistance of limestone and/or silica fume mortars. *Construction and Building Materials*, *26*(1), 613–618. https://doi.org/https://doi.org/10.1016/j.conbuildmat.2011.06.064

Sharma, N. K., Swain, S. K., & Sahoo, U. C. (2012). Stabilization of a Clayey Soil with Fly Ash and Lime: A Micro Level Investigation. *Geotechnical and Geological Engineering*, *30*(5), 1197–1205. https://doi.org/10.1007/s10706-012-9532-3

Sherwood, P. (1993). *Soil stabilization with cement and lime*.

Shi, B., Jiang, H., Liu, Z., & Fang, H. Y. (2002). Engineering geological characteristics of expansive soils in China. *Engineering Geology*, *67*(1), 63–71. https://doi.org/https://doi.org/10.1016/S0013-7952(02)00145-X

Shuai, F., & Fredlund, D. G. (1998). Model for the simulation of swelling-pressure measurements on expansive soils. *Canadian Geotechnical Journal*, *35*(1), 96–114.

Siddique, R., & Chahal, N. (2011). Use of silicon and ferrosilicon industry by-products (silica fume) in cement paste and mortar. *Resources, Conservation and Recycling*, *55*(8), 739–744. https://doi.org/https://doi.org/10.1016/j.resconrec.2011.03.004

Silva, L. R. R. da, Silva, J. A. da, Francisco, M. B., Ribeiro, V. A., de Souza, M. H. B., Capellato, P., Souza, M. A., dos Santos, V., Cesar Gonçalves, P., & de Lourdes Noronha Motta Melo, M. (2020). Polymeric Waste from Recycling Refrigerators as an Aggregate for Self-Compacting Concrete. *Sustainability*, *12*(20). https://doi.org/10.3390/su12208731

Sivapullaiah, P. V. (2006). Pozzolanic stabilization of expansive soils. *Expansive Soils: Recent Advances in Characterization and Treatment*, *1*, 419–434.

Slade, P. G., Quirk, J. P., & Norrish, K. (1991). Crystalline Swelling of Smectite Samples in Concentrated NaCl Solutions in Relation to Layer Charge. *Clays and Clay Minerals*, *39*(3), 234–238. https://doi.org/10.1346/CCMN.1991.0390302

Snethen, D. R. (1986). Expansive Soils: Where Are We? *Ground Failure*, *3*, 12–16.

Tangstad, M. (2013). Chapter 6 - Ferrosilicon and Silicon Technology. In M. Gasik (Ed.), *Handbook of Ferroalloys* (pp. 179–220). Butterworth-Heinemann. https://doi.org/https://doi.org/10.1016/B978-0-08-097753-9.00006-X

Terrel, R. L., Epps, J. A., Barenberg, E. J., Mitchell, J. K., & Thompson, M. R. (1979). *Soil stabilization in pavement structures-a user's manual volume 1: Pavement design and construction considerations*.

Terzaghi, K., & Peck, R. B. (1967). *Soil Mechanics in Engineering Practice, 2nd Edition*. John Wiley & Sons. https://books.google.com.tr/books?id=AnbHzgEACAAJ

Thompson, M. R. (1966). Lime Reactivity of Illinois Soils. *Journal of the Soil Mechanics and Foundations Division*, *92*(5), 67–92. https://doi.org/10.1061/JSFEAQ.0000911

Thompson, M. R. (1968). Lime stabilization of soils for highway purposes. *Ill Univ Hwy Res Lab Civil Eng Studies*.

Ting, M. Z. Y., Wong, K. S., Rahman, M. E., & Selowarajoo, M. (2021). Prediction model for hardened state properties of silica fume and fly ash based seawater concrete incorporating silicomanganese slag. *Journal of Building Engineering*, *41*, 102356. https://doi.org/https://doi.org/10.1016/j.jobe.2021.102356

Tiwari, N., & Satyam, N. (2019). Experimental Study on the Influence of Polypropylene Fiber on the Swelling Pressure Expansion Attributes of Silica Fume Stabilized Clayey Soil. *Geosciences*, *9*(9). https://doi.org/10.3390/geosciences9090377

Topçu, I. B., & Kaval, M. (2001). Economical analysis of use of silica fume in concrete. *Journal of Eng. &Arch. Fac. Osmangazi University*, *14*(1), 18–31.

Topçuoğlu, Y. A., & Gürocak, Z. (2023). Determination Of Molecular Changes Occuring In Bentonite Stabilized With Fly Ash, Silica Fume And Tuff By Fouirer Transform Infrared Spectroscopy (Ft-Ir) Method. *Journal*, *11*(1), 94–112.

Tran, T. D., Cui, Y.-J., Tang, A. M., Audiguier, M., & Cojean, R. (2014). Effects of lime treatment on the microstructure and hydraulic conductivity of Héricourt clay. *Journal of Rock Mechanics and Geotechnical Engineering*, *6*(5), 399–404. https://doi.org/https://doi.org/10.1016/j.jrmge.2014.07.001

Türköz, M., Savaş, H., & Tasci, G. (2018). The effect of silica fume and lime on geotechnical properties of a clay soil showing both swelling and dispersive features. *Arabian Journal of Geosciences*, *11*(23), 735. https://doi.org/10.1007/s12517-018-4045-x

Türköz, M., Umu, S. U., & Öztürk, O. (2021). Effect of silica fume as a waste material for sustainable environment on the stabilization and dynamic behavior of dispersive soil. *Sustainability*, *13*(8), 4321.

Turkoz, M., & Vural, P. (2013). *The effects of cement and natural zeolite additives on problematic clay soils*. *20*(4), 395–405. https://doi.org/doi:10.1515/secm-2012-0104

U.S ARMY CORPS OF ENGINEERS WASHINGTON DC. (1999). *Use of Waste Materials in Pavement Construction*.

Walker, D. D. (1992). *Innovations and Uses for Lime*. ASTM. https://books.google.com.tr/books?id=oAA5a4raA5EC

Wang, X., Huang, J., Dai, S., Ma, B., & Jiang, Q. (2020). Investigation of silica fume as foam cell stabilizer for foamed concrete. *Construction and Building Materials*, *237*, 117514. https://doi.org/https://doi.org/10.1016/j.conbuildmat.2019.117514

West, G., & Carder, D. R. (1997). *Review of lime piles and lime-stabilised soil columns* (Vol. 305). Thomas Telford.

Winterkorn, H. F., & Pamukcu, S. (1991). Soil Stabilization and Grouting. In H.-Y. Fang (Ed.), *Foundation Engineering Handbook* (pp. 317–378). Springer US. https://doi.org/10.1007/978-1-4757-5271-7_9

Yarbaşı, N., Kalkan, E., & Akbulut, S. (2007). Modification of the geotechnical properties, as influenced by freeze–thaw, of granular soils with waste additives. *Cold Regions Science and Technology*, *48*(1), 44–54. https://doi.org/https://doi.org/10.1016/j.coldregions.2006.09.009

Yeğinobalı, A. (2011). *Silis Dumanı ve Çimento ile Betonda Kullanımı*. https://www.turkcimento.org.tr/uploads/pdf/silis_dumanı_ve_çimento_ile_betonda_kullanımı.pdf

Yoder, E. J., & Witczak, M. W. (1975). *Principles of Pavement Design*. Wiley. https://books.google.com.tr/books?id=eDVSAAAAMAAJ

Yong, R. N., & Warkentin, B. P. (1975). *Soil properties and behaviour* (Vol. 5). Elsevier Scientific Pub. Co.

Yongshan, W., James, K., G, B. H., & C, J. R. (2002). Influence of Amorphous Clay-Size Materials on Soil Plasticity and Shrink-Swell Behavior. *Journal of Geotechnical and Geoenvironmental Engineering*, *128*(12), 1026–1031. https://doi.org/10.1061/(ASCE)1090-0241(2002)128:12(1026)

Zaini, M. S. I., & Hasan, M. (2023). Effect of Optimum Utilization of Silica Fume and Lime On the Stabilization of Problematic Soils. *International Journal of Integrated Engineering*, *15*(1), 352–366. https://penerbit.uthm.edu.my/ojs/index.php/ijie/article/view/9573

Zhang, Z., Zhang, B., & Yan, P. (2016). Comparative study of effect of raw and densified silica fume in the paste, mortar and concrete. Construction and Building Materials, 105, 82–93. https://doi.org/https://doi.org/10.1016/j.conbuildmat.2015.12.045

APPENDICES

A. Swell Percent vs Square-Root of Time Graphs of Treated Samples

Swell percent versus square root of time graphs of 3% L, 3% L + 5% SF, 3% L + 10% SF, 3% L + 15% SF, 3% L + 20% SF, 5% L, 5% L + 5% SF, 5% L + 10% SF, 5% L + 15% SF, 5% L + 20% SF treated samples with 0-7-28 days curing results were presented separately.

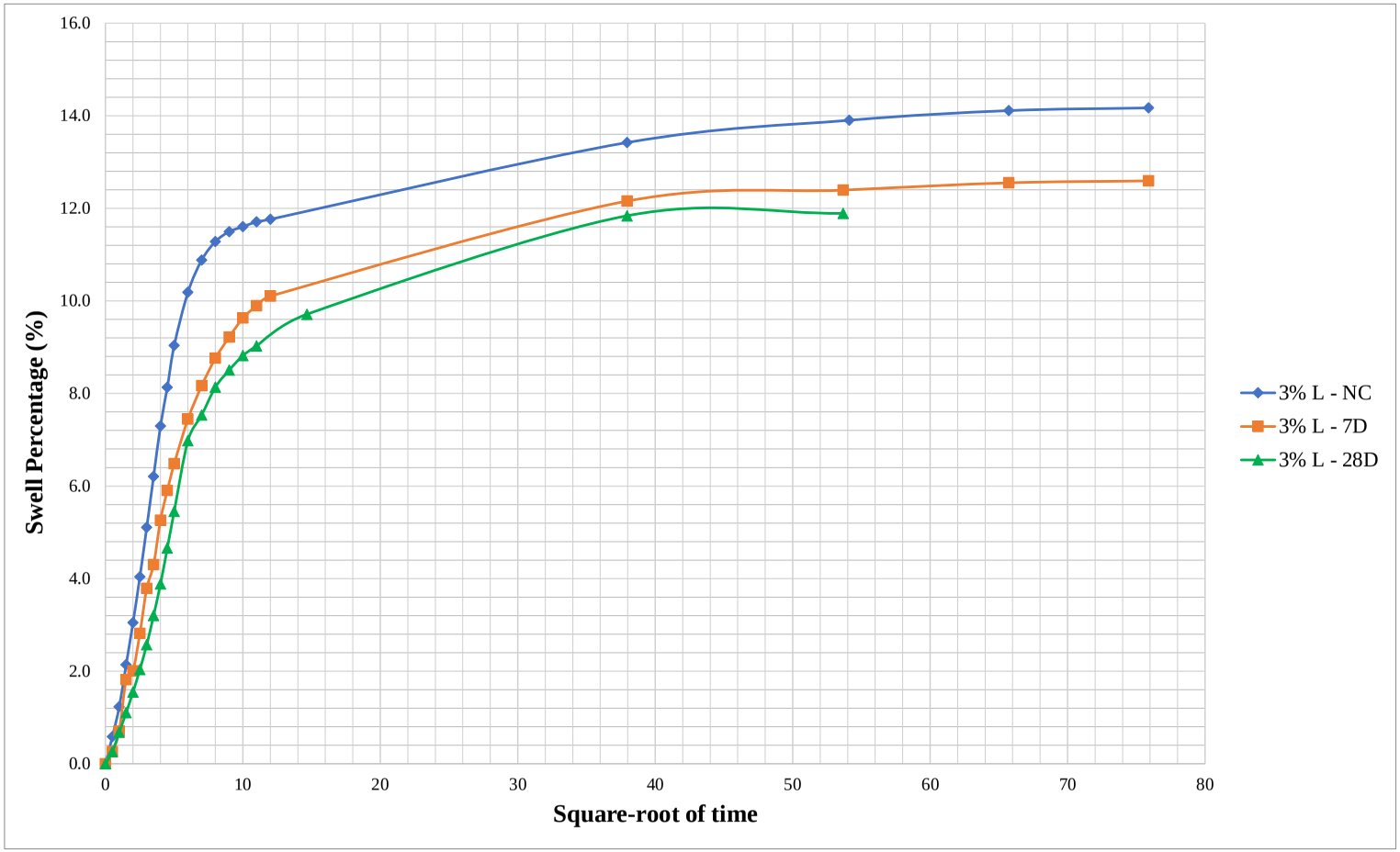

Figure A.1 Percent Swell vs Square-Root of Time Relationships for 3% L Samples with 0-7-28 Days of Curing

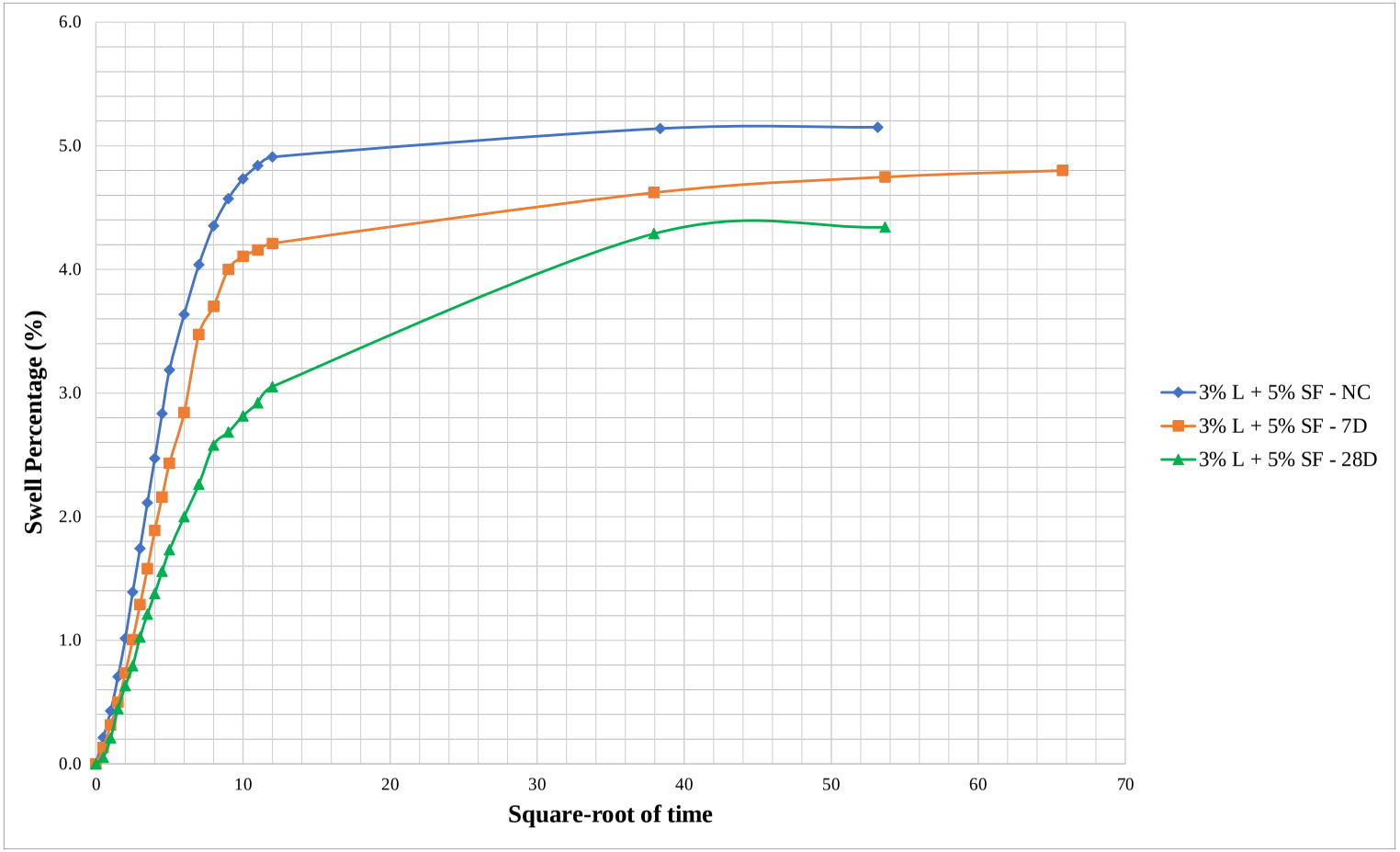

Figure A.2 Percent Swell vs Square-Root of Time Relationships for 3% L + 5% SF Samples with 0-7-28 Days of Curing

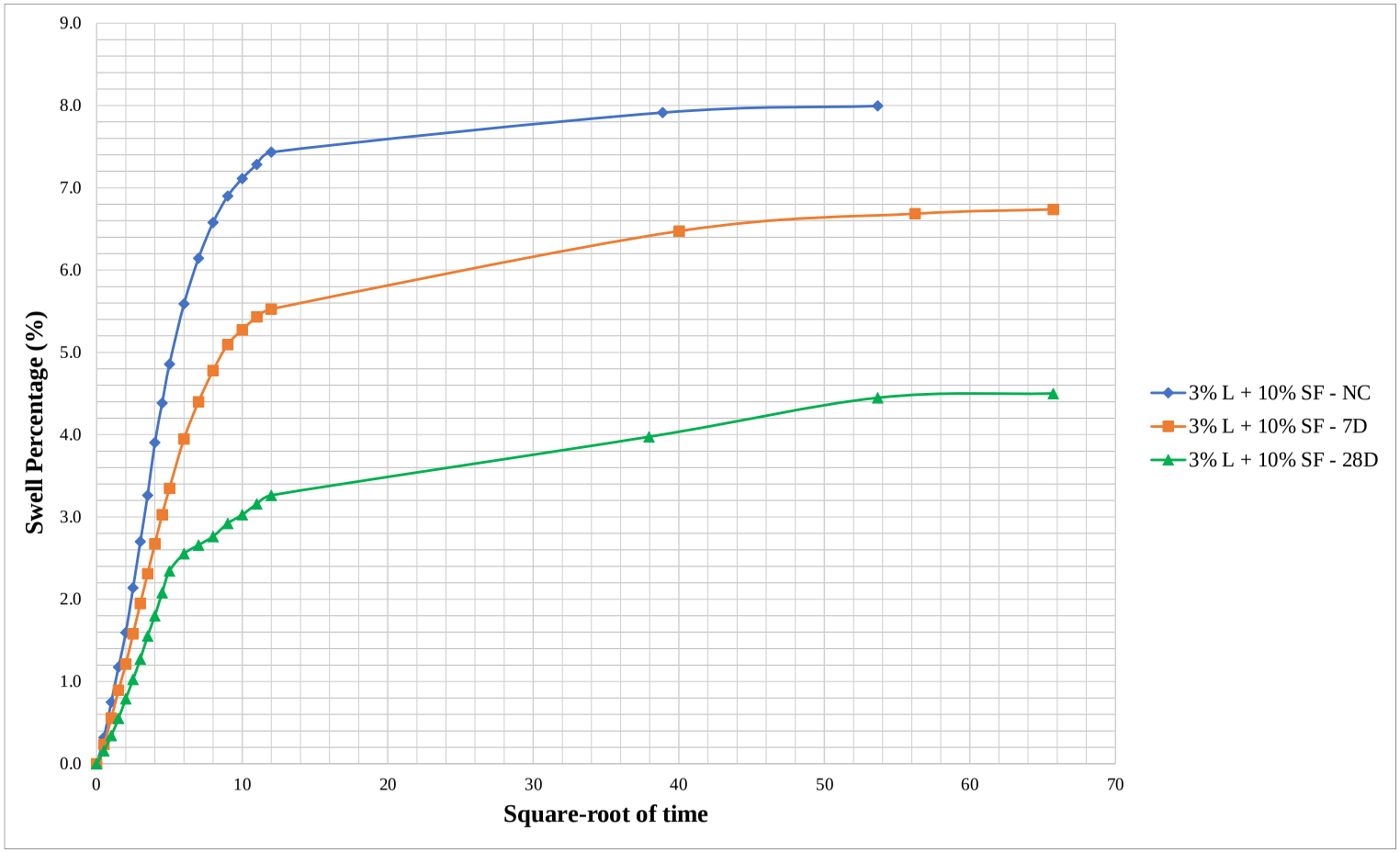

Figure A.3 Percent Swell vs Square-Root of Time Relationships for 3% L + 10% SF Samples with 0-7-28 Days of Curing

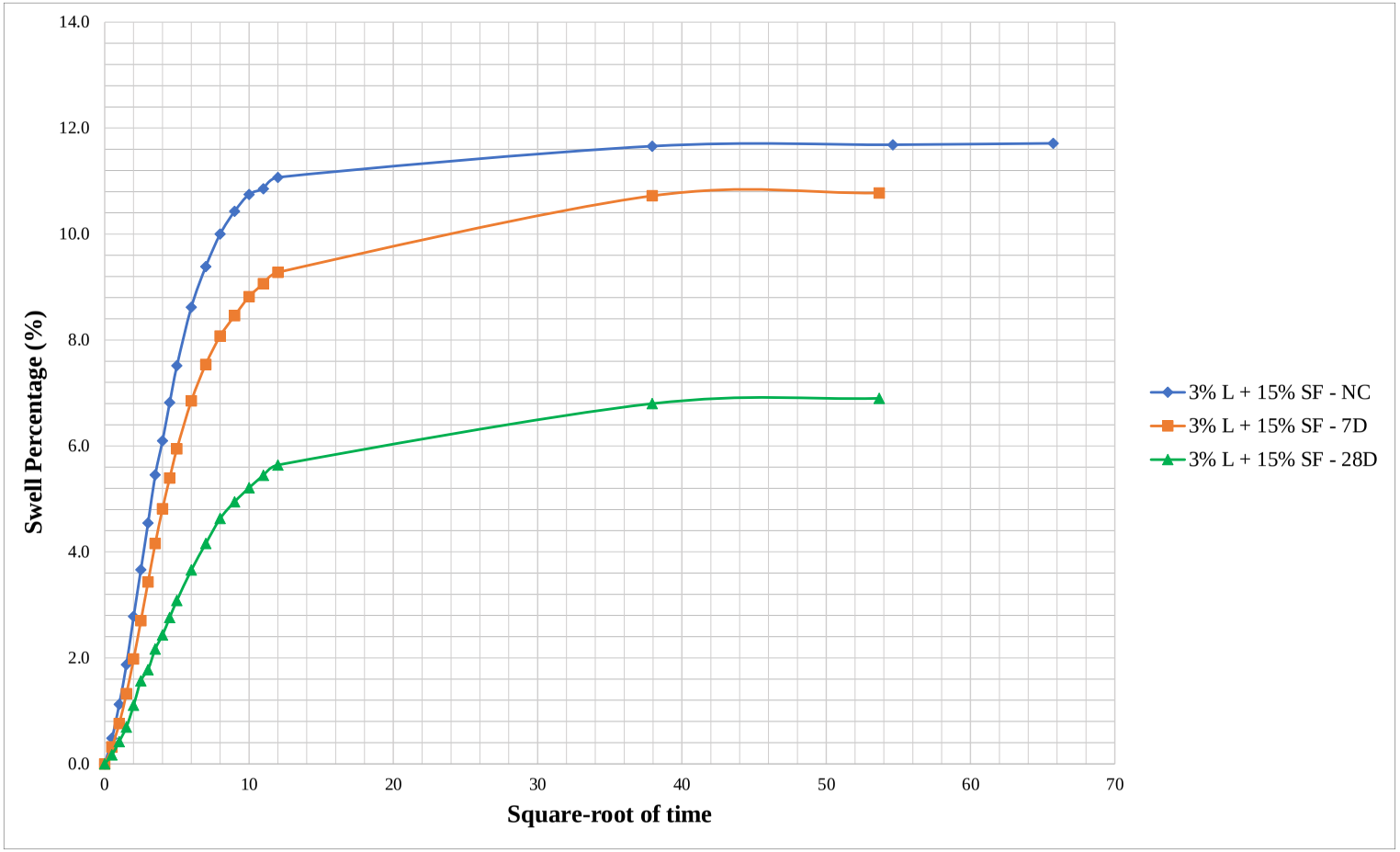

Figure A.4 Percent Swell vs Square-Root of Time Relationships for 3% L + 15% SF Samples with 0-7-28 Days of Curing

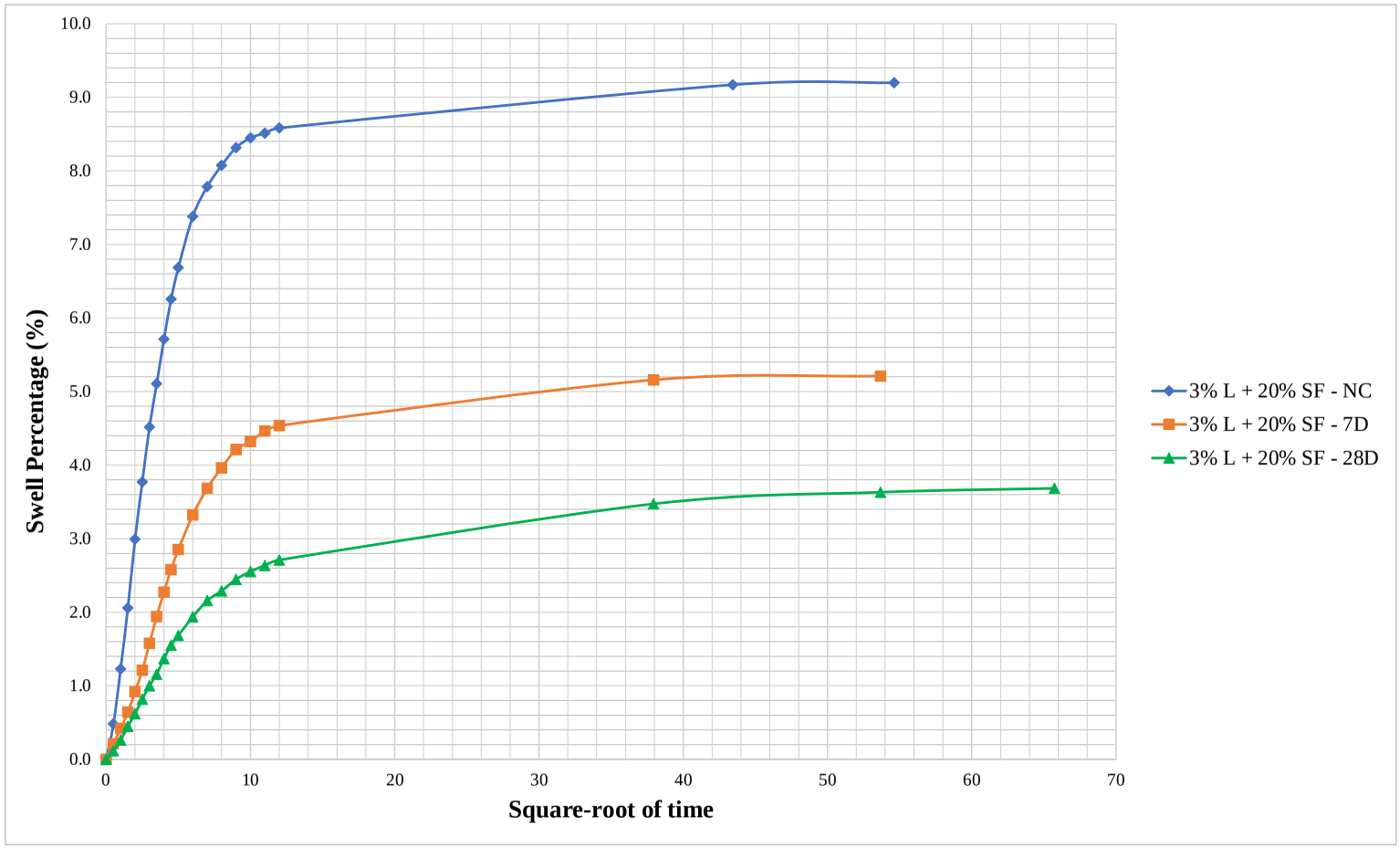

Figure A.5 Percent Swell vs Square-Root of Time Relationships for 3% L + 20% SF Samples with 0-7-28 Days of Curing

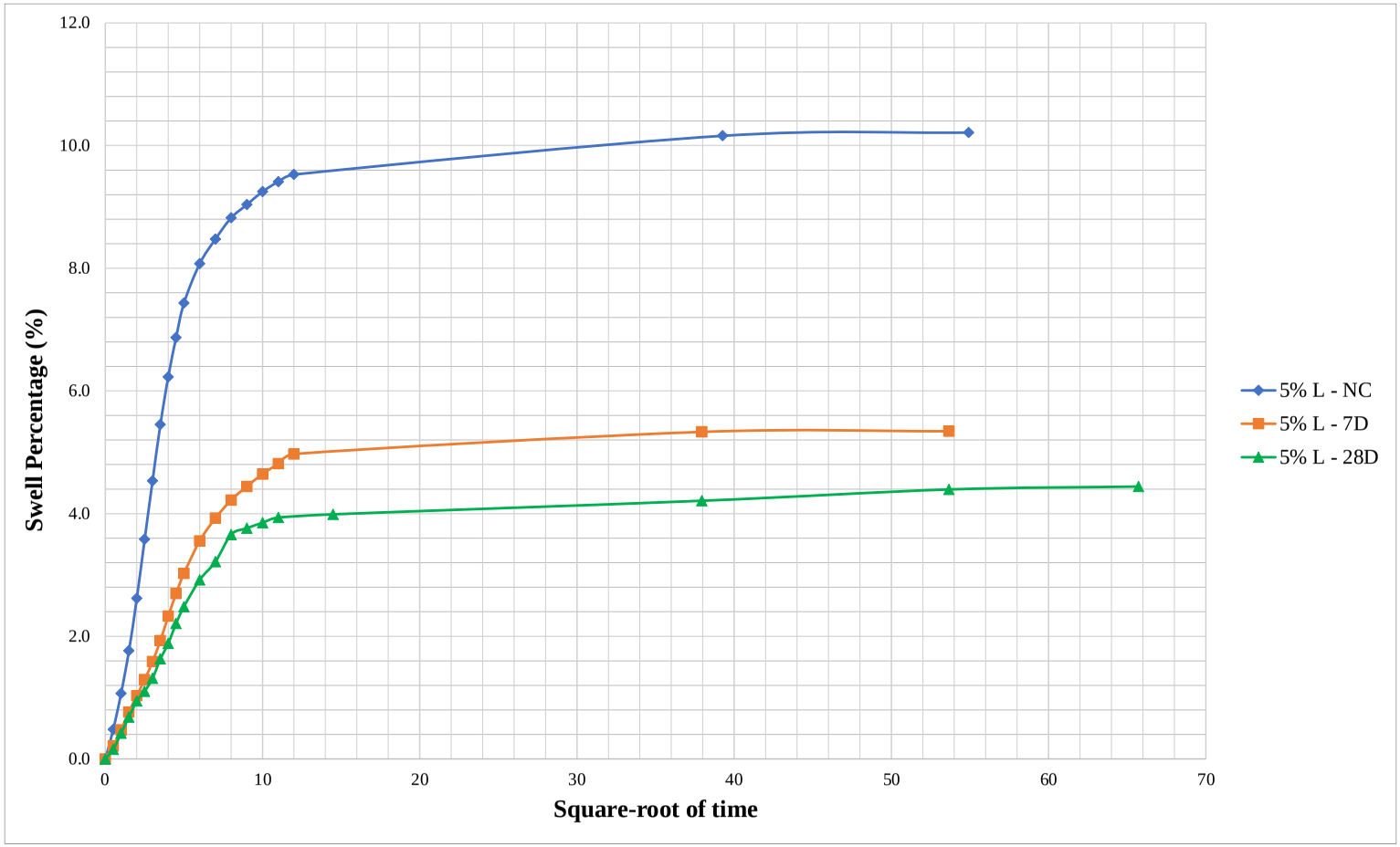

Figure A.6 Percent Swell vs Square-Root of Time Relationships for 5% L Samples with 0-7-28 Days of Curing

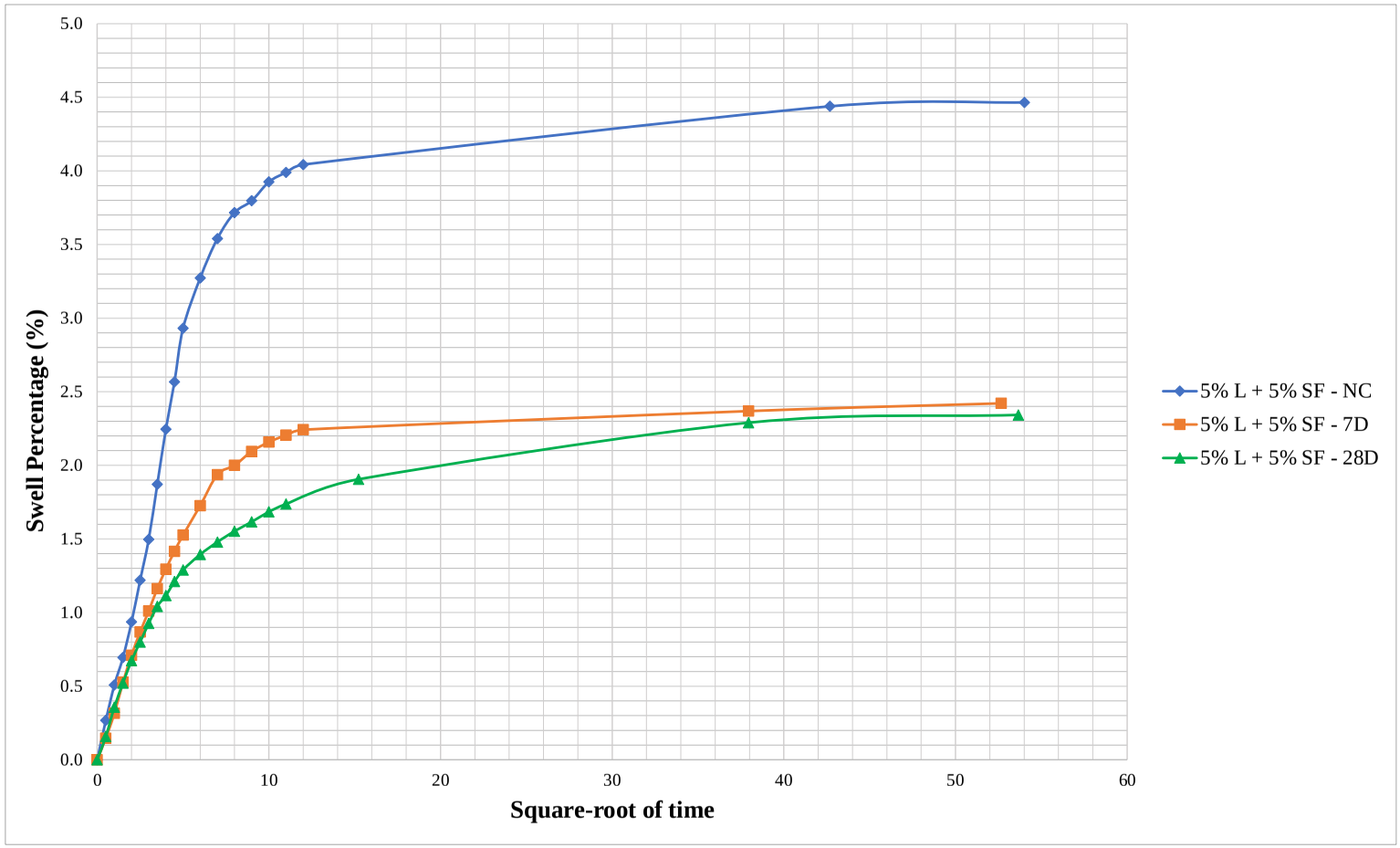

Figure A.7 Percent Swell vs Square-Root of Time Relationships for 5% L + 5% SF Samples with 0-7-28 Days of Curing

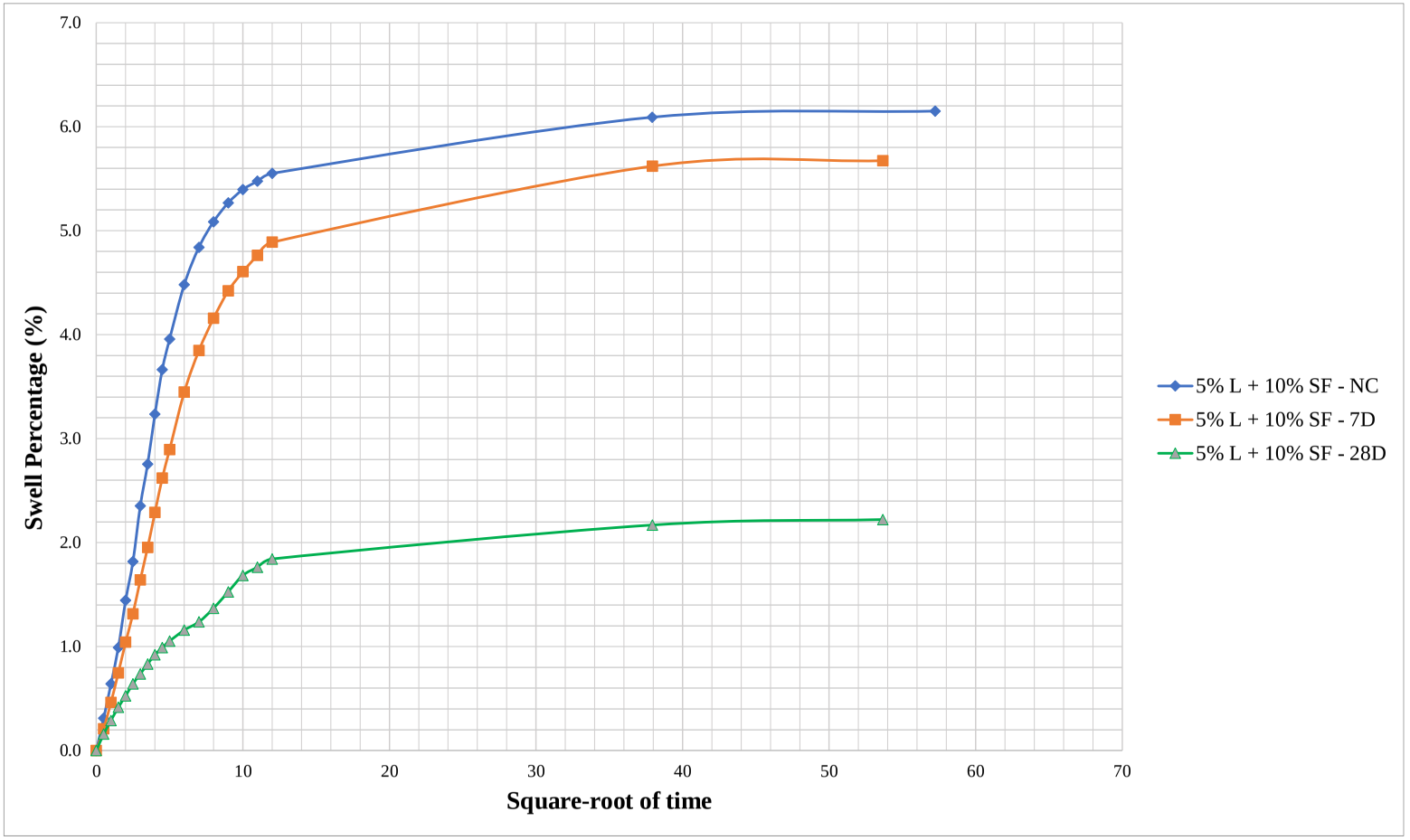

Figure A.8 Percent Swell vs Square-Root of Time Relationships for 5% L + 10% SF Samples with 0-7-28 Days of Curing

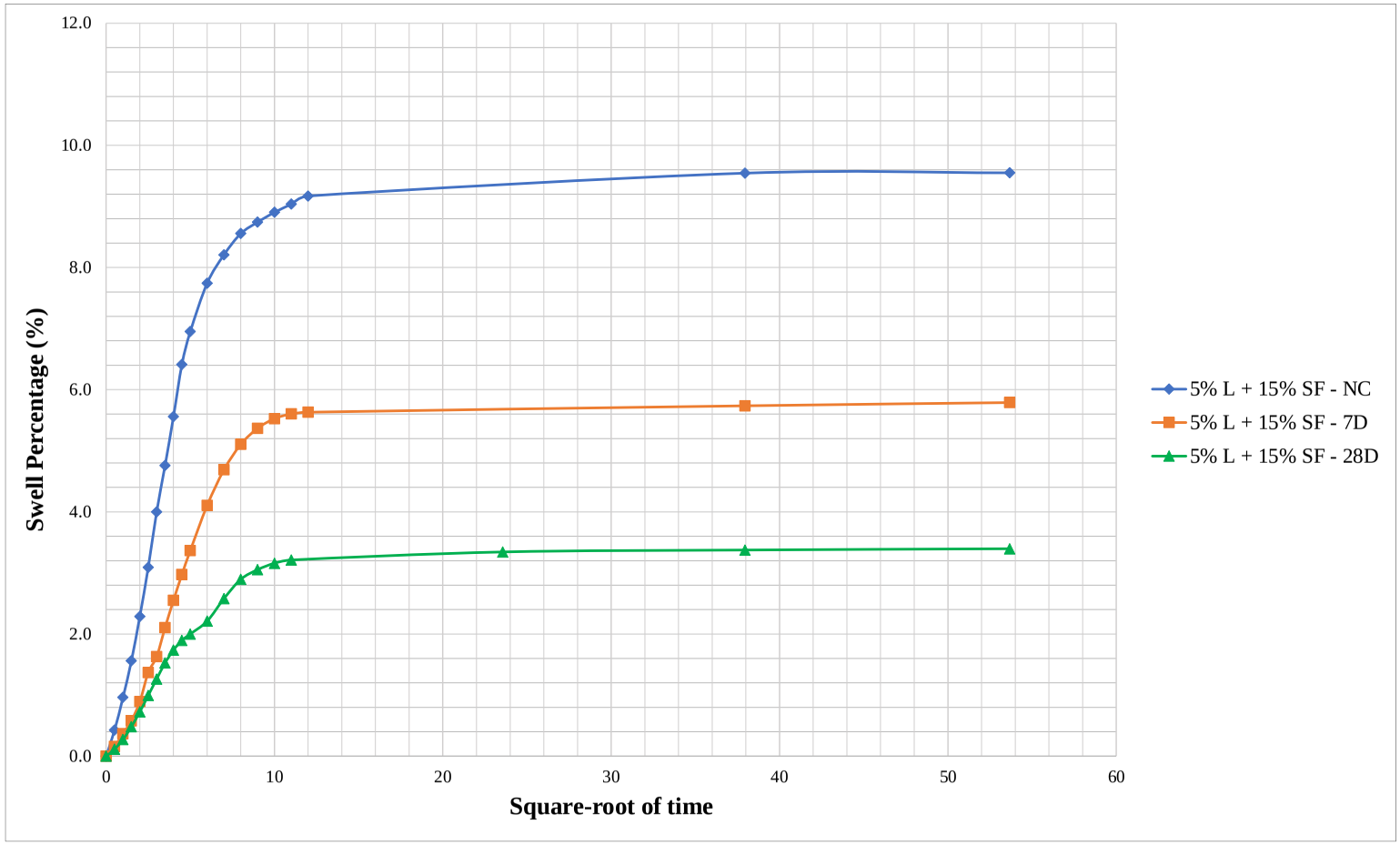

Figure A.9 Percent Swell vs Square-Root of Time Relationships for 5% L + 15% SF Samples with 0-7-28 Days of Curing

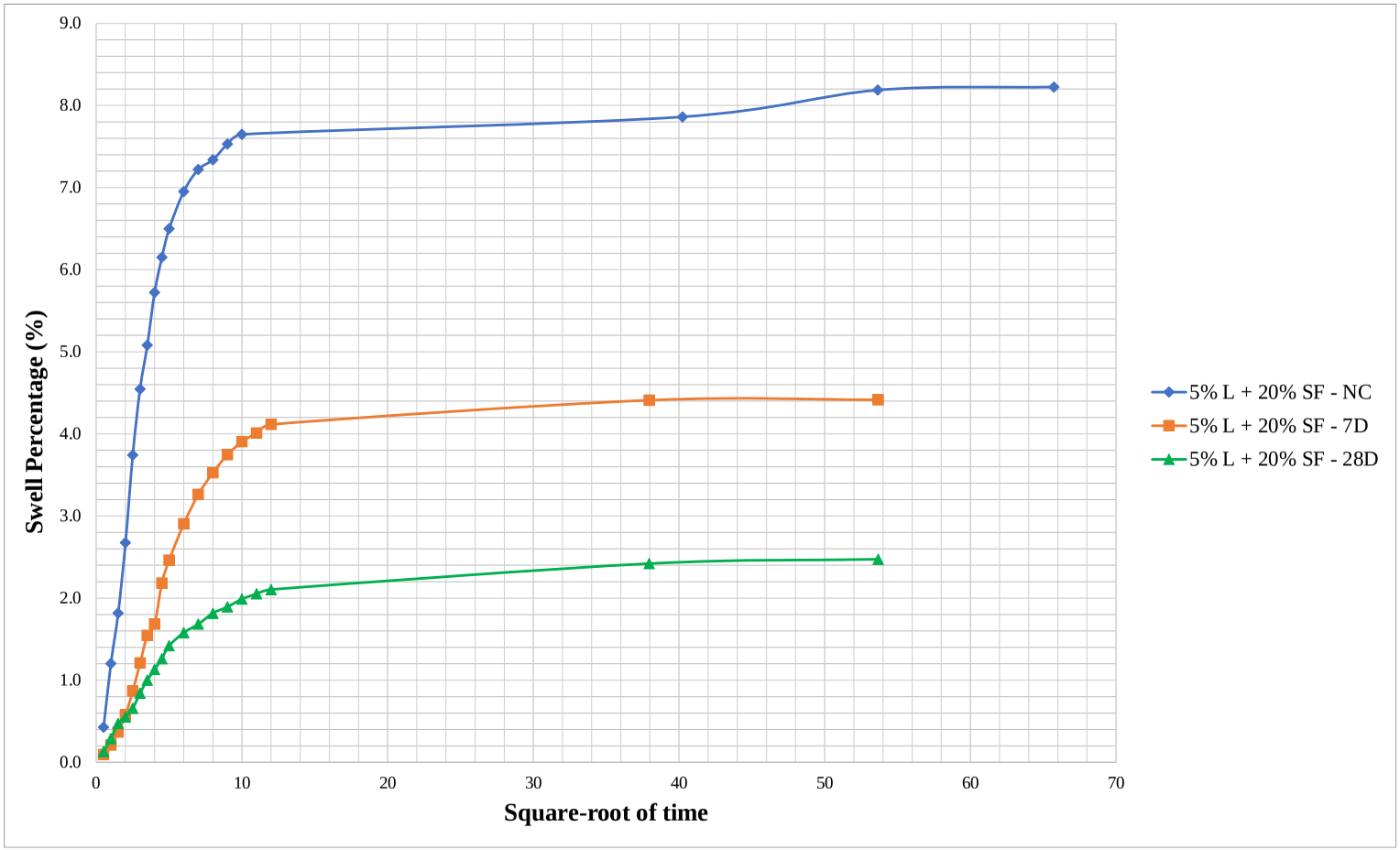

Figure A.10 Percent Swell vs Square-Root of Time Relationships for 5% L + 20% SF Samples with 0-7-28 Days of Curing

B. Axial Compressive Stress vs Axial Strain of Treated Samples

Axial compressive stress versus axial strain graphs of 3% L, 3% L + 5% SF, 3% L + 10% SF, 3% L + 15% SF, 3% L + 20% SF, 5% L, 5% L + 5% SF, 5% L + 10% SF, 5% L + 15% SF, 5% L + 20% SF treated samples with 0-7-28 days curing results were presented separately.

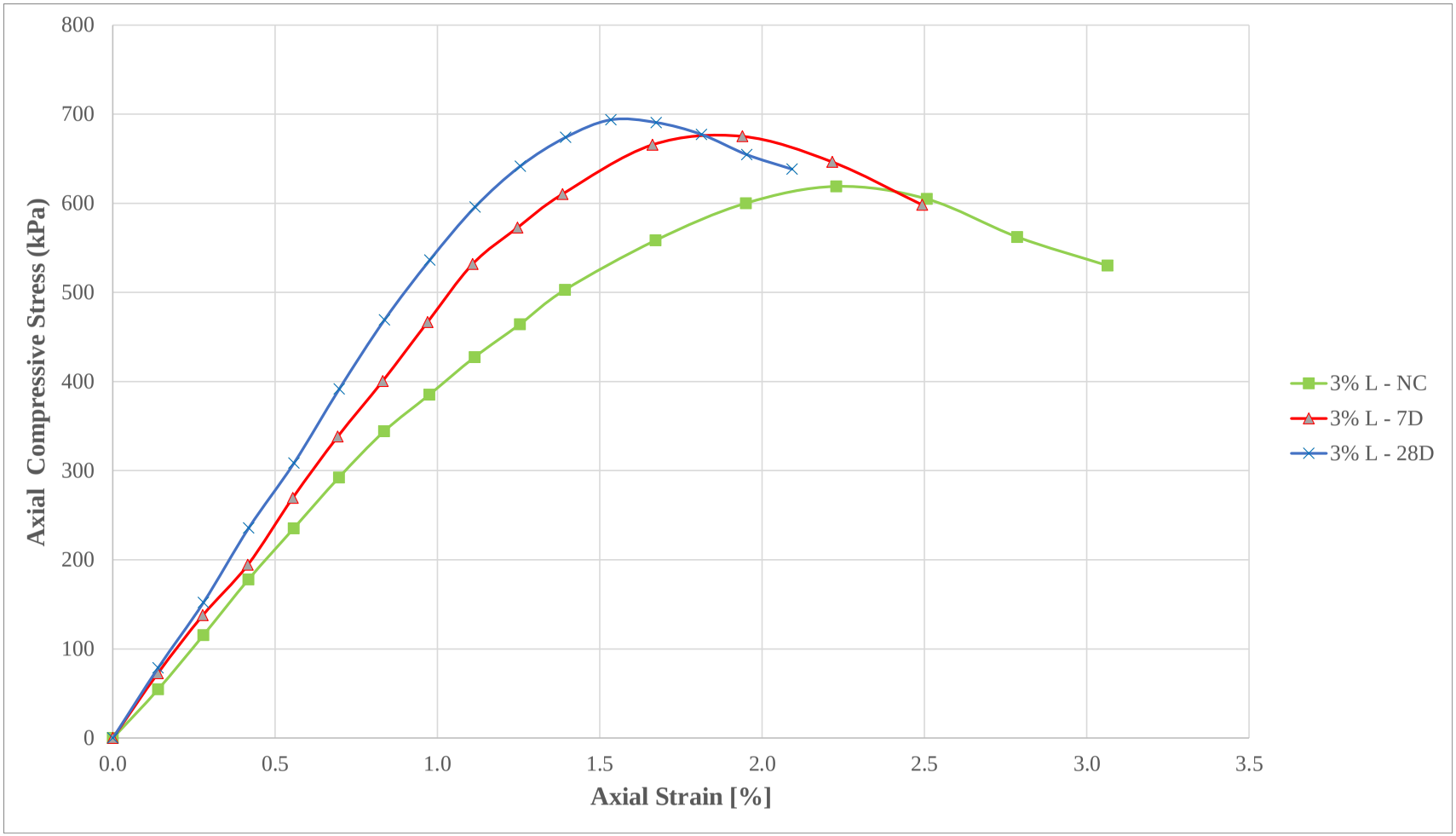

Figure B.11 Axial Compressive Stress vs Axial Strain Relationships for 3% L Samples with 0-7-28 Days of Curing

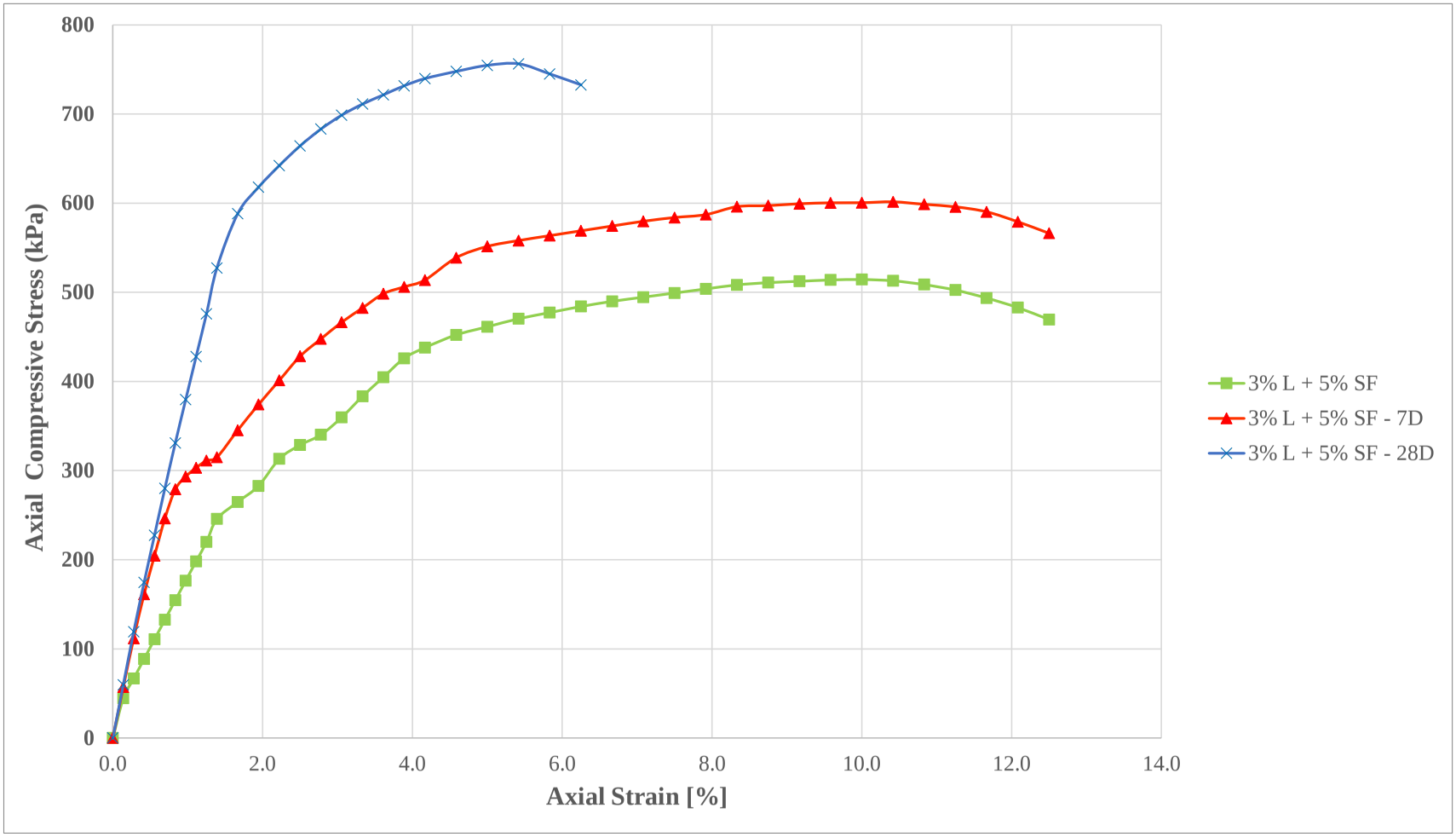

Figure B.12 Axial Compressive Stress vs Axial Strain Relationships for 3% L + 5% SF Samples with 0-7-28 Days of Curing

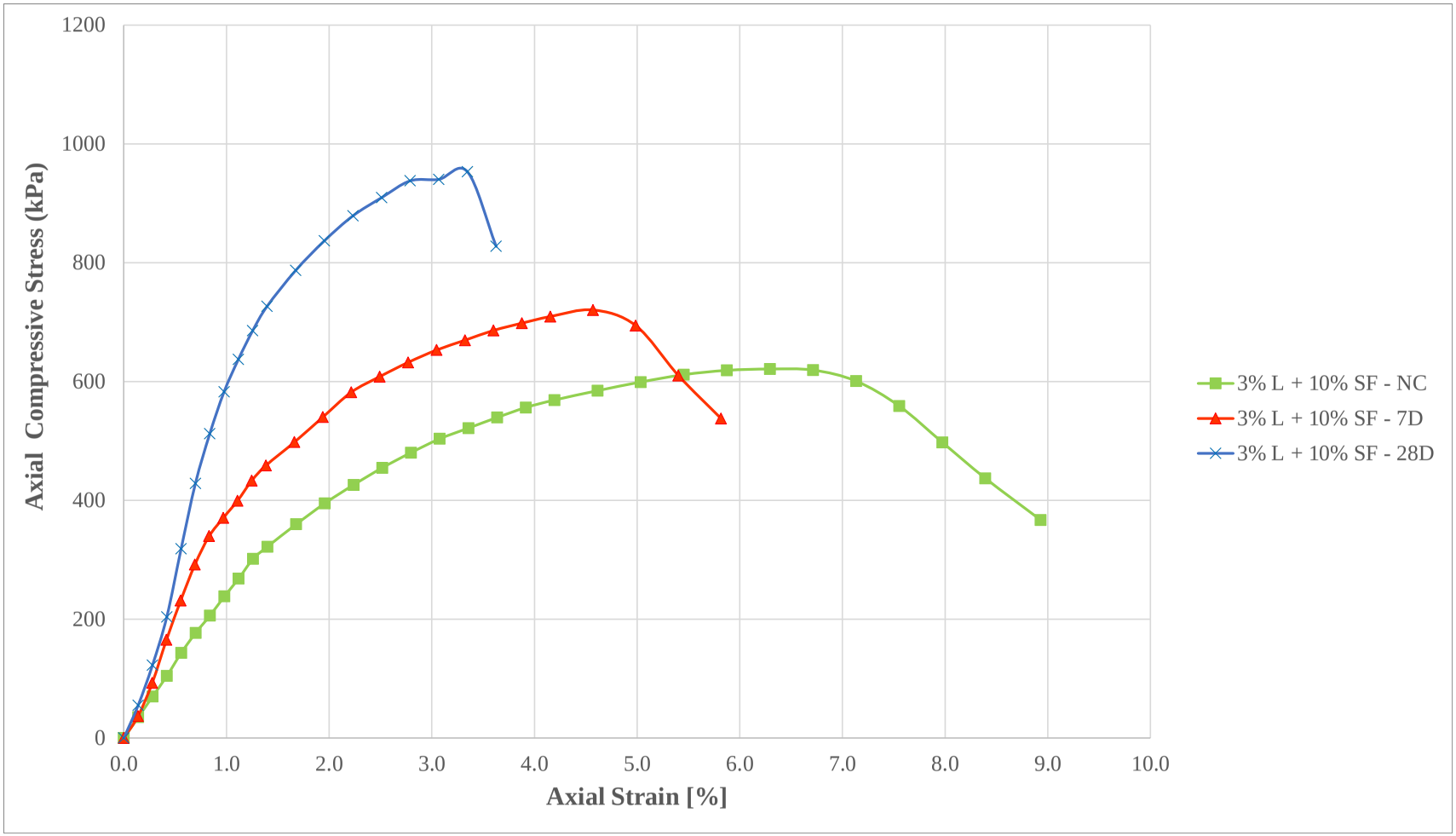

Figure B.13 Axial Compressive Stress vs Axial Strain Relationships for 3% L + 10% SF Samples with 0-7-28 Days of Curing

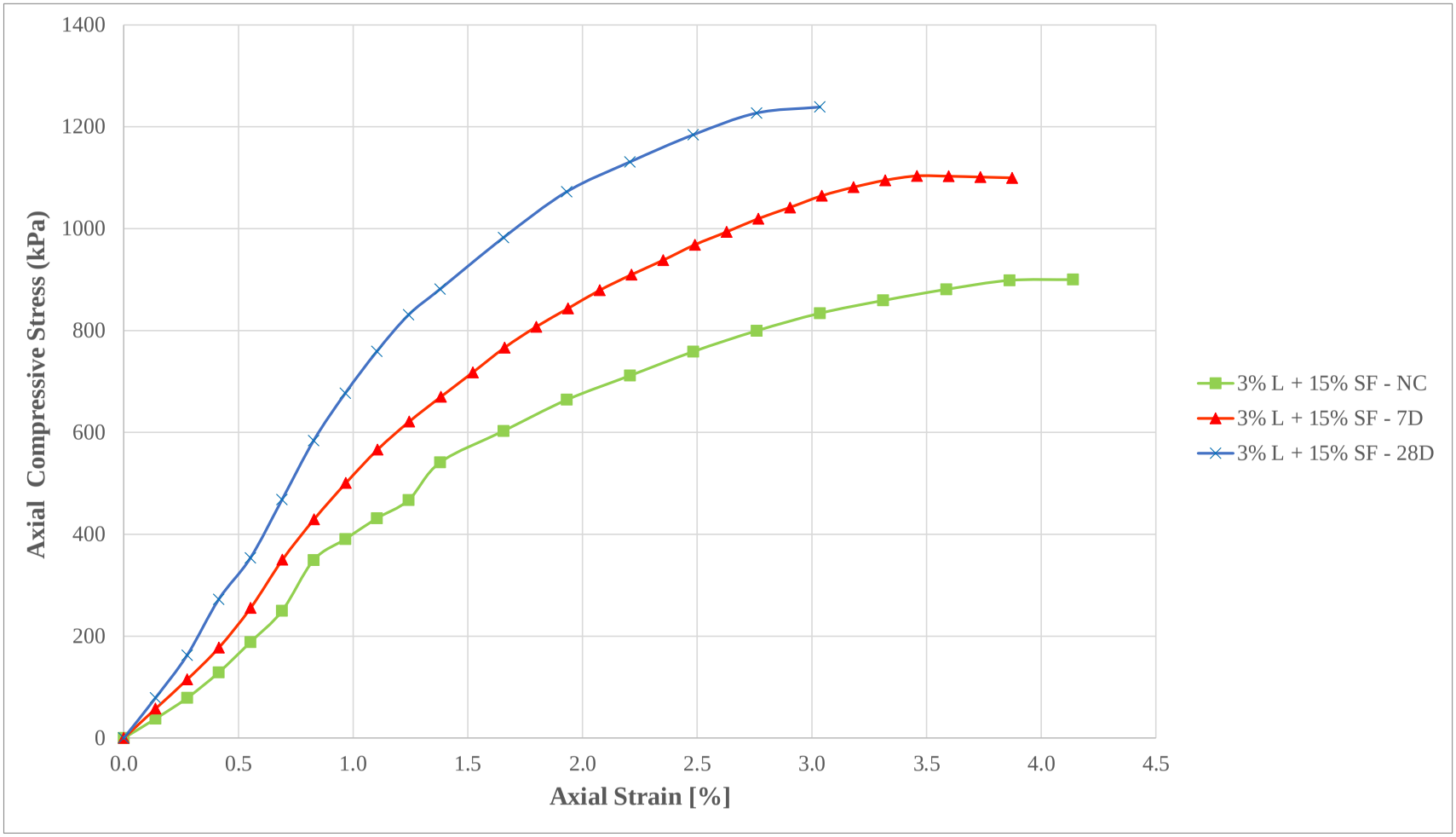

Figure B.14 Axial Compressive Stress vs Axial Strain Relationships for 3% L + 15% SF Samples with 0-7-28 Days of Curing

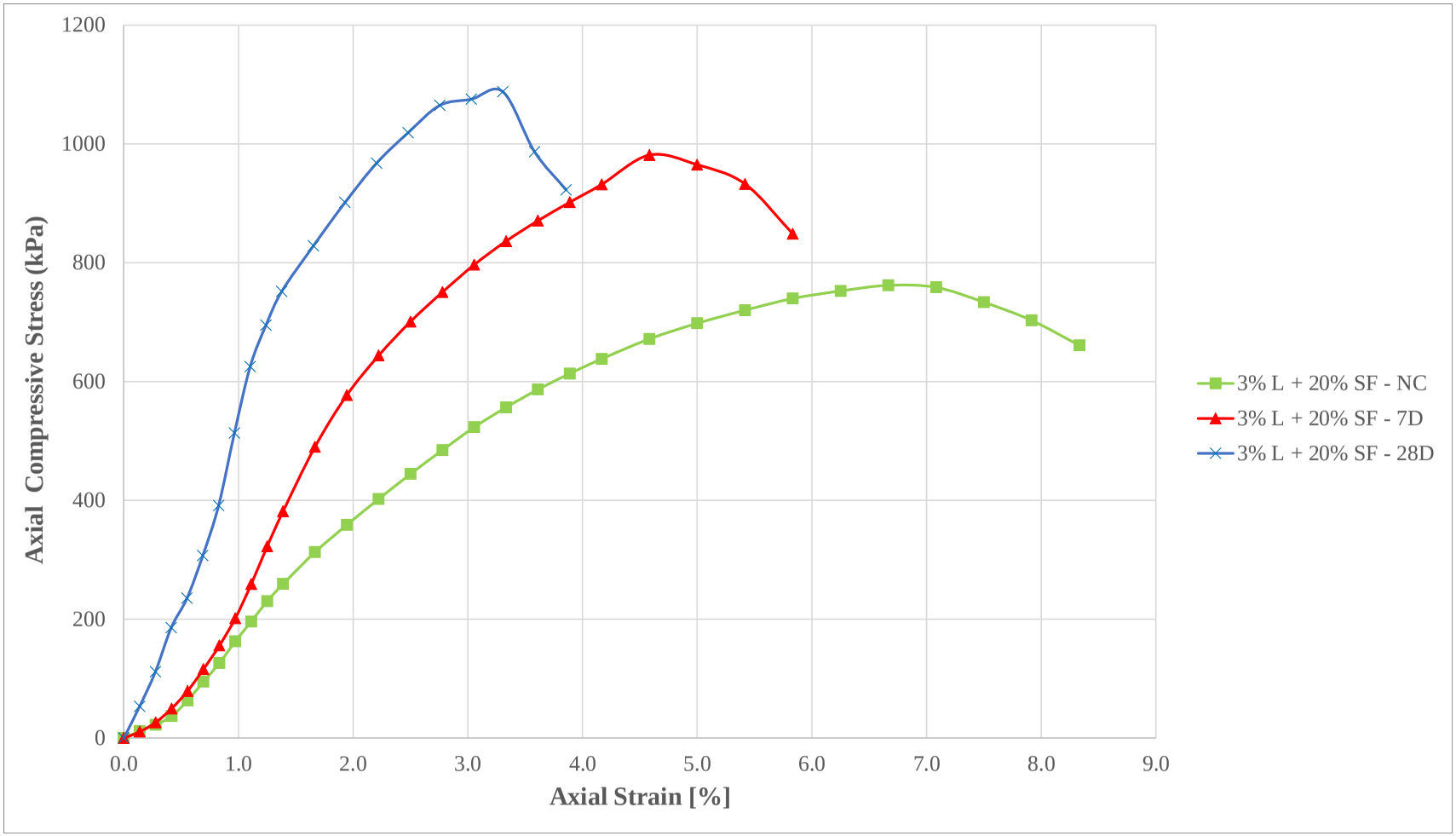

Figure B.15 Axial Compressive Stress vs Axial Strain Relationships for 3% L + 20% SF Samples with 0-7-28 Days of Curing

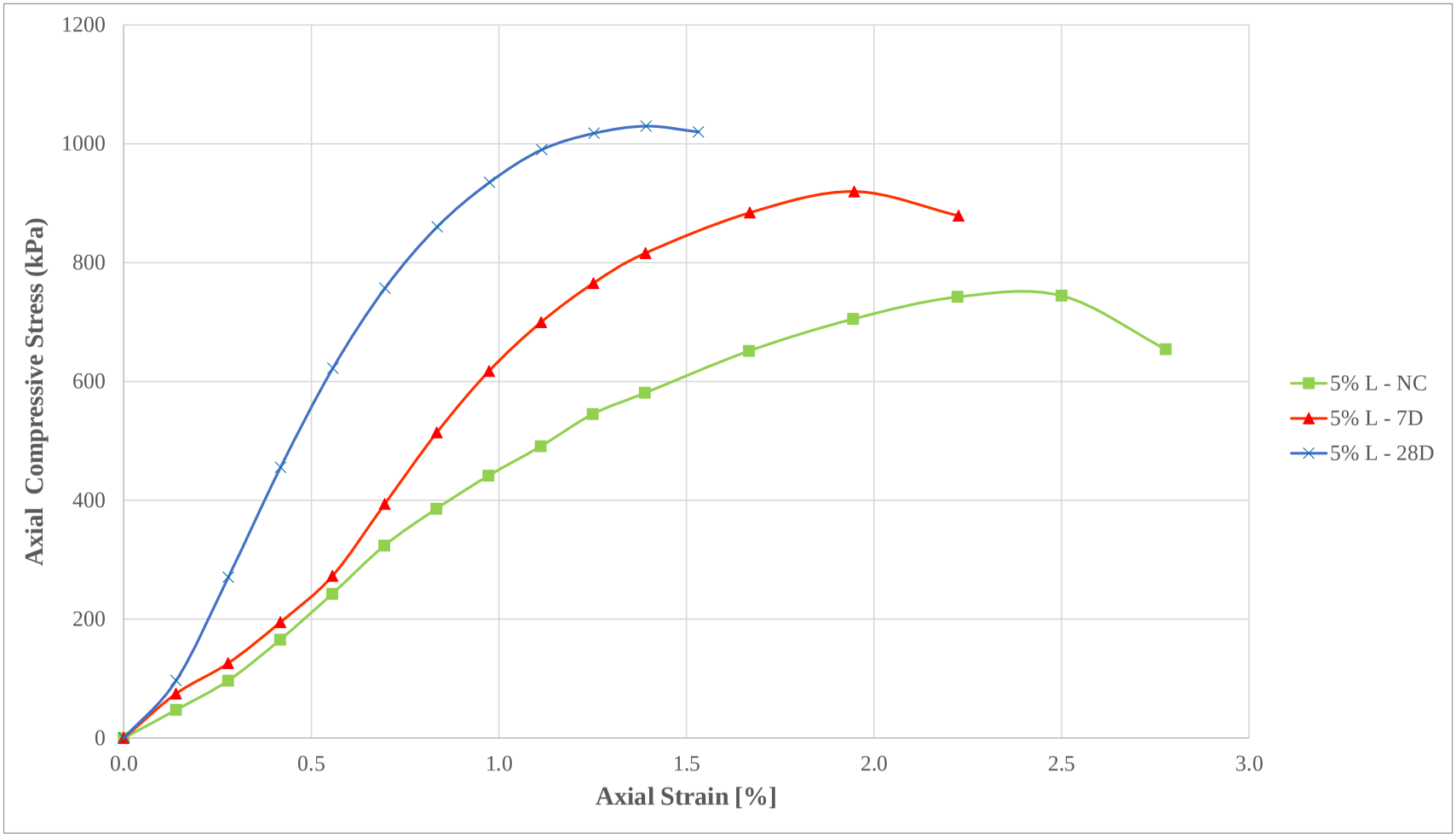

Figure B.16 Axial Compressive Stress vs Axial Strain Relationships for 5% L Samples with 0-7-28 Days of Curing

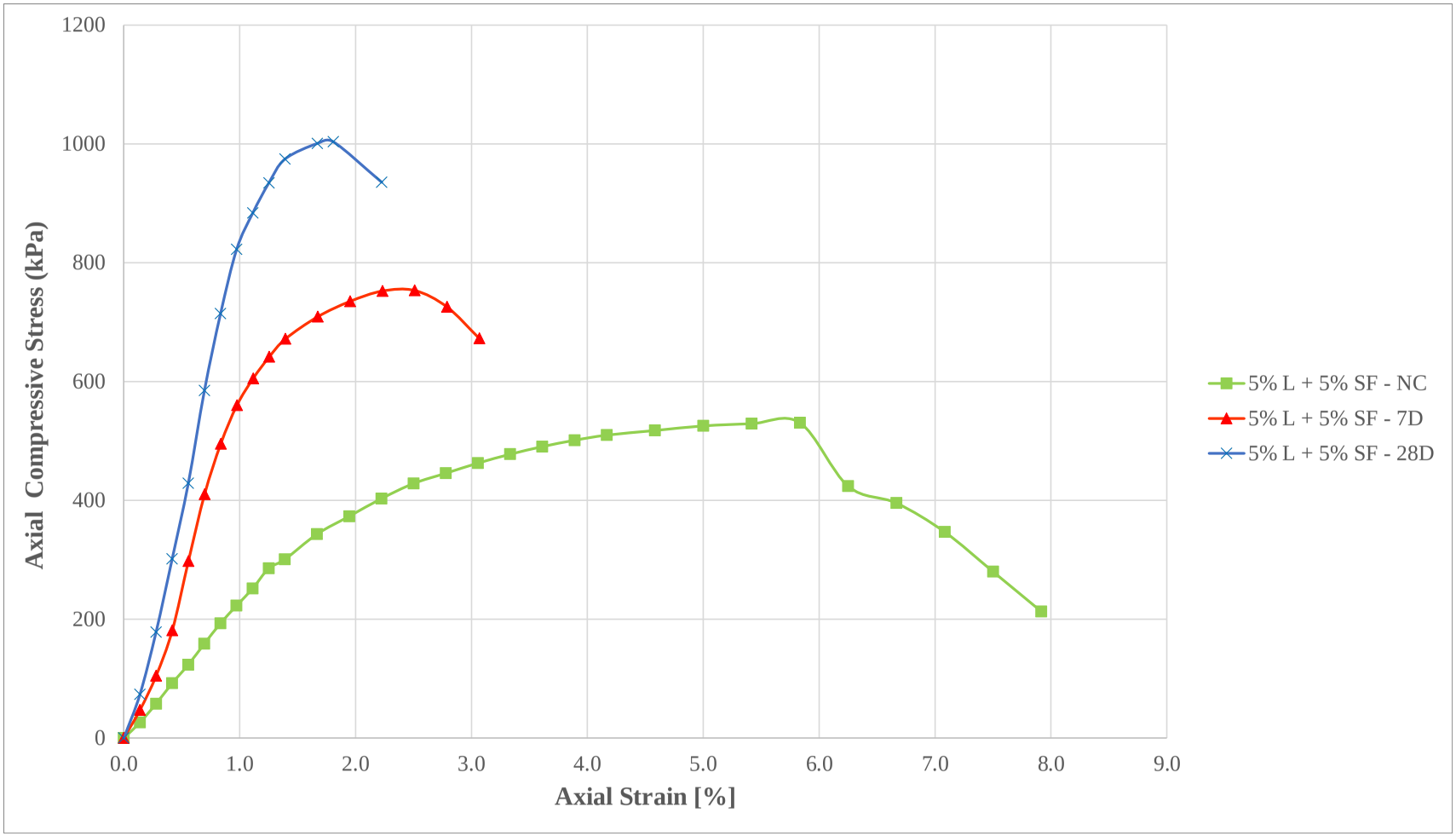

Figure B.17 Axial Compressive Stress vs Axial Strain Relationships for 5% L + 5% SF Samples with 0-7-28 Days of Curing

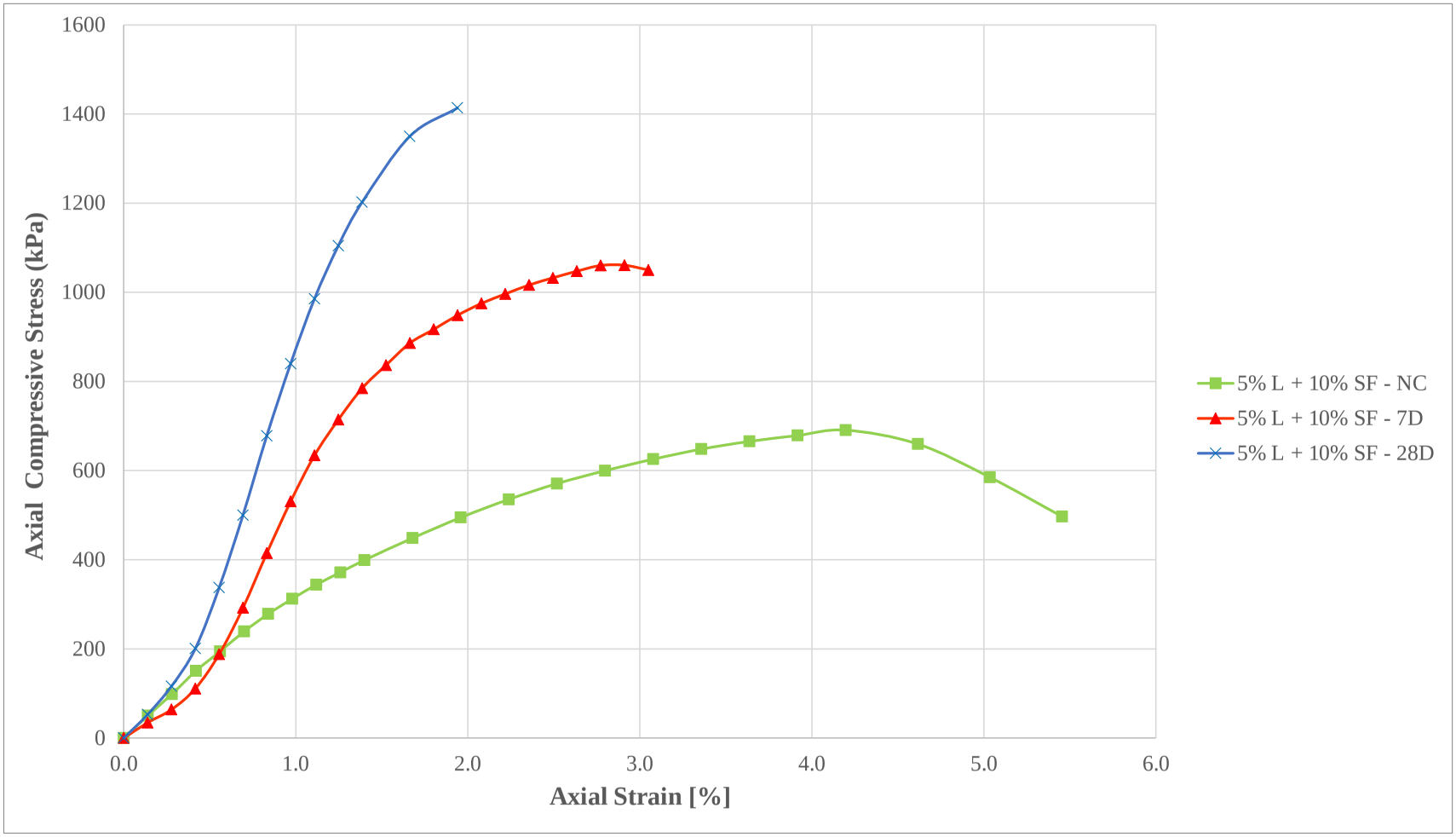

Figure B.18 Axial Compressive Stress vs Axial Strain Relationships for 5% L + 10% SF Samples with 0-7-28 Days of Curing

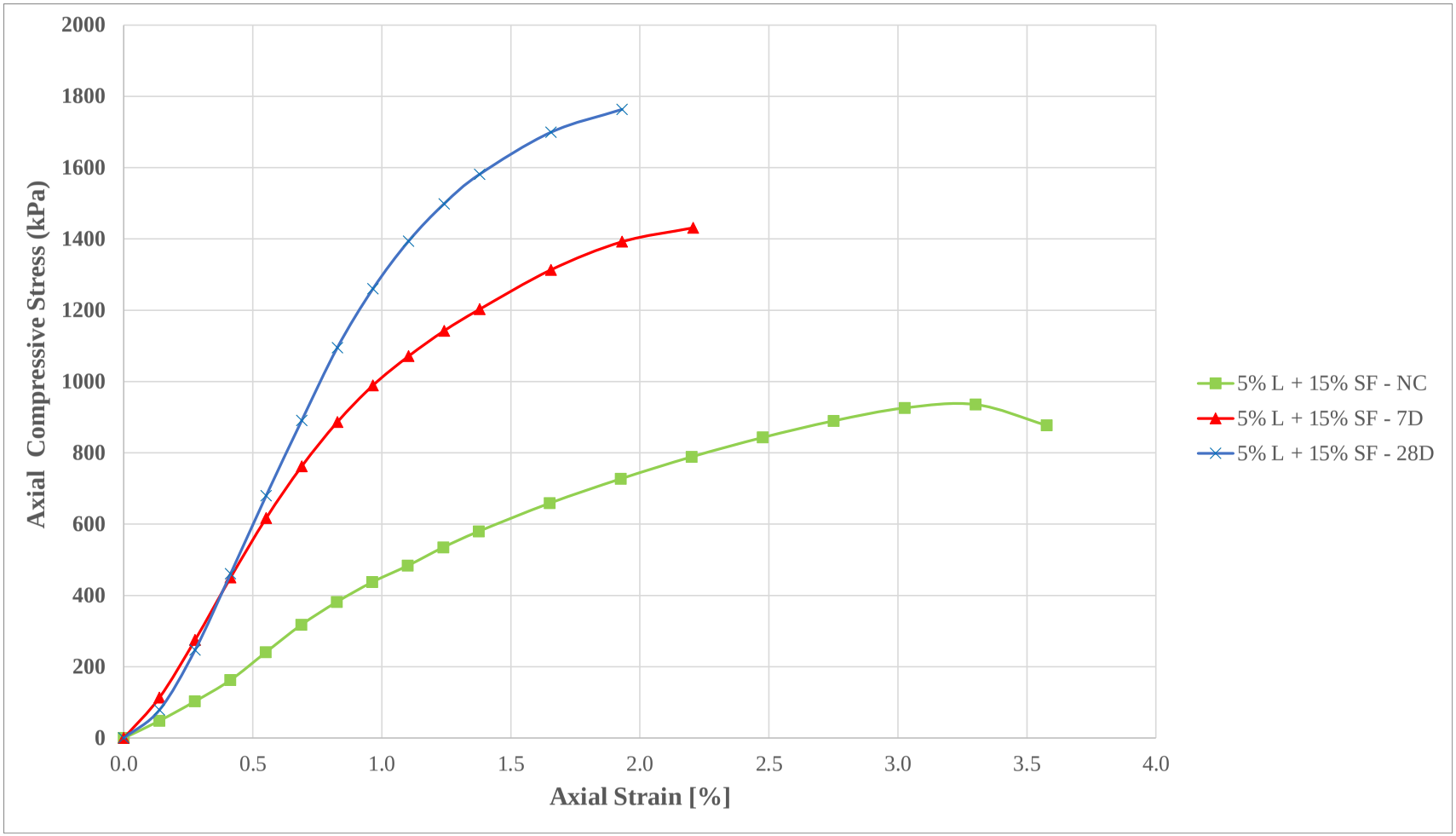

Figure B.19 Axial Compressive Stress vs Axial Strain Relationships for 5% L + 15% SF Samples with 0-7-28 Days of Curing

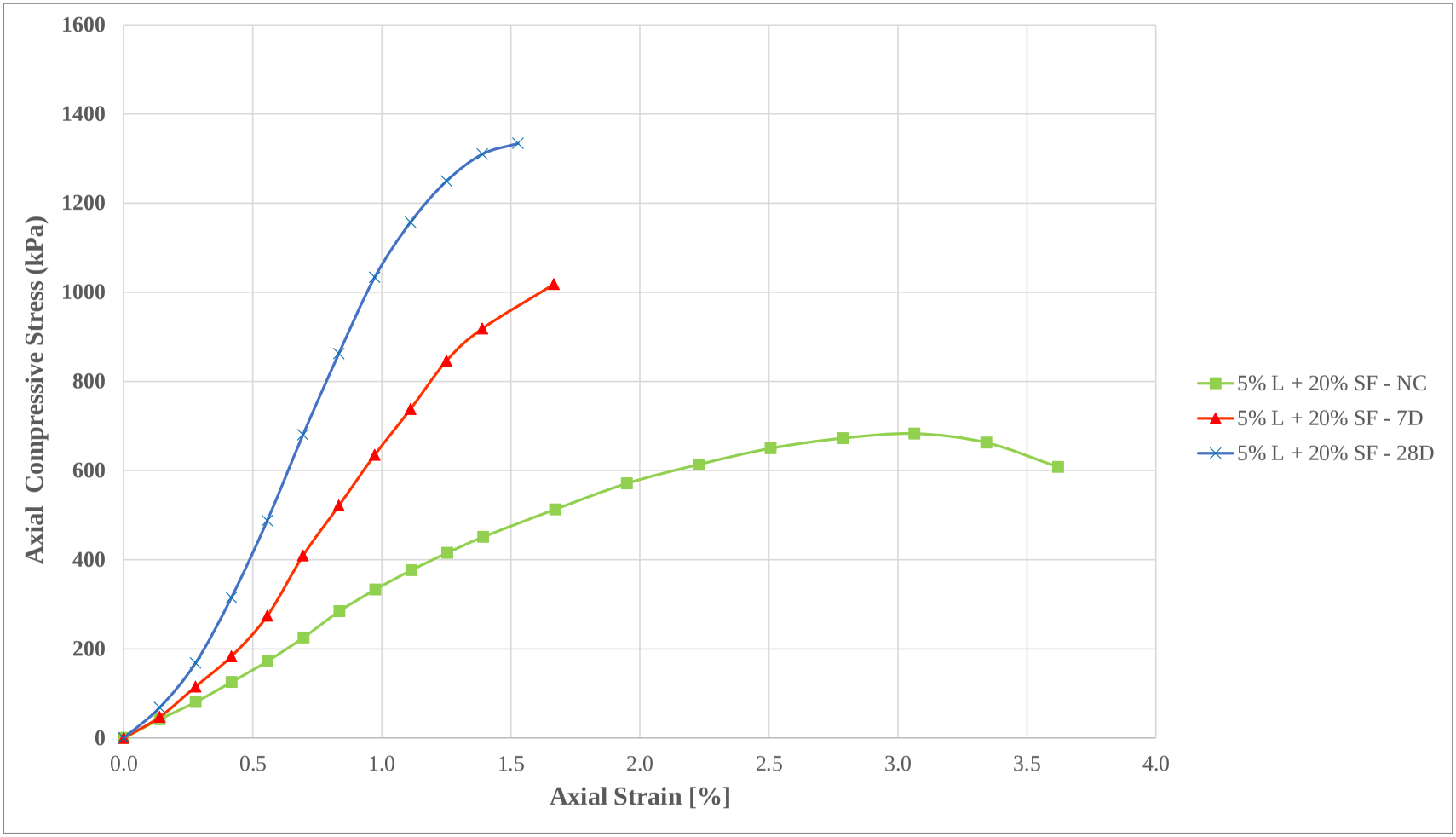

Figure B.20 Axial Compressive Stress vs Axial Strain Relationships for 5% L + 20% SF Samples with 0-7-28 Days of Curing

C. Swell Rate vs Percent Additive

Swell percent versus percent additive of treated samples with 0-7-28 days curing results were presented in one graph.

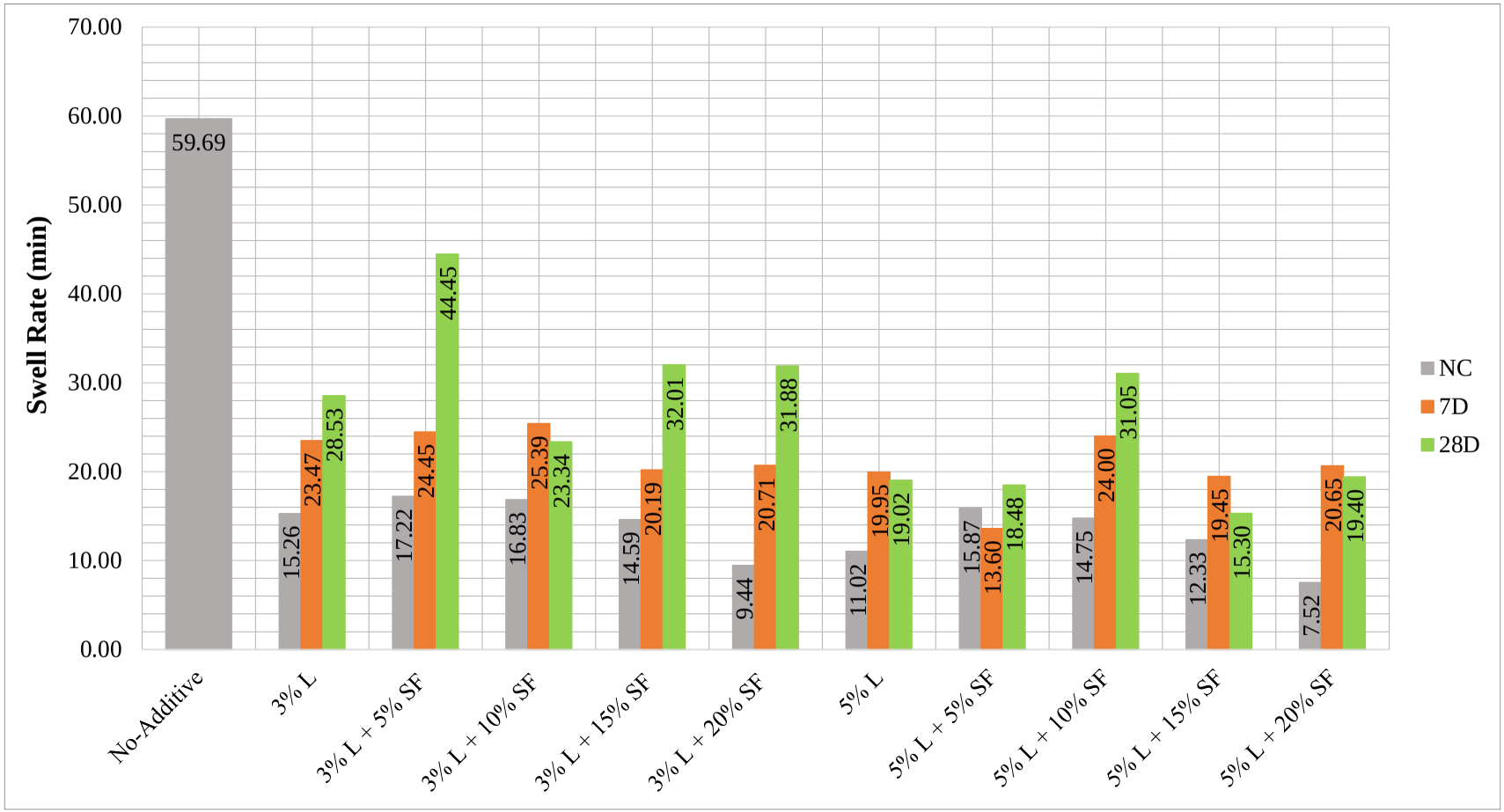

Figure C.21 Swell Rate vs Percent Additive Graph of All Samples with 0-7-28 Days of Curing

D. Net Swell Percentage and Stabilization Percentages

Net swell percent vs percent additive of treated samples graph is given in Figure D.1, and stabilization percent in net swell vs percent additive graph is given in Figure D.2.

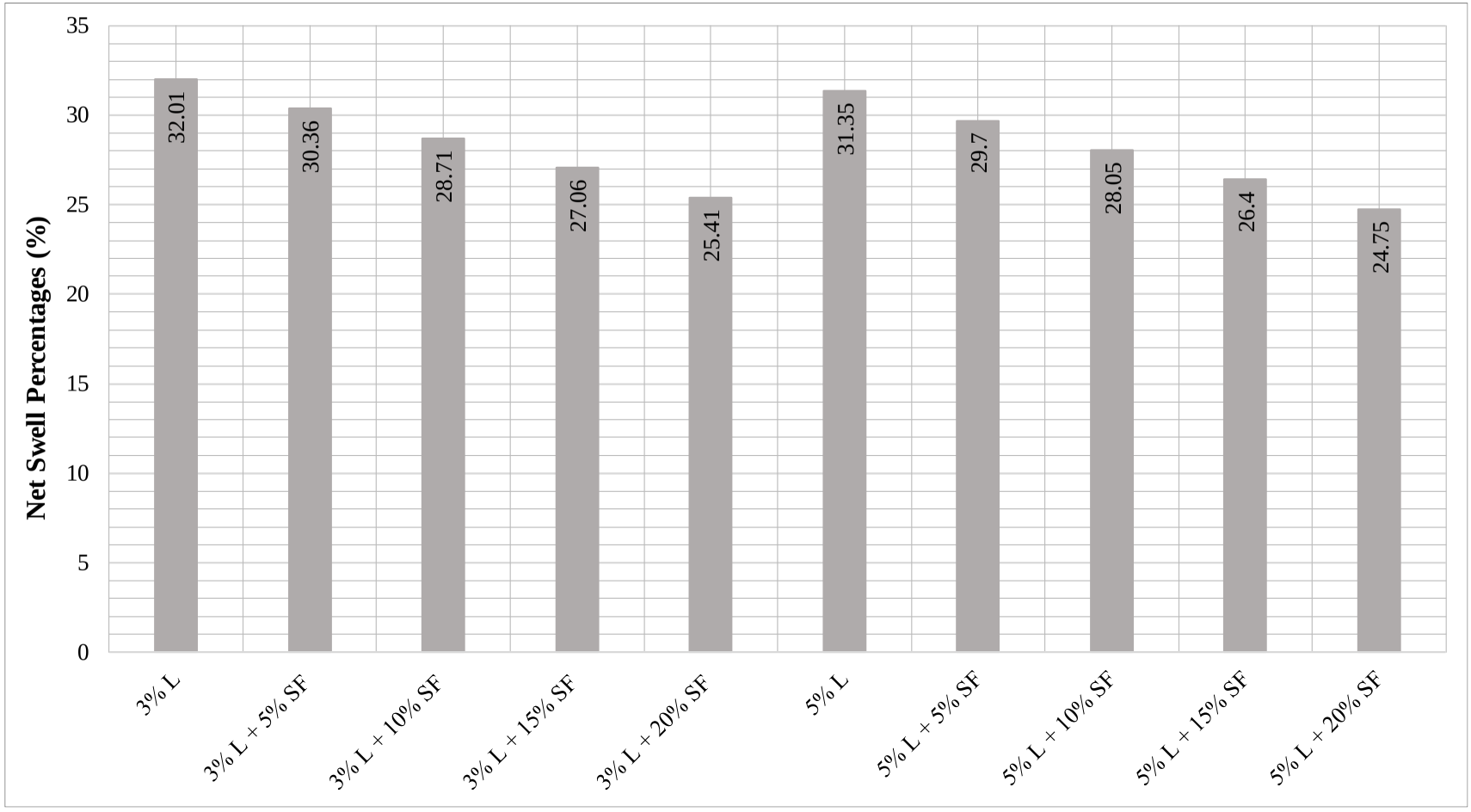

Figure D.22 Net Swell Percentages vs. Percent Additive of Treated

Figure D.23 Stabilization Percent in Net Swell Vs Percent Additive Graph of All Treated Samples